NPS-SP-16-002CR


# NAVAL POSTGRADUATE SCHOOL

**MONTEREY, CALIFORNIA**

**BATTERY SIMULATION AND INVESTIGATION UTILIZING MATLAB SIMULINK**

by

Annika Klussmann

August 2016

THIS PAGE INTENTIONALLY LEFT BLANK

# REPORT DOCUMENTATION PAGE

*Form Approved OMB No. 0704–0188*



| 1. AGENCY USE ONLY *(Leave Blank)* | 2. REPORT DATE | 3. REPORT TYPE AND DATES COVERED |
|---|---|---|
| | August 2016 | Research Report 05-10-2016 to 08-10-2016 |

**4. TITLE AND SUBTITLE**

BATTERY SIMULATION AND INVESTIGATION UTILIZING MATLAB SIMULINK

**5. FUNDING NUMBERS**

**6. AUTHOR(S)**

Annika Klussmann

**7. PERFORMING ORGANIZATION NAME(S) AND ADDRESS(ES)**

Naval Postgraduate School
Monterey, CA 93943

**8. PERFORMING ORGANIZATION REPORT NUMBER**

NPS-SP-16-002 CR

**9. SPONSORING / MONITORING AGENCY NAME(S) AND ADDRESS(ES)**

N/A

**10. SPONSORING / MONITORING AGENCY REPORT NUMBER**

**11. SUPPLEMENTARY NOTES**

The views expressed in this document are those of the author and do not reflect the official policy or position of the Department of Defense or the U.S. Government. IRB Protocol Number: N/A.

**12a. DISTRIBUTION / AVAILABILITY STATEMENT**

Approved for public release. Distribution is unlimited

**12b. DISTRIBUTION CODE**

**13. ABSTRACT** *(maximum 200 words)*

As a self-sufficient power system, a satellite has to be equipped with an electrical energy storage system enabled with a rechargeable battery. To improve the quality of the energy supply at space satellite systems the new high performance battery cell technology, lithium iron phosphate ($LiFePO_4$), is presented and investigated in this work.
Evaluation factors of battery cells for an assessment of the technology are explained and the data of the lithium iron phosphate battery cell are demonstrated. Experimental tests of the cell are performed with MACCOR, a battery test system software. Additionally, a power supply system simulation of the currently used lithium ion battery in the NPSAT1 implemented in Matlab Simulink is investigated for a battery consisting of lithium iron phosphate cells.

| 14. SUBJECT TERMS | 15. NUMBER OF PAGES 121 |
|---|---|
| | 16. PRICE CODE |

| 17. SECURITY CLASSIFICATION OF REPORT | 18. SECURITY CLASSIFICATION OF THIS PAGE | 19. SECURITY CLASSIFICATION OF ABSTRACT | 20. LIMITATION OF ABSTRACT |
|---|---|---|---|
| Unclassified | Unclassified | Unclassified | UU |

NSN 7540-01-280-5500

Standard Form 298 (Rev. 2–89)
Prescribed by ANSI Std. 239–18

THIS PAGE INTENTIONALLY LEFT BLANK

**NAVAL POSTGRADUATE SCHOOL**
**Monterey, California 93943-5000**

Ronald A. Route
President

James Newman
Interim Provost

The report entitled "*Battery Simulation and Investigation Utilizing MatLab Simulink*" was prepared for the Naval Postgraduate School.

**Further distribution of all or part of this report is authorized.**

**This report was prepared by:**

_____
Annika Klussmann
Ensign, German Navy

**Reviewed by:**

_____
Rudolf Panholzer, Chairman
Space Systems Academic Group

**Released by:**

_____
Jeffrey D. Paduan
Dean of Research

THIS PAGE INTENTIONALLY LEFT BLANK

**Approved for public release. Distribution is unlimited**

# BATTERY SIMULATION AND INVESTIGATION UTILIZING MATLAB SIMULINK

Annika Klussmann
Ensign, German Navy
[B.S., Helmut Schmidt Universitaet Hamburg, 2015]

Submitted in partial fulfillment of the
requirements for the degree of

**MASTER OF SCIENCE IN AUTOMOTIVE ENGINEERING**

from the

**NAVAL POSTGRADUATE SCHOOL**
**August 2016**

Approved by:

Thesis Advisor

Second Reader

Rudy Panholzer
Chair, Space Systems Academic Group

THIS PAGE INTENTIONALLY LEFT BLANK

# ABSTRACT

As a self-sufficient power system, a satellite has to be equipped with an electrical energy storage system enabled with a rechargeable battery. To improve the quality of the energy supply at space satellite systems the new high performance battery cell technology, lithium iron phosphate ($LiFePO_4$), is presented and investigated in this work.

Evaluation factors of battery cells for an assessment of the technology are explained and the data of the lithium iron phosphate battery cell are demonstrated. Experimental tests of the cell are performed with MACCOR, a battery test system software. Additionally, a power supply system simulation of the currently used lithium ion battery in the NPSAT1 implemented in Matlab Simulink is investigated for a battery consisting of lithium iron phosphate cells.

THIS PAGE INTENTIONALLY LEFT BLANK

# Contents

# List of Figures

THIS PAGE INTENTIONALLY LEFT BLANK

# List of Tables

THIS PAGE INTENTIONALLY LEFT BLANK

# List of Abbreviations

| | |
|---|---|
| % | Percent |
| $(CH_2O_2)_2CO$ | Ethylene carbonate |
| $Fe_2SiO_4$ | Fayalite |
| $LiCoO_2$ | Lithium cobalt oxide |
| $LiFePO_4$ | Lithium iron phosphate |
| $LiMn_2O_4$ | Lithium manganese oxide |
| $LiNiO_2$ | Lithium nickel oxide |
| $Mg_2SiO_4$ | Forsterite |
| $OC(OCH_3)_2$ | Dimethyl carbonate |
| $\eta$ | Efficiency |
| $\Omega$ | Ohm |
| $\rho$ | Energy density |
| $\rho_S$ | Specific energy density |
| $\rho_V$ | Volumetric energy density |
| **°C** | Degree Celsius |
| **A** | Ampere |
| **AC Imp** | Alternating Current Impedance |
| **Ah** | Ampere-hours |
| **C** | C-Rate |
| $\mathbf{C}_N$ | Capacity |
| **CCCV** | Constant Current, Constant Voltage |
| **CID** | Circuit interrupt device |

| | |
|---|---|
| **CL** | Cycle life |
| **cm** | Centimeter |
| **Co** | Cobalt |
| **$Co^+$** | Cobalt ion |
| **DOD** | Depth of discharge |
| **Fe** | Iron |
| **$Fe^+$** | Iron ion |
| **g** | Gram |
| **h** | Hours |
| **I** | Discharge current |
| **kg** | Kilogram |
| **L** | Liter |
| **Li** | Lithium |
| **$Li^+$** | Lithium ion |
| **M** | Molecular weight |
| **mm** | Millimeter |
| **$Mn^+$** | Manganese ion |
| **n** | Number of electrons |
| **Ni** | Nickel |
| **$Ni^+$** | Nickel ion |
| **NPS** | Naval Postgraduate School |
| **NPSAT1** | Naval Postgraduate School Small Satellite |
| **O** | Oxide |
| **OCVD** | Open Circuit Voltage Decay |
| **P** | Phosphate |

| | |
|---|---|
| $\mathbf{R}_i$ | resistance |
| **s** | Siemens |
| **SD** | Self discharge |
| **SOC** | State of charge |
| **STK** | Satellite Tool Kit |
| **T** | Temperature |
| $\mathbf{U}_N$ | Nominal voltage |
| **US$** | US Dollar |
| **V** | Volt |
| $\mathbf{V}_b$ | Measured voltage |
| $\mathbf{V}_i$ | Voltage source |
| **Wh** | Watt hours |
| **X** | Cost |

THIS PAGE INTENTIONALLY LEFT BLANK

# CHAPTER 1:
# Introduction

The variety in battery cell technology is large but, nowadays, the most sustainable technology is the lithium ion battery cell. During 30 years of development lithium based cells experienced a tremendous advancement to increase their level of performance. Particularly, the research of new electrode materials, especially cathode materials, has been a focus to improve the electrochemical performance and to reduce the potential of danger and the material cost. One of the most innovative positive electrode material for lithium ion batteries is lithium iron phosphate. It is a phosphate olivine which distinguishes itself by offering high safety standards, environmental friendliness and high thermodynamic stability.

A significant challenge is to develop battery cell types for applications which do not operate under normal environmental conditions or have special requirements for power supply. For example, battery cells for space systems, in particular satellite systems, have to meet certain requirements to ensure an accurate operation under space conditions. In this case, models can help to simulate the operation under investigating conditions and to reduce or avoid costly and time-consuming physical testing. Additionally, the current challenge with lithium ion batteries used in satellite systems is to ensure the safe operation of the battery cells.

This thesis deals with an investigation which contributes if the lithium iron phosphate battery cell APR18650M1 of A123 Systems is useful for space satellite systems of the Space Systems Academic Group of Naval Postgraduate School. Chapter 2 gives an overview of the function and the evaluation of a battery cell to introduce the reader to battery technology. The lithium iron phosphate battery cell and its characteristics are presented in Chapter 3 in detail. Chapter 4 deals with a test series of the lithium iron phosphate battery cell performed to determine its performance characteristics. These tests are implemented with MACCOR, a battery cell test system. Furthermore, in Chapter 5 the Matlab Simulink model for power supply of the Naval Postgraduate School Small Satellite NPSAT1 is tested by using collected data of the experimental testings to examine a simulated battery consisting of lithium iron phosphate battery cells. The result of this investigation is presented and shows that the battery cycles

through the entire simulation timeframe. The collected data of the testing and the simulation contribute to determine a potential use of the lithium iron phosphate battery cell in further space satellite systems of NPS.

# CHAPTER 2:
# Background

Batteries are an essential component of most electrical applications like portable devices, cars and consumer electronics. As a result, a battery cell is the most familiar electrical energy storage system. New electrical engineering challenges force the power industry to develop the battery continually to improve its levels of performance.
This chapter deals with the battery as an electrical energy storage system. The battery technology and the function of a battery cell are explained. In addition, the evaluation factors of a battery are presented and a short introduction of the usage of batteries in space systems with particular focus on the safety aspects is given.

## 2.1 Electrical Energy Storage

The demand for electrical power does not necessarily coincide with its generation. Additionally, mostly renewable energy sources like solar plants or wind turbines have intermittent availability caused by the dependence on discontinuous resources so that it is necessary to store the produced energy for later use.
Electrical energy storage is implemented in different ways. To differentiate the various methods they are characterized by their physical operating principles. There are mechanical, chemical, thermal, electromagnetic and electrochemical energy storage systems. This thesis is limited to the explanation of electrochemical storage systems. In particular, the battery as an electrochemical energy storage system is reviewed.
The electrochemical energy storage mechanism is the most traditional energy storage technology and it is widely used in electrical devices and systems. In this method, the energy stored in a chemical form is converted into electrical energy on demand.

## 2.2 Battery Technology

The battery as an electrochemical energy storage system is a widely used and preferred technology to power electrical devices like portable electronics. Nowadays, batteries are an essential component of most electronic applications and the industry

is continually developing new battery types to improve their level of performance. In general, the basic structure of every battery is the same and does not depend on the used electrochemical materials. Each battery consists of one or more cells connected to each other. The materials in the cells are active materials which store the essential chemical energy. The cell including two electrodes and an electrolyte is able to convert the chemical energy into electrical energy. As shown in Figure 2.1, the two electrodes are the anode and the cathode. Both are connected to each other by an external circuit, which allows a flow of electrons. The electrolyte acts like an ionic conductor between the electrodes and allows an ion flow. A separator between the electrodes is needed to prevent an internal short-circuit.

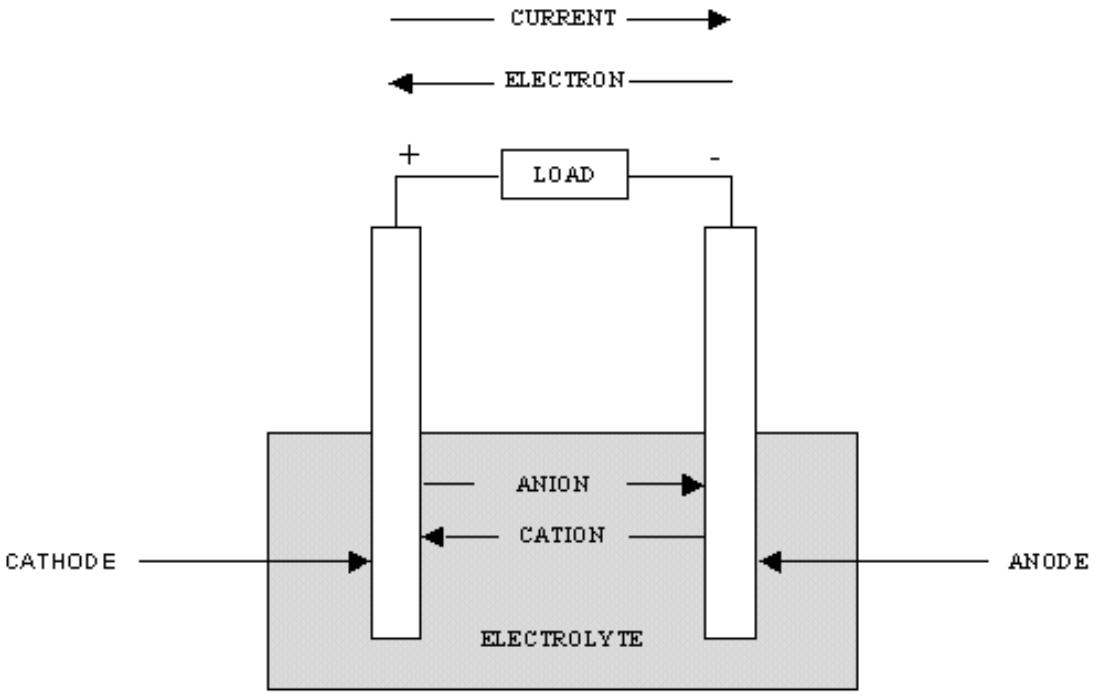


Figure 2.1. Discharge process of a galvanic cell [1]

In the discharge process, the anode is negatively charged and the cathode is positively charged. The negatively charged anions from the cathode flow through the electrolyte to the anode. In return, the positively charged cations from the anode flow through the electrolyte to the cathode. This procedure is called the oxidization of the anode and the reduction of the cathode. The described process causes the anode to give up

electrons to the external circuit. The cathode accepts these electrons and a current flow is generated. This process is called a redox reaction. Formula 2.1 shows the oxidization in a cell where the substance A loses an electron as the reducing agent. The reduction is shown in Formula 2.2 whereby the oxidation agent B receives the electron. Formula 2.3 demonstrates the overall reaction of the oxidation and reduction agents.

$$\mathrm{A} \longrightarrow \mathrm{A}^{+} + e^{-} \tag{2.1}$$

$$\mathrm{B} + e^{-} \longrightarrow \mathrm{B}^{-} \tag{2.2}$$

$$\mathrm{A} + \mathrm{B} \longrightarrow \mathrm{A}^{+} + \mathrm{B}^{-} \tag{2.3}$$

Batteries are divided into two categories, primary and secondary batteries. Primary batteries are not rechargeable whereas secondary batteries are rechargeable. The rechargeability depends on the material used.

Secondary batteries are able to be recharged by implementing the described discharge process in reverse resulting in the charging process. If ions stop moving through the electrolyte the battery cell is discharged. No electrons are able to move through the external circuit anymore so that it has to be recharged. During the charging process the positively charged anode oxidizes and the negatively charged cathode reduces, so that the Formulas 2.1, 2.2 and 2.3 describe the process in reverse respectively. The electron flow is produced by an external power supply, so that the materials of the electrodes are recharged.

The anode, the cathode and the electrolyte consist of different materials and they must meet certain requirements. The anode has to be efficient as a reducing agent with high coulombic output. This is important to provide the external circuit with electrons. The anode material needs good conductivity and should be stable in contact with the electrolyte. Metals like zinc, lithium or lithium alloys and lithium carbons are the most commonly used materials for anodes. The cathode material has to work efficiently as an oxidizing agent. It has to be stable in contact with the electrolyte like the anode material and it must have a useful working voltage. Oxygen in zinc air batteries or metal oxides like halogens or sulfur and its oxides are examples of cathode materials. To separate the anode and the cathode, a separator is used. It is permeable to the electrolyte and ions are able to flow through it so that the desired ionic conductivity is maintained. The electrolyte acts like an ionic conductor and

has to have good conductivity. To prevent an internal short-circuit, the electrolyte must not react with the electrode material. Most electrolytes are liquid and include aqueous solutions, but materials like molten salt are also used.
To prevent potential dangers, a cell has to be equipped with safety features like venting mechanisms or seals. To protect the cell against harmful influences, containers serve as safe enclosures. Some of these safety devices and their functions are explained in detail in Section 2.4.
The described components of a cell can be arranged in various ways resulting in different cell shapes. There are, for example, cylindrical, flat, button or prismatic cells. The shape of a battery cell is not affecting the performance level but rather established to standardize the size and shape of the installation position at the powered application.

## 2.3 Evaluation Factors

The evaluation factors of a battery cell are physical parameters used to describe the cell and its procedure or to compare the performance level of different kinds of cells. This section deals with some of these factors used to classify cells which are discussed further in the following chapters. The factors are listed alphabetically in Table 2.1. In the text the physical units of the factors are noted in square brackets.
The nominal voltage $U_N$ [V] of a cell is the value of the voltage supplied during normal operation. The nominal voltage of most zinc cells, for example, is 1.5V, whereas lithium cells provide a nominal voltage of 3V.
To indicate the amount of electrical charge, the capacity $C_N$ [Ah] of a cell is specified. The amount of the capacity of secondary batteries is always stated with regard to a certain discharge current I [A] and decreases with increasing discharge current.
Batteries are available in different shapes. Therefore, it is not easy to compare different battery shapes with regard to its stored energy. Consequently, it is useful to characterize the energy distribution of a cell with regard to a certain weight or size. The energy density $\rho$ is the amount of energy stored in the cell and it is indicated as the specific energy density $\rho_S$ [Wh $kg^{-1}$] or the volumetric energy density $\rho_V$ [Wh $L^{-1}$]. The higher the density the more energy can be stored.
To characterize the charge level of a cell, the state of charge SOC [%] is specified.

Table 2.1. Evaluation factors

| Name | Formula symbol | Unit |
|---|---|---|
| Ambient temperature | T | °C |
| Capacity | $C_N$ | Ah |
| Charging efficiency factor | $\eta$ | - |
| Cost | X | US$ $kWh^{-1}$ |
| C-rate | C | - |
| Cycle life | CL | - |
| Depth of discharge | DOD | % |
| Discharge current | I | A |
| Internal resistance | $R_i$ | Ω |
| Nominal voltage | $U_N$ | V |
| Self-discharge | SD | % |
| Specific energy density | $\rho_S$ | Wh $kg^{-1}$ |
| State of charge | SOC | % |
| Volumetric energy density | $\rho_V$ | Wh $L^{-1}$ |

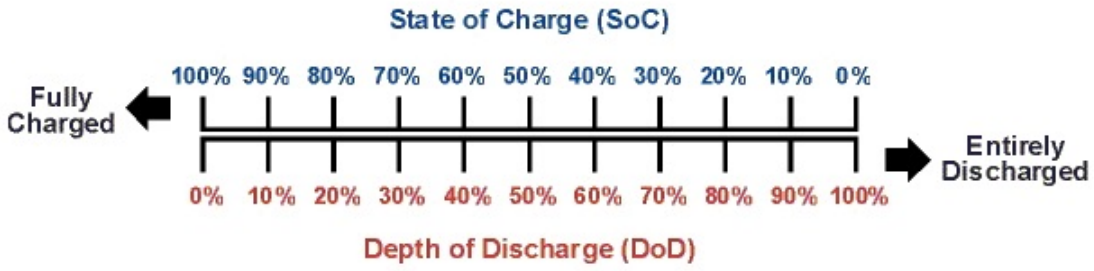


Figure 2.2. Comparison of SOC and DOD [2]

An SOC of 100% represents a fully charged cell whereas an SOC of 0% represents a fully discharged cell. The reciprocal of the SOC is the depth of discharge DOD [%]. A DOD of 100% characterizes an SOC of 0% indicating an entirely discharged cell, whereas a DOD of 0% represents a fully charged cell with an SOC of 100% as shown in Figure 2.2.

Another value to characterize a secondary cell is the C-rate C, used to indicate the maximum charge and discharge currents $I_{max}$ under certain boundary conditions. The C-rate is a rate at which a cell is charged or discharged relative to its maximum capacity. The C-rate is calculated by dividing the maximum current $I_{max}$ by the capacity

$C_N$ of the cell. It is usual to specify the C-rate as, for example, 1C. This means that a cell with the capacity of 100Ah is charged or discharged in one hour with a charge or discharge current of 100A respectively. A C-rate of 2C, for example, indicates that the cell is charged or discharged twice as fast.

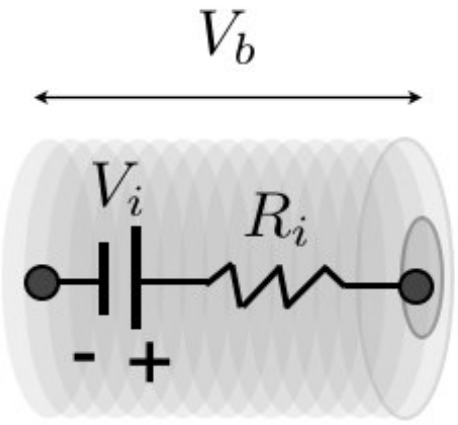


Figure 2.3. Internal resistance of a battery cell [3]

The equivalent circuit of a battery cell is modeled as a voltage source $V_i$ in series with a resistance $R_i$ [Ω] as shown in Figure 2.3. This internal resistance $R_i$ depends on temperature. The higher the temperature the lower the resistance. If the cell is used to power an electrical load a part of the voltage is lost across the internal resistance in the form of heat. This effect results in a difference between the measured voltage $V_b$ that the cell delivers and the higher no-load voltage $V_i$. The voltage difference is known as the voltage drop. To determine the effect of the internal resistance more precisely, the charging efficiency factor $\eta$ [-] is specified. It is defined by dividing the externally supplied charge quantity by the total supplied charge quantity.
The storage of battery cells is a challenge and depends on which active materials are used in the cell. If a cell is not used longer than a certain period of time it is possible for it to lose a part of its stored energy. The loss is caused by internal chemical reactions. This phenomenon is known as self-discharge SD [%]. The amount depends on the state of charge, the charging current and other material affecting factors like ambient temperature. Lead acid batteries experience a self-discharge of 5% per month whereas lithium ion batteries distinguish themselves having a self-discharge of 1% up

to 2% per month [16].
A secondary cell which is fully charged and subsequently entirely discharged run through one cycle. To record the cycle life of a cell, the number of cycles are added before the nominal capacity of the cell falls below 70% of its initially capacity. In general lithium ion batteries are able to offer a lifetime of 1000 or more cycles [17].
An other important factor is the cost. The manufacturing and the maintenance costs are summarized in a cost factor X which is expressed per kilowatt hour [US$ $(\mathrm{kWh})^{-1}$]. In 2014 a lithium ion battery costs US$500 to US$600 per kilowatt hour. Efforts are underway to reduce cost in five years to US$200 per kilowatt hour [17]. However, lead acid batteries have cost of US$150 per kilowatt hour [18].
Most evaluation factors presented depend on the ambient temperature T [°C] in which the battery is operating. In general, batteries operate best at room temperature because most of them are designed to work at that temperature. Cold temperatures increase the internal resistance and lower the capacity and the energy density. Warm temperatures decrease the internal resistance. The cell life is stressed enormously by temperature changes. It can be determined that every 8°C rise in temperature cuts the life of a lead acid battery in half like mentioned in [19]. This implies the life time of the cell of 10 years would reduce to 5 years if the ambient temperature is just 8°C higher than expected during battery cell development.

## 2.4 Safety Issues

The battery cell is an electrochemical device operating with active material. As a result of that, an incorrect design or abuse causes potential danger. This potential danger requires prudent handling and exact operating procedures in accordance with user instructions. In this section safety issues and accident prevention measures are presented.
Nowadays, new battery technologies are based on non-toxic active materials whenever possible. For example, lead acid batteries are being replaced by new designs over time because lead is a toxic metal. However, innovative battery materials which are used to increase energy density or capacity of the cell show a risk in case of cell failures or abuse.

When a lithium cell has an SOC of 100% the cathode contains a powerful oxidizing transition metal oxide and the anode contains the lithiated carbon, a strong reducing material. The electrolyte between the electrodes consists of a lithium salt and a carbonate solvent which tends to be readily oxidized and reduced [20]. Due to this fact, a lithium containing battery cell is thermodynamically unstable and, additionally, very sensitive to thermal and overcharge abuse. Therefore, possible fire hazards are most likely.

The main safety issue is overcharging of battery cells. In general, overcharging occurs during charging a battery pack containing a number of cells arranged in series. During the charge process a charger measures the voltage of the battery pack continuously and calculates the SOC of the whole battery requiring each cell is identical to the others with regard to the capacity and the SOC. It may happen that the cells used in the battery are not truly identical with small variations in cell capacity and cell performance due to different cell ageing. This results into the fact that a number of cells in the battery can be fully charged before the charger estimates an SOC of 100% and continues to charge the battery. An overcharge of a lithium ion battery cell might lead to chemical and electrochemical reactions in the cell between the components. A gas release and rapid increase of cell temperature might occur which triggers self-accelerating reactions in the cell resulting in thermal runaway and possible explosions [20].

To reduce the risk of overcharging batteries are equipped with an external voltage regulation. This technology activates an external bypass circuit when one of the cell voltages moves outside of the prescribed range. Instead through the battery, the charging current will flow through the external circuit. Alternatively, inactivation agents, like biphenyl or furan, in the electrolyte are used to avoid overcharging. The advantage of these organic compounds is that they operate in small amounts and thus do not increase the volume or the weight of the cell. Otherwise, after required for usage they permanently disable the cell resulting into the failure of the battery.

Another safety issue is overheating which occurs often, because the negative electrode produces heat while operating. A temperature sensor detects a rise in cell temperature when it is, for example, charging. When the temperature reaches a certain level the charging process is interrupted to reduce the temperature.

A tear-away tab or a circuit interrupt device (CID) is installed to disable the cell if

its internal pressure exceeds a prescribed amount. To release the surplus pressure a vent is provided. For example, safety vents are useful if other safety devices fail and overheating occurs. A possible release of gas and expansion of active materials with rising temperature cause the pressure in the cell to increase. Safety vents are able to release the internal pressure.

The described safety devices prevent explosions, fires and leakages of the cell. Safety devices will only work successfully if the manufacturing process of the cell is very precise without parts or work steps containing errors [17]. Figures 2.4 and 2.5 show two versions of a primary cylindrical lithium iron disulfide ($LiFeS_2$) battery cell including some of the described safety devices. The anode (18) and the cathode (20) are isolated from each other by a separator (26) in Figure 2.4. To limit the current flow under abusive electrical conditions a positive temperature coefficient PTC device (42) is located between the positive terminal (40) of the battery and the sealing plate (14). To release pressure out of the battery a vent well (28) and a vent hole (30) are provided in Figure 2.5. A vent ball (32) which has to close and seal the aperture if the pressure level is permitted and a vent bushing are forced to move out of the aperture and the emergent gas can be released.

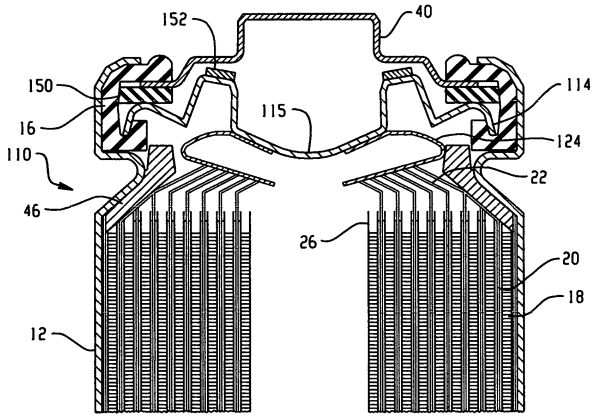


Figure 2.4. Circuit interrupt device, Part 1 [4]

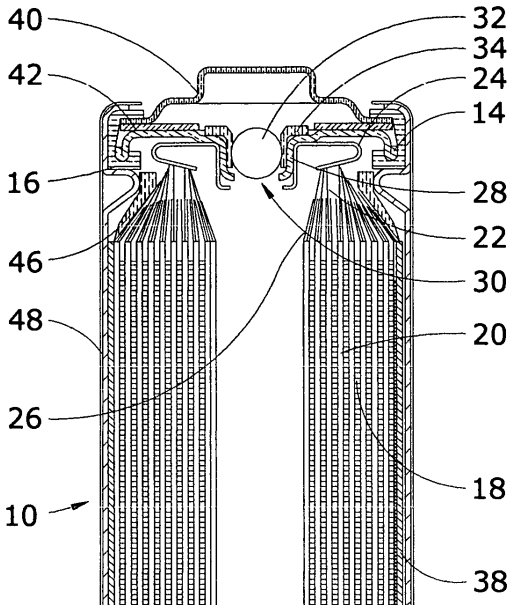

Figure 2.5. Circuit interrupt device, Part 2 [4]

## 2.5 Batteries in Space Systems

Battery technology development is fast-paced and focused on decreasing cost by reducing weight and increasing the cycle life of battery cells. Including space technology, batteries are indispensable nowadays and the above named aims are supposed to be achieved to ensure sustainable success of a new battery technology in space systems. Battery cells are used in satellites to store electrical energy and to supply electrical power when needed. They are recharged via photovoltaic using solar panels. Because of the special environmental conditions in space there are certain requirements for battery cells used in space systems. This section deals with these environmental conditions and introduces the reader to different satellite battery applications. Particularly, reference is made to NPSAT1, a Naval Postgraduate School Small Satellite. As mentioned, satellites are supplied with electrical energy from solar panels. During launch phase and eclipse periods batteries are used to provide needed power. During peak power demand, energy storage systems are used to augment power from solar panels.

In general, and in the case of NPSAT1, the battery cells are connected in series to form strings. One string provides the voltage required by the bus. Strings are con-

nected in parallel to provide the needed capacity of the battery. Figure 2.6 shows a basic block diagram of a bus power supply system. If the solar panels are exposed to the sun, the voltage of the connected solar generator and the bus is maintained at a constant amplitude by a voltage regulator across the solar generator. A battery charge regulator enables that the battery is charged during this time.

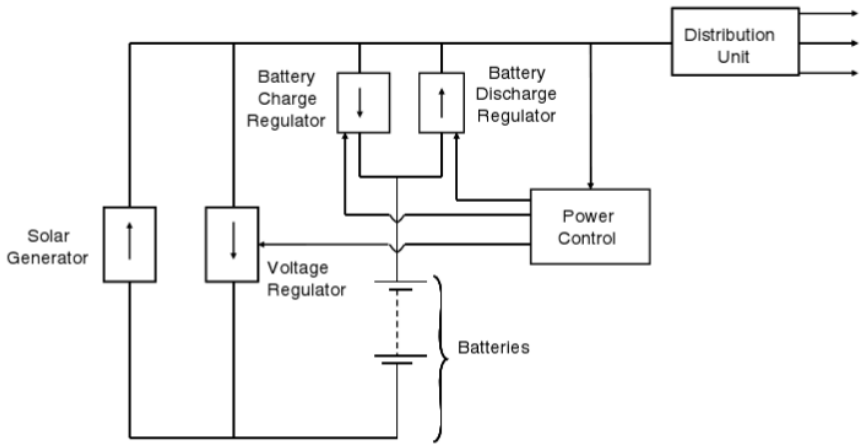


Figure 2.6. Bus power supply system [5]

There are many different battery types used in space systems. All of them have to meet special requirements such as an acceptable specific and volumetric energy density. The higher the energy density the smaller the cells. Battery cells with a high energy density deliver a higher amount of energy per volume or weight unit than cells with a lower energy density. This results in the space which is provided for the cells might be much smaller and the mass of the satellite might be much lighter.
The capacity of a cell affects the battery size as well. The larger the cell of one type is, the higher the capacity of the cell would be because more place for the electrochemical material is available. Depending on the discharge current the capacity is used faster or slower. Manufacturers of satellites have to find the balance between needed capacity and the available space. For this purpose it is useful to use a cell material which offers a high capacity on small space.
The lithium- ion battery used in the NPSAT1 is a battery consisting lithium cobalt oxide battery cells with a graphite anode as shown in Figure 2.7. Seven cells are con-

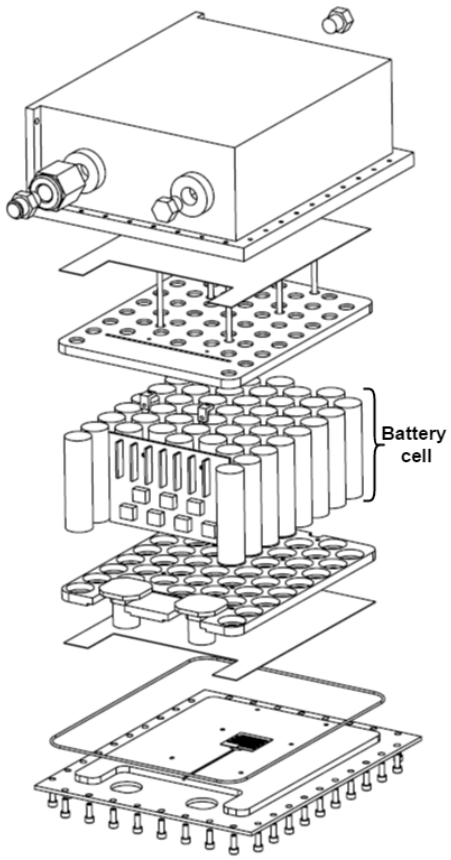


Figure 2.7. NPSAT1 battery assembly [6]

nected in series to strings and seven of these strings are connected in parallel resulting in a compact and rectangular arrangement. This design offers an overall capacity of 226 Wh and a voltage of 29.5V. This corresponds to a capacity of 7.66Ah [21]. The advantage of this design is that if one cell is failing just the string which includes this cell is separated from the battery. Additionally, several tests were performed during the development phase to ensure the resistance of the battery to vibration and temperature during launch phase and operation in the space.

# CHAPTER 3:
# Lithium Iron Phosphate Battery Cell

Nowadays, the most sustainable battery systems are lithium ion batteries, because lithium offers the smallest energy carrying ions in battery material technologies. This thesis is based on a lithium iron phosphate battery cell, a subset of lithium ion batteries.

This chapter deals with the presentation of the lithium iron phosphate battery cell ($LiFePO_4$) APR18650M1 of A123 Systems. First, the function of a lithium ion battery cell is explained in general. Additionally, the characteristics of the lithium iron phosphate cell are elucidated by means of the evaluation factors explained in Section 2.3. Finally, an overview is given of safety devices used in the lithium iron phosphate battery cell.

## 3.1 Lithium Ion Battery Cell

A lithium ion battery cell is a rechargeable battery cell used in many portable applications. This section presents the function of a lithium ion battery in general by elucidating used cathode and anode materials and explaining the ion exchange during operation.

Lithium is used in battery cells because it offers the highest electro-negative potential in battery material technologies. Additionally, lithium is the lightest metal in the periodic table. When it reacts with a high electro-positive material, a high cell voltage and consequently a high energy content is produced. In general, a distinction can be made between lithium ion and lithium metal batteries. A Li-ion cell includes an anode, which contains different lithium intercalation compounds [7] like graphite, whereas a lithium metal cell uses alloying or pure metal as an anode material [17].

The cathode material of a lithium cell affects the capacity and the energy characteristics of the battery much more than the anode material because the positive electrode is the heaviest of both [17]. Furthermore, 40% of the total cost is for cathode material [7]. Therefore, the cathode material offers the largest potential for improvement to enhance battery performance and efficiency. Common cathode materials are, for ex-

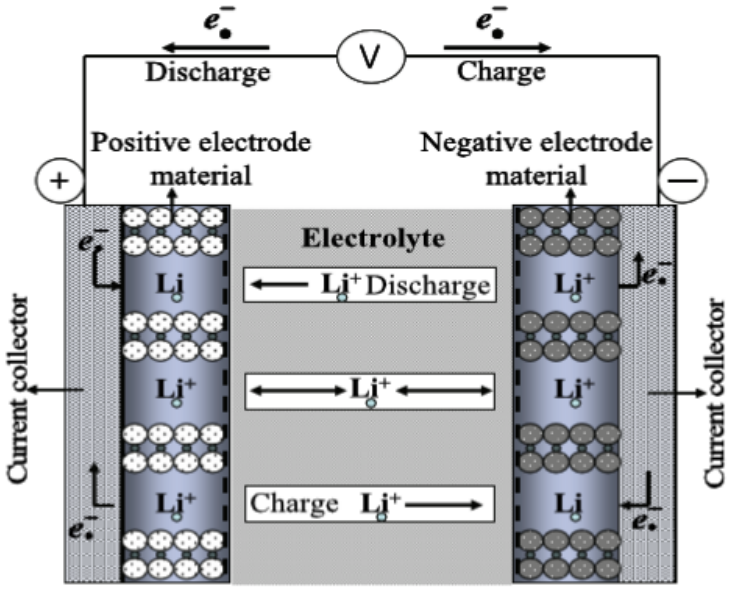


Figure 3.1. Schematic diagram of the charge and discharge process of a rechargeable Li-ion battery cell [7]

ample, lithium cobalt oxide, lithium manganese oxide or lithium iron phosphate [17]. This thesis deals with a lithium iron phosphate battery cell so that the following sections cover the structure and the properties according to this battery type.
The schematic operation of a typical Li-ion battery cell is shown in Figure 3.1 [7]. The anode consists of carbon in a graphitic form and the cathode consists of lithium-insertion compound. As explained in Section 2.2, a $Li^+$ exchange between the electrodes takes place at the charging and discharging process to allow an electron flow through the external circuit. The effectiveness of the ion insertion and extraction depends on factors like the availability of ions at the electrodes and the lightness of transport of ions through the electrolyte [7].

## 3.2 Characteristics of the Lithium Iron Phosphate Cell

The characteristics of the lithium iron phosphate battery cell are explained by presenting the materials of the cell components, anode, cathode and electrolyte. Additionally, the crystal structure of the cathode material is elucidated in detail and the

charging and discharging process is presented by indicating the chemical reactions of the battery cell materials during operation.

### 3.2.1 Cell Components

The investigated lithium iron phosphate cell in this thesis is a A123 Systems cell of the type APR18650M1A as shown in Figure 3.2 [8]. It has a nominal capacity of 1.1Ah and a nominal voltage of 3.3V. The cell consists of a graphite anode with intercalated metallic lithium. A non-aqueous solution is needed for the electrolyte because the voltage (3.3V) of the lithium ion battery is higher than the decomposition voltage of water (1.23V). Additionally, the solution has to be electrochemically resistant, useful in a wide temperature range and sufficiently reactive with the electrodes. Therefore, common lithium ion electrolytes consist of a lithium hexafluorphosphate ($LiPF_6$) as the conducting salt dissolved in organic carbonates [22]. For example, the lithium iron phosphate battery cell used in this investigation includes solvents like ethylene carbonate ($(CH_2O_2)_2CO$) and dimethyl carbonate ($OC(OCH_3)_2$). The cathode is a lithium iron phosphate electrode. Compared with common lithium cobalt oxide cathodes, lithium iron phosphate has become more important as a cathode material in recent years [17].


Figure 3.2. A123 Systems' APR18650M1A lithium ion cylindrical cell and its dimensions [8]

According to Molenda [9], lithium iron phosphate as a cathode material is the most

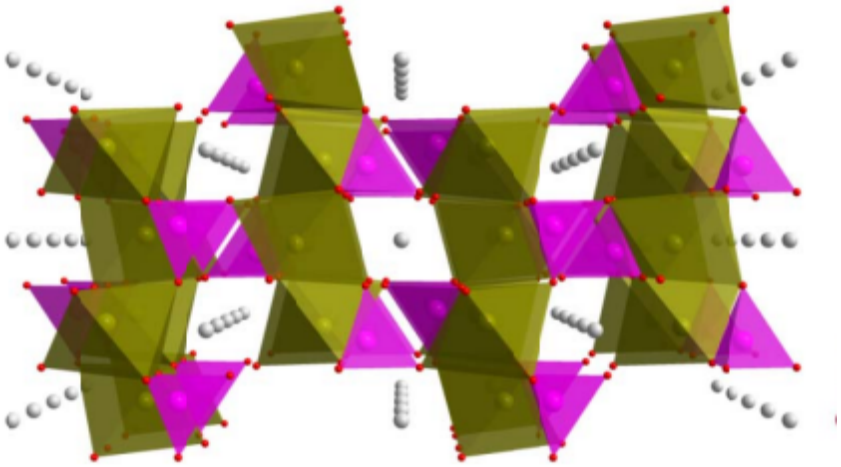

Figure 3.3. Crystal structure of $LiFePO_4$ [9]

promising material for lithium ion batteries and applications like portable devices or electric vehicles. The material offers a high reversible capacity with 170mAh $g^{-1}$ [9], a high chemical stability and an appropriate voltage like conventional lithium ion batteries [17]. Most important, lithium iron phosphate is not toxic and less costly than other used cathode materials so that most of the safety issues with lithium ion batteries and high manufacturing costs can be reduced. Due to this fact, this battery type is gaining more and more attention in battery technologies.

### 3.2.2 Crystal Structure of Lithium Iron Phosphate

Lithium iron phosphate as a cathode material belongs to the olivine structured battery material technology. Olivine is a rock-forming mineral. It is chemically called magnesium iron silicate and exhibits a chemical formula which typically ranges between Forsterite ($Mg_2SiO_4$) and Fayalite ($Fe_2SiO_4$). In general, the chemical formula of the olivine structured cathode is $LiXPO_4$ in which the X complies with Ferrum (Fe), Mangan (Mn), Cobalt (Co) or Nickel (Ni). Therefore, the battery cell with a $LiFePO_4$ cathode is a member of the olivine group.

As shown in Figure 3.3 [9] the crystal structure of lithium iron phosphate exhibits an orthorhombic unit cell. The $FeO_6$ atoms (green and red), which occur octahedral, are connected to each other by $PO_4$ atoms (pink and red), which occur tetrahedral,

through edge-sharing layers. The $Li^+$ cations (white) occupy the octahedral positions and form chains along one-dimensional tunnels. The orthorhombic olivine structure of lithium iron phosphate exhibits robust characteristics and thermal stability. This results in higher safety performances of cells using lithium iron phosphate as cathode material.

### 3.2.3 Charge and Discharge Process

As explained in Section 2.2, the charge and discharge process of battery cells is enabled by an ion exchange. The electrodes in lithium iron phosphate battery cells are changing lithium ions resulting in a lithium insertion and extraction during the discharge and the charge at the lithium iron phosphate cathode respectively. These two reactions are demonstrated in Formula 3.1 for the discharge and 3.2 for the charge process [7].

$$FePO_4 + xLi^+xe^- \longrightarrow xLiFePO_4 + (1-x)FePO_4 \tag{3.1}$$

$$LiFePO_4 - xLi^+ - xe^- \longrightarrow xFePO_4 + (1-x)LiFePO_4 \tag{3.2}$$

During the discharge process $Li^+$ ions are inserted into the $FePO_4$ structure. The $Fe^{3+}$ ions are reduced to $Fe^{2+}$ ions by gaining electrons as shown in Formula 3.1. Upon charging, as shown in Formula 3.2, $Li^+$ ions are extracted from $LiFePO_4$. Additionally, the $Fe^{2+}$ ions lose electrons and oxidize to $Fe^{3+}$ while the $LiFePO_4$ phase is formed. Because the $LiFePO_4$ and the $FePO_4$ phases occur as an olivine-type orthorhombic structure, the lattice constant of the structures are similar [17]. According to Bazzi [14], a change from the $LiFePO_4$ phase to the $FePO_4$ phase involves a lattice volume reduction of 6.77%. This minimal structural phase change results in a good cycle performance. Furthermore the bond between the O, Fe and P atoms is very strong. This fact inhibits the electrochemical reaction in lithium iron phosphate by impeding the separation of the atoms.

The ionic diffusivity ($10^{-13}$ to $10^{-16}$ $cm^2$ $s^{-1}$ [23], [24]) and electronic conductivity ( $10^{-9}$ S $cm^{-}1$ [23], [24]) as a result of the described phenomenon are low in contrast to other cathode materials. Both properties lead to poor battery performance caused by affecting the electrochemical reaction. As a result, the capacity, cycle-life and rate capability may be impaired [14]. Nonetheless, lithium iron phosphate is a valued

cathode material because it offers many more advantages than other commonly used materials. Further evaluation factors are contained in the following section.

## 3.3 Basic Properties and Evaluation Factors

Table 3.1 [7] at page 21 shows a comparison of properties of battery cells using lithium cobalt oxide ($LiCoO_2$), lithium nickel oxide ($LiNiO_2$), lithium manganese oxide ($LiMn_2O_4$) or lithium iron phosphate ($LiFePO_4$) as a cathode material. The table entries are average values of commonly used battery cells. The properties are explained in detail in the following sections. Furthermore, the capacities and the energy densities are identified as practical or theoretical values, because factors like the intrinsic kinetic energy, the conductivity limitations of the material, the impact of electrode components, the current density or the ambient temperature [7] influences the theoretical performance of the cell determined under ideal experimental conditions.

### 3.3.1 Specific Capacity

As an example, the theoretical capacity C [mAh $g^{-1}$] of the active material in a battery cell is a measurement of the quantity of electricity involved in the electrochemical reaction and can be estimated as shown in Formula 3.3, according to Cheruvally [7].

$$C = \frac{n \cdot 26.8 \cdot 1000}{M} mAh \tag{3.3}$$

n = Number of electrons involved in the redox reaction process [-]
M = Molecular weight of the material [g]

For lithium iron phosphate battery cells the number of electrons n is 1 [17] and the molecular weight M amounts to 157.76g [17] provided that $FePO_4$ converts completely during the intercalation [7]. Hence, the theoretical capacity of $LiFePO_4$ amounts to 169.88mAh $g^{-1}$ rounded to 170mAh $g^{-1}$ in Table 3.1 [7].
As demonstrated by the comparison in Table 3.1 [7], the theoretical capacity of lithium iron phosphate is higher than the capacity of lithium manganese oxide but lower than the capacity of lithium cobalt oxide and lithium nickel oxide. However,

Table 3.1. Comparison of Li-ion batteries by means of certain evaluation factors [7]

| Features | $LiCoO_2$ | $LiNiO_2$ | $LiMn_2O_4$ | $LiFePO_4$ |
|---|---|---|---|---|
| Availability | Low | Fair | High | High |
| Cost | High | Fair | Low | Low |
| Discharge capacity[2] [mAh $g^{-1}$] | 145 | 160 | 105 | 155 |
| Environment friendliness | Poor | Fair | Good | Good |
| Nominal Voltage [V] | 3.6 | 4.0 | 3.9 | 3.5 |
| Redox couple | $Co^{4+}/Co^{3+}$ | $Ni^{4+}/Ni^{3+}$ | $Mn^{4+}/Mn^{3+}$ | $Fe^{3+}/Fe^{2+}$ |
| Safety | Fair | Poor | Good | Good |
| Specific capacity[1] [mAh $g^{-1}$] | 274 | 274 | 148 | 170 |
| Specific energy density[2] [Wh $kg^{-1}$] | 520 | 640 | 410 | 540 |
| Structure | Layered | Layered | Spinel | Orthorhombic |
| True density [g $cm^{-3}$] | 5.1 | 4.8 | 4.2 | 3.6 |
| Volumetric energy density[2] [Wh $L^{-1}$] | 2650 | 3070 | 1720 | 1940 |

[1] Theoretical
[2] Practical

the layered structure of $LiCoO_2$ and $LiNiO_2$ enables a complete reversible insertion-extraction process within a limited compositional range, so that a practical capacity of $\sim$ 150mAh $g^{-1}$ can be implemented.

### 3.3.2 Cell Voltage

Furthermore, the nominal voltage of lithium iron phosphate cells with 3.5V (see Table 3.1 [7]) is not extraordinarily high for lithium ion battery cells. Presented in detail by Cheruvalley [7], the typical charge and discharge curves (see Figure 3.4) demonstrate the charging voltage of 3.5V and discharging voltage of 3.3V. Although these are not the highest voltage values in Table 3.1 [7], the voltage difference between charge and discharge plateaus is smaller than those of other common cathode materials. It can be established that the kinetic energy of the transition process between $LiFePO_4$ and $FePO_4$ is better than of other used cathode materials.

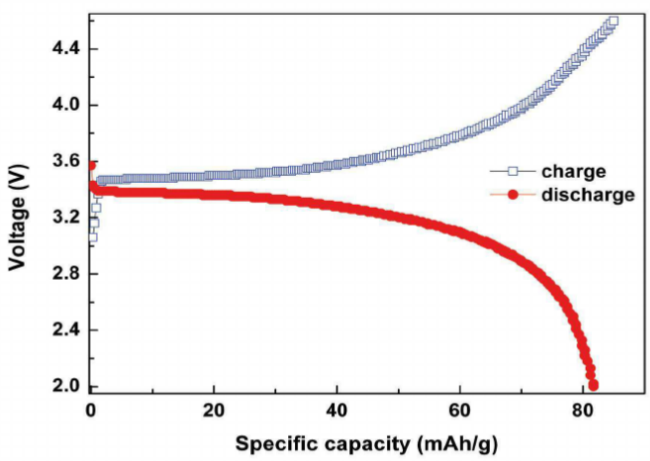


Figure 3.4. Typical charge and discharge curves for $LiFePO_4$ [7]

### 3.3.3 Cycle Life

Lithium ion battery cells diminish in quality of performance during their lifetime, measured by the number of charging and discharging cycles the battery can complete

before its charge capacity is reduced to 70%. Figure 3.5 (a) [7] shows the current-voltage curves of a lithium iron phosphate cell for the first cycles. The electrochemical reaction occurs with almost no loss in the reversibility and no change in the charging and discharging voltage. Because of these minimal losses, the battery has good cycle performance during the first cycles. The extended cycle life is shown in Figure 3.5 (b) [17]. The discharge capacity of the cell during the first 55 cycles decreases slightly. The capacity at the first cycle is 109mAh $g^{-1}$. After 55 cycles the discharge capacity diminishes to 79.57mAh $g^{-1}$. This results in a capacity loss of 27% for 55 cycles and a 0.5% capacity loss per cycle. Compared to the other cathode materials [17], lithium iron phosphate has an excellent cycle performance which is traceable to the olivine chemical structure and the similarity of $LiFePO_4$ and $FePO_4$ as explained in Section 3.2.

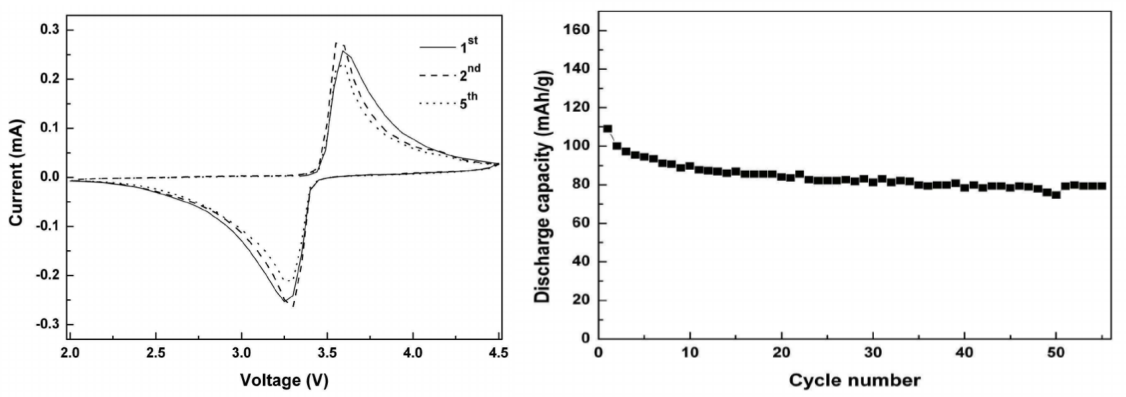


((a)) Current-Voltage curves of $LiFePO_4$ [7] ((b)) Capacity-Cycle number curve of $LiFePO_4$ [7]

Figure 3.5. Cycle life of $LiFePO_4$ [7]

### 3.3.4 Energy Density

As mentioned in Section 2.3, the density of the used cathode material greatly affects the performance of the Li-ion battery cell and is a relevant factor for the final cost of the cell. The true density, listed in Table 3.1 for each cathode material, is the density of the particles which make up the material. This value is determined by its molecular weight and the lattice constant. The olivine structured lithium iron phosphate has a true density of 3.6g $cm^{-3}$ which is explicitly lower than other listed density values.

The product of the theoretical capacity [Ah $kg^{-1}$] and the average voltage [V] results in the theoretical specific energy. These theoretical values, shown in Table 3.2, are compared to the practical specific energy [Wh $kg^{-1}$] in Figure 3.6 (a). Figure 3.6 (b) shows the practical and theoretical volumetric energy density [Wh $L^{-1}$] of considered cathode materials. The practical and theoretical values are calculated by multiplying the true energy with the practical or theoretical specific energy respectively and are listed in Table 3.2. Figure 3.6 (a) [7] demonstrates that the theoretical specific energy of lithium iron phosphate is one of the lower ones. However, the practical specific energy value shows that $LiFePO_4$ has a higher property than $LiCoO_2$ and $LiMn_2O_4$. Figure 3.6 (b) [7] shows that the practical volumetric energy density of lithium iron phosphate is slightly higher than that of $LiMn_2O_4$ but significantly lower than that of the other considered materials. This relates to the low true density of $LiFePO_4$.

Table 3.2. Theoretical energy densities

| Factor | $LiCoO_2$ | $LiNiO_2$ | $LiMn_2O_4$ | $LiFePO_4$ |
|---|---|---|---|---|
| Theoretical specific energy density [Wh $kg^{-1}$] | 986.4 | 1096 | 577.2 | 595 |
| Theoretical volumetric energy density [Wh $L^{-1}$] | 5030.6 | 5260.8 | 2424.2 | 2142 |

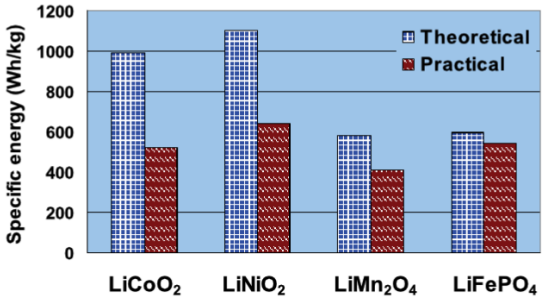


((a)) Theoretical specific energy densities

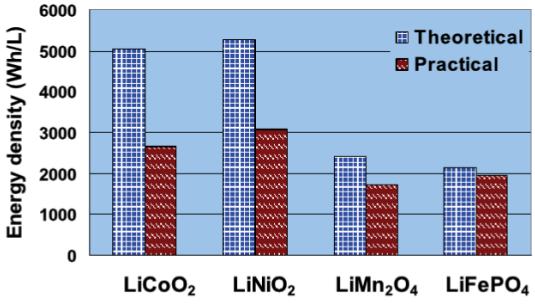


((b)) Theoretical volumetric energy densities

Figure 3.6. Comparison of energy characteristics [7]

### 3.3.5 Safety

Because of the high overheating potential of lithium battery cells and the concern about catching fire, cells with cathode materials including lithium are subject to

special requirements [17]. As explained in Section 3.2, lithium iron phosphate is thermally stable because of its olivine structure. $LiFePO_4$ and $FePO_4$ structures remain unchanged at temperature of up to 400°C, according to Cheruvalley [7], and the oxygen atoms are unavailable to oxidize the electrolyte solvent as further discussed by Xiao [25]. Thus it is possible to let the cell operate under abusive conditions without losses in terms of safety.

Lithium iron phosphate is able to tolerate an overvoltage of 1.6V up to 5.1V with no significant structural rearrangements, in contrast to the redox couple $Li/Li^+$ [17], [25]. This tremendous range ensures safety in operations without decomposing the electrolyte [25]. Redox couples like $M^{4+}/M^{3+}$ in layered oxides and spinel cathodes cannot offer good structural and chemical characteristics, so these materials are less suitable for cathodes with regard to the safety factor. $LiCoO_2$ and $LiNiO_2$ occur in a layered structure with interstitial connections via van der Waals forces, which are reduced during overvoltage conditions and high temperature changes [17]. This effect results into $O_2$ loss, irreversible capacity loss and, in the end, significant safety hazards [7].

### 3.3.6 Environment, Availability and Cost

The factors this section deals with do not directly affect the battery cell performance. However they are considered during the development of new battery cells and in particular during the selection of the active materials.

Lithium iron phosphate is an environment-friendly material because it is not toxic, in contrast to lithium cobalt oxide, for example. Therefore, the usage and the disposal of lithium iron phosphate is ecologically harmless and the storage of cells including this material is possible without determining losses in stability.

There are two ways to obtain lithium iron phosphate, from natural sources or synthesized materials. The former is implemented by extracting lithium iron phosphate from the naturally occurring ore, triphylite. Triphylite is a lithium ion phosphate which forms solid solutions with lithiophilite, a lithium manganese phosphate to the chemical formula $LiFe_xMn_{1-x}PO_4$ [14]. These ores are abundant and inexpensive, so they are attractive for battery technology [7]. Furthermore, these ores commonly occur in phases with a lot of impurity or partial bigger particles. This effect results

Table 3.3. Comparison of cost of $LiFePO_4$ and $LiCoO_2$ based on a 18650 cell [14], [7]

| Factor | $LiCoO_2$ | $LiFePO_4$ |
|---|---|---|
| | 5.05 [14] | 6.31 [14] |
| Material cost [US\$ $kg^{-1}$] | 40 [7] | 15 [7] |

in lower electrochemical performance [17]. To avoid this loss, synthesized materials are used to produce lithium iron phosphate [7] whose raw materials are inexpensive and easily available [14].

Compared to other metal oxide-based materials like lithium cobalt oxide, the cost of lithium iron phosphate production is much lower. The cost of cathode material per kilogram for lithium cobalt oxide is US\$40. For lithium iron phosphate the cost is US\$15 (see Table 3.3) [7]. An extraction of 5.05Wh is possible for lithium cobalt oxide, and 6.31Wh for lithium iron phosphate per US\$ [14]. This shows that $LiFePO_4$-based cells are highly economical compared to $LiCoO_2$-based cells.

### 3.3.7 Summary

As presented in Sections 3.3.1 to 3.3.6, lithium iron phosphate offers a number of characteristics as a useful cathode material for lithium ion battery cells. The factors worth mentioning are its non-toxicity, low cost, high disposability, environment-friendliness, safety and thermal stability because of its robust, close-packed orthorhombic, olive structure. Additionally, lithium iron phosphate provides a relatively high theoretical capacity of 170mAh $g^{-1}$ and a useful operating voltage of 3.5V. The main advantages are the high reversibility of its redox reaction and its stable performance during cycling compared to other cathode materials.

The main drawbacks of lithium iron phosphate used in battery cells are its poor electronic and ionic conductivities which affect the mass transport of the lithium ions and ultimately the cell performance. To avoid these limitations it is possible to synthesize small particles with uniform morphology and to produce active particles with conductive coatings, as explained in detail by Cheruvalley [7].

## 3.4 Safety Devices

As mentioned in Section 2.4, battery cells are subject to safety regulations to avoid potential hazards. The safety data sheet of the lithium iron phosphate battery cell [15] provides an identification of hazards for the cell. The sheet notes that the cell is not classified as dangerous or hazardous because it contains active material whose release is not expected in normal use. The chemical material is contained in a sealed enclosure so that a risk of exposure is excluded as long as the cell is not mechanically, thermally or electrically abused to the point of compromising the enclosure. A damage of the enclosure results in a leakage of the electrolyte which could affect health by burning the skin or eyes. Additionally, the liquid electrolyte used in lithium iron phosphate battery cells is flammable when subject to high temperatures (150°C [15]) or is abused for example, when the cell is overcharged (>3.6V [8]). The cell should not be opened, dissembled, crushed or burned and it has to be stored in a dry location at room temperature (25°C [15]) to avoid shortened cell life. There are special transportation requirements, requiring testing, packaging and marking instructions which are presented in detail in the Cylindrical Battery Pack Design, Validation and Assembly Guide by A123 Systems [26].

The lithium iron phosphate battery cell produced by A123 Systems includes a shutdown separator and a thermal interrupt which stop the charging or discharging process when higher temperatures occur caused by overcharging or over-current, for example. To avoid a high internal pressure a tear-away tab is provided and if increasing pressure occurs a vent is used [15]. These devices, already presented in Section 3.2.3, occupy useful space inside the cell. They reduce their reliability and they disable the cell irreversibly [26]. However they are necessary because the anode produces heat while the cathode produces oxygen during operation as mentioned in Section 3.2.3. The risk of explosion or fire is greatly reduced by installing safety devices while the cost of the lithium cells increases.

THIS PAGE INTENTIONALLY LEFT BLANK

# CHAPTER 4:
# Experimental Cell Testing

A lithium iron phosphate cell of the type APR18650M1A is considered and tests are performed to determine its characteristics under special conditions. This work helps to ascertain if lithium iron phosphate cells work more efficiently in satellite systems than the lithium ion battery cells currently used in NPSAT1. The following sections provide a summary of screening tests that are performed to characterize the cells and to prove if it is suitable for space battery systems. Each cell test is described by explaining its motivation, approach and result. Certain relations between influence factors and collected data are illustrated in figures. Additionally, the test implementation is explained and the collected data are presented and analyzed.

## 4.1 Test Concepts

The following subsections deal with the description of the cell tests to investigate the lithium iron phosphate battery cell of the type APR18650M1A. First, the open circuit voltages of the cells are measured with a digital voltmeter. Then the described tests are performed with the MACCOR software. Additional tests to determine the cell performance are provided in Appendix A.

The main data of the lithium iron phosphate battery cell specified by the manufacturer are listed in Table 4.1. They are used to determine the test settings. As listed, the nominal capacity of the cell is 1.1Ah so that a 1C rate, equivalent to a discharge current of 1.1A, discharges the cell in one hour as explained in Section 2.3 the nominal voltage is 3.3V and therefore lower than the averaged value of 3.5V mentioned in Chapter 2. Additionally, the voltage of the charging and discharging procedures is regulated between 2V and 3.6V to avoid safety issues or lifetime reduction. Therefore, the battery cell is not discharged lower than 2V and is not charged higher than 3.6V during the tests.

Table 4.1. Data sheet of the A123 Systems' lithium ion rechargeable APR18650M1A cell [15]

| Factor | Value |
|---|---|
| Core cell weight [g] | 39 |
| Cycle life at 5C discharge, 100% DOD | Over 1,000 cycles |
| Internal Impedance (kHz AC) [mΩ] | 18 |
| Internal Resistance (10A, 1s DC) [mΩ] | 27 |
| Maximum continuous discharge [A] | 30 |
| Nominal capacity [Ah] | 1.1 |
| Nominal voltage [V] | 3.3 |
| Operating temperature range [°C] | -30 to +60 |
| Recommended standard charge method | 1.5A to 3.6V CCCV, 45min |
| Recommended fast charge current | 4A to 3.6V CCCV, 15min |
| Recommended charge and cut-off voltage at 25°C [V] | 3.6 to 2 |
| Storage temperature range [°C] | -40 to +60 |

### 4.1.1 Break-In and Capacity

In previous lithium ion cell tests [7] Cheruvally detected that the capacity increases slightly after the first two cycles of charging and discharging as shown in Figure 4.1 as the formatting phase. Afterwards the capacity starts to decrease while passing a peak phase and a decline phase. Therefore, two full cycles of this test are performed at a temperature of 25°C and a C-Rate of 1C, equivalent to 1.1A. It is important to ensure that the DOD of 100% is fully established to break the cells in. The cycles are used to measure the capacity of the cells. To determine the electrical impedance in alternating current AC Imp [Ω] of the cells the complex ratio of the voltage and the current at the end of charge voltage EOCV is generated.

### 4.1.2 Discharge Capacity and Watt Hour Efficiency

To measure the constant current charge and constant current discharge capacity of the cells, three cycles at different temperatures (5°C, 10°C and 30°C) are implemented. At each cycle the discharge capacity and the charge capacity are required to calculate the ratio of these data and to determine the watt hour efficiency of the cells for a specific cycle. The watt hour efficiency is the ratio of the amount of energy available during the discharge process to the amount of energy used during the charge process [13].

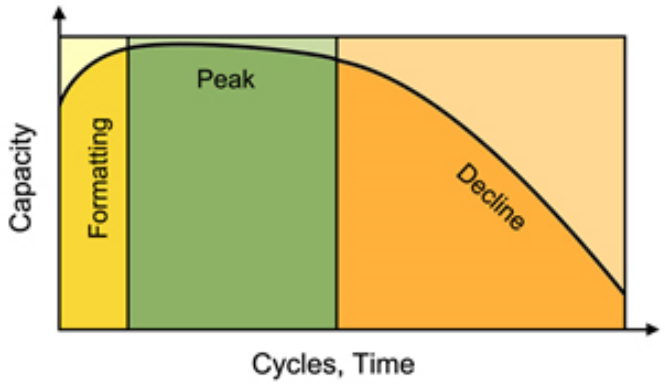


Figure 4.1. Battery lifespan [10]

### 4.1.3 Rate Variation

In preparation for the simulation of the battery cells with Matlab Simulink a test procedure has to be implemented to discharge the cells with different discharge rates. The cells are charged with a rate of 1.1A and discharged eleven times with discharge rates of 3.5A, 3.0A, 2.5A, 2.0A, 1.5A, 1.0A, 0.75A, 0.5A, 0.375A, 0.25A and 0.1A. Rest steps between the charge and discharge processes allow the chemical reaction in the cells to complete.

### 4.1.4 Temperature Variation

In preparation for the simulation of the battery cells with Matlab Simulink an additional test procedure has to be implemented to discharge the cells at different temperatures. The cells are charged and discharged with a rate of 1.1A at eight different temperatures of 40°C, 35°C, 30°C, 25°C, 20°C, 15°C, 10°C and 5°C. Pause steps during the cycles allow to adjust the ambient temperature of the cells. Due to possible condensation in the enclosure which affects the safety performance of the test, the procedure starts with a cycle at 40°C to eliminate potential moisture in the enclosure.

## 4.2 Experiment Implementation

The tests performed to verify the function of the lithium iron phosphate battery cells are implemented in MACCOR, a software program used to test a wide range of products like batteries, fuel cells or supercapacitors. Therefore the procedures of

the tests have to be programmed. Subsection 4.2.1 and 4.2.2 deal with the setup and the implementation of the tests. The steps of the procedures are explained with the break-in test procedure as an example. Afterwards, the experimental data collection with MACCOR is presented and the obtained data are analyzed and evaluated.

### 4.2.1 Experimental Setup

The test setup shown in Figure 4.2 (a) is used to perform the battery cell tests and is located in Bullard Hall 112, a battery test laboratory. Located in a 6.35mm thick enclosure made out of polycarbonate, eight pods (see Figure 4.2 (b)) are equipped with a lithium cell during the tests. The pods are named Channels 1 to 8.

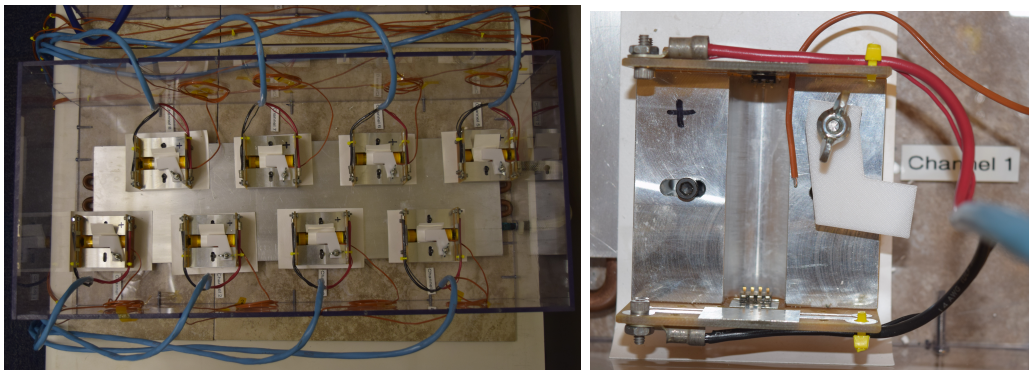


((a)) Test setup ((b)) Channel 1

Figure 4.2. Experimental setup

The MACCOR software is able to access the channels via electrical leads and the interface of the software allows to select a specific pod for a test procedure. A temperature sensor in every channel measures the ambient temperature regulated by a Polyscience Recirculator which is connected to a cold plate located underneath the channels.

For safety reasons and to enable stand-alone and unattended operation the box made out of polycarbonate is necessary to avoid safety issues caused by flames or escaping gas, for example. Additionally, the cells have to be stored during non-usage in metal storage lockers approved by Naval Postgraduate School (NPS). To prevent contact between cell electrodes during storage, the cells are arranged in parallel in a storage box as shown in Figure 4.3. Additional safety and handling guidelines for the exper-

imental setup and the testing of lithium ion batteries are provided in Appendix B.

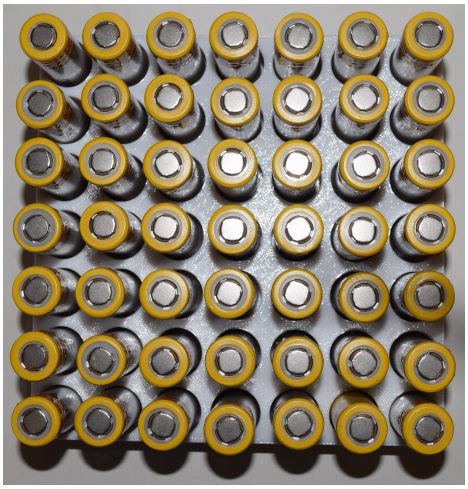

Figure 4.3. Storage of the battery cells

### 4.2.2 Test Procedures

The tests described in Section 4.1 are implemented in MACCOR. The test procedures have to be implemented in the MACCOR BuildTest Software to retrieve them in the MACCOR Software. As an example, the test procedure of the break-in test (see Subsection 4.1.1) is shown in Figures 4.4 and 4.5. The steps of the test are numbered and listed chronologically. Step 1 includes a safety section which provides an automatic switch to Step 25 if the voltage falls outside the approved range between 2V and 3.6V. This means that the test is ended prematurely. Additionally, the thermocouple of 30°C ends the test automatically if the temperature increases above 30°C. Step 2 is the alternating current impedance (AC Imp) test to ensure that the battery cell is correctly connected to the contact points of the battery cell test channels or to determine bad cells, which are not tested and used to verify the battery model. Afterwards, a discharge of the cell and another AC Imp test occur while giving the cells rest steps to ensure that the chemical reaction in each cell is completed before the next step in the test procedure starts. Steps 7 to 11 include the first cycle the cells traverse. A second cycle from Step 16 to 20 follows after another AC Imp test and rest steps. After these two cycles the break-in test is performed. The capacity

of the cell is extracted from the data. Additionally, the cells are charged to 3.3V in step 23 to achieve a safe storage voltage. Other procedures used to test the battery cells are shown in Appendix C.

Build Test - [C:\Maccor\Procedur\AK_Flight_breakin_ac_imp.000]

File Edit Options Window Help

Description

Breakin

| Step | Type | Mode | Value | Limit | Value | End Type | Op | Value | Goto | Report Type | Value | Options |
|---|---|---|---|---|---|---|---|---|---|---|---|---|
| 1 | Rest | | | | | Step Time | = | 00:00:05 | 002 | Step Time | 00:00:01 | ANNN |
| | | | | | | Voltage | >= | 3.601 | 025 | | | |
| | | | | | | Voltage | <= | 1.99 | 025 | | | |
| | | | | | | Thermocouple | >= | 1 / 30.0 | 025 | | | |
| 2 | AC Imp | Current | 1.1 | | | | | | | | | |
| 3 | Discharge | Current | 1.1 | Voltage | 2.0 | Voltage | <= | 2.0 | 004 | Step Time | 00:00:05 | 4NNN |
| 4 | Rest | | | | | Step Time | = | 00:01:00 | 005 | Step Time | 00:00:05 | 4NNN |
| 5 | AC Imp | Current | 1.1 | | | | | | | | | |
| 6 | Rest | | | | | Step Time | = | 00:01:00 | 007 | Step Time | 00:00:05 | ANNN |
| 7 | Charge | Current | 1.1 | Voltage | 3.6 | Voltage | >= | 3.6 | 008 | Step Time | 00:00:05 | 4NNN |
| 8 | Rest | | | | | Step Time | = | 00:01:00 | 009 | Step Time | 00:00:05 | 4NNN |
| 9 | AC Imp | Current | 1.1 | | | | | | | | | |
| 10 | Rest | | | | | Step Time | = | 00:01:00 | 011 | Step Time | 00:00:05 | ANNN |
| 11 | Discharge | Current | 1.1 | Voltage | 2.0 | Voltage | <= | 2.0 | 012 | Step Time | 00:00:05 | 4NNN |
| 12 | Advance Cycle | | | | | | | | | | | |
| 13 | Rest | | | | | Step Time | = | 00:05:00 | 014 | Step Time | 00:00:05 | 4NNN |
| 14 | AC Imp | Current | 1.1 | | | | | | | | | |
| 15 | Rest | | | | | Step Time | = | 00:01:00 | 016 | Step Time | 00:00:05 | 4NNN |

Figure 4.4. Break-in test sequence, Part 1

| | | | | | | | | | | | | |
|---|---|---|---|---|---|---|---|---|---|---|---|---|
| 16 | Charge | Current | 1.1 | Voltage | 3.6 | Voltage | >= | 3.6 | 017 | Step Time | 00:00:05 | 4NNN |
| 17 | Rest | | | | | Step Time | = | 00:01:00 | 018 | Step Time | 00:00:05 | 4NNN |
| 18 | AC Imp | Current | 1.1 | | | | | | | | | |
| 19 | Rest | | | | | Step Time | = | 00:01:00 | 020 | Step Time | 00:00:05 | ANNN |
| 20 | Discharge | Current | 1.1 | Voltage | 2.0 | Voltage | <= | 2.0 | 021 | Step Time | 00:00:05 | ANNN |
| 21 | Advance Cycle | | | | | | | | | | | |
| 22 | Rest | | | | | Step Time | = | 00:01:00 | 023 | Step Time | 00:00:05 | ANNN |
| 23 | Charge | Current | 1.1 | Voltage | 3.3 | Voltage | >= | 3.3 | 024 | Step Time | 00:00:05 | ANNN |
| 24 | AC Imp | Current | 1.1 | | | | | | | | | |
| 25 | End | | | | | | | | | | | |

Figure 4.5. Break-in test sequence, Part 2

### 4.2.3 Test Realisation

MACCOR is used to implement the tests of the lithium iron phosphate battery cell. The test software is able to retrieve the procedures of the BuildTest software, perform the tests, and view and store the measured data. Figure 4.6 shows the detailed screen as the main screen of MACCOR, the interface of the user and the hardware during a break-in test. The main screen constantly monitors the status of the test position in the system as the state. In Figure 4.6 the status of Channel 1 is active and the software is charging the battery cell in Channel 1 with a current of 1.1Amps as stated in Step 16 of the test procedure (see Figure 4.4). The detailed screen enables to start and stop the test for each channel with the buttons on the top and view the actual readings as shown on the right of Figure 4.6.

The interface is further segmented into the intermediate screen, the normal screen, the chart screen and the quick voltage screen. The intermediate screen shown in Figure A.1 in Appendix D displays the cycle number, test steps, current, voltage and other information in real-time readouts. The chart screen provides a test chart of experimental data based on user specifications. The real-time reading chart in Figure

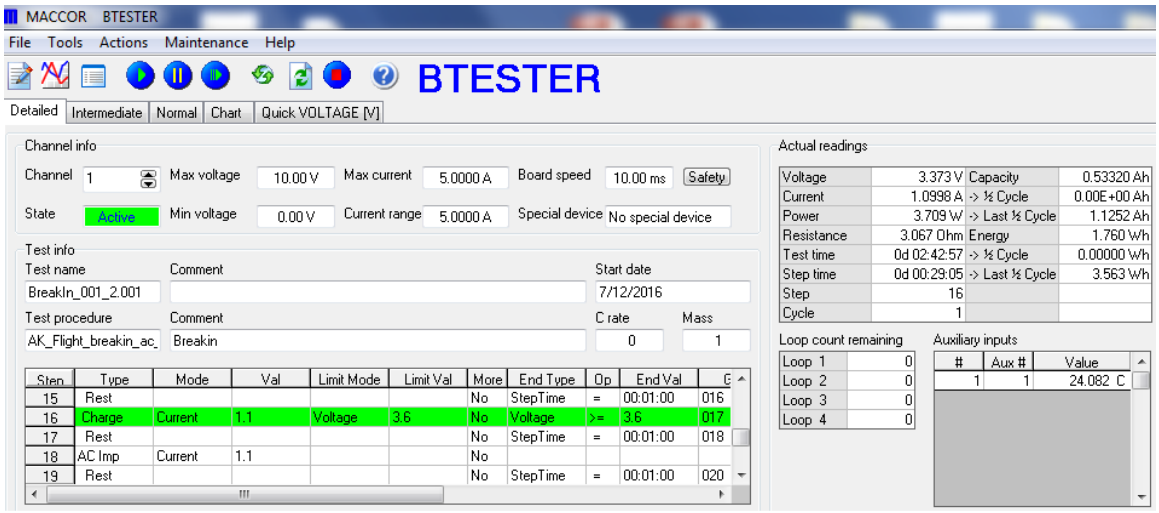


Figure 4.6. Detailed screen of MACCOR

A.2 in Appendix D is based on the voltage of all eight channels during the break-in test. The quick voltage screen (see Figure A.3 in Appendix D) shows the voltage of the active channels in real-time readings.

## 4.3 Experimental Data Analysis

The data collected in the described tests with MACCOR are presented in detail in this section with illustrating diagrams which were implemented in Matlab with exponential interpolation. The collected data stored in text files are converted to excel spreadsheets and read in the Matlab workspace to enable further processing.

### 4.3.1 Open Circuit Voltage

To examine if the main data which characterize the cells conform the data in the data sheet, the open circuit voltage is measured with a digital voltmeter. The OCV for each cell listed in Table A.1 in Appendix A.1 are between 3.2881V and 3.2928V with an average of 3.291006V. The data do not differ essentially on the nominal voltage of 3.3V in the data sheet.

### 4.3.2 Break-In

Figure 4.7 shows the break-in of Cell 001. The cell runs through two full cycles. At the first step in the test procedure the voltage of Cell 001 amounts 2.78V. After the cell is discharged to a voltage of 2V with a discharge rate of 1.1A the break-in starts with a charge and discharge rate of 1.1A to 3.6V and 2V. During this process, the voltage is increasing strongly at the beginning and the end of the charge and decreasing strongly at the beginning and the end of the discharge procedure. During the rest step between the two cycles the voltage of the cell strongly increases to an amount of 2.465V because the cell is recovering. This phenomenon is called voltage drift. At the AC Imp test, which occurs between the rest steps and before each charge or discharge, an AC Imp of 20m$\Omega$ is measured. In the third cycle, the cell is charged until the voltage achieves the safe storage voltage of 3.3V whereas the voltage decreases again during the rest step at the end of the procedure.

At the beginning and the end of the charging and discharging phases the voltage strongly increases or decreases. Most of the time, the charging or discharging voltage is stable with an averaged value of 3.363V for the charge and 3.165V for the discharge process. A flat charge or discharge curve signifies a constant voltage supply so that the power delivered by the cell is mostly steady. Low-power applications, which need a stable supply voltage during operation, and high-power applications, which need a stable supply voltage especially at the end of the discharge cycle [17], can be powered with cells exhibiting these discharge characteristics. A lower internal resistance of the cell results in a flatter charge and discharge curve.

The nominal voltage of 3.3V for the cell noted in the data sheet (see Table 4.1) cannot be achieved during the discharge process. The difference is caused by losses due to cell resistance and polarization of the active materials at the electrodes [17] as well as voltage drop caused by the product of the current and the internal resistance. Furthermore, the exhaustion of the active material in the cell effects a strong drop of the voltage at the end of the discharge.

### 4.3.3 Capacity

Table A.2 in Appendix A.2 shows the capacities of the cells at the end of the break-in test. These capacities vary between 1.1Ah and 1.14Ah with an averaged value of 1.1275Ah. This averaged capacity meets the nominal capacity in the data sheet of

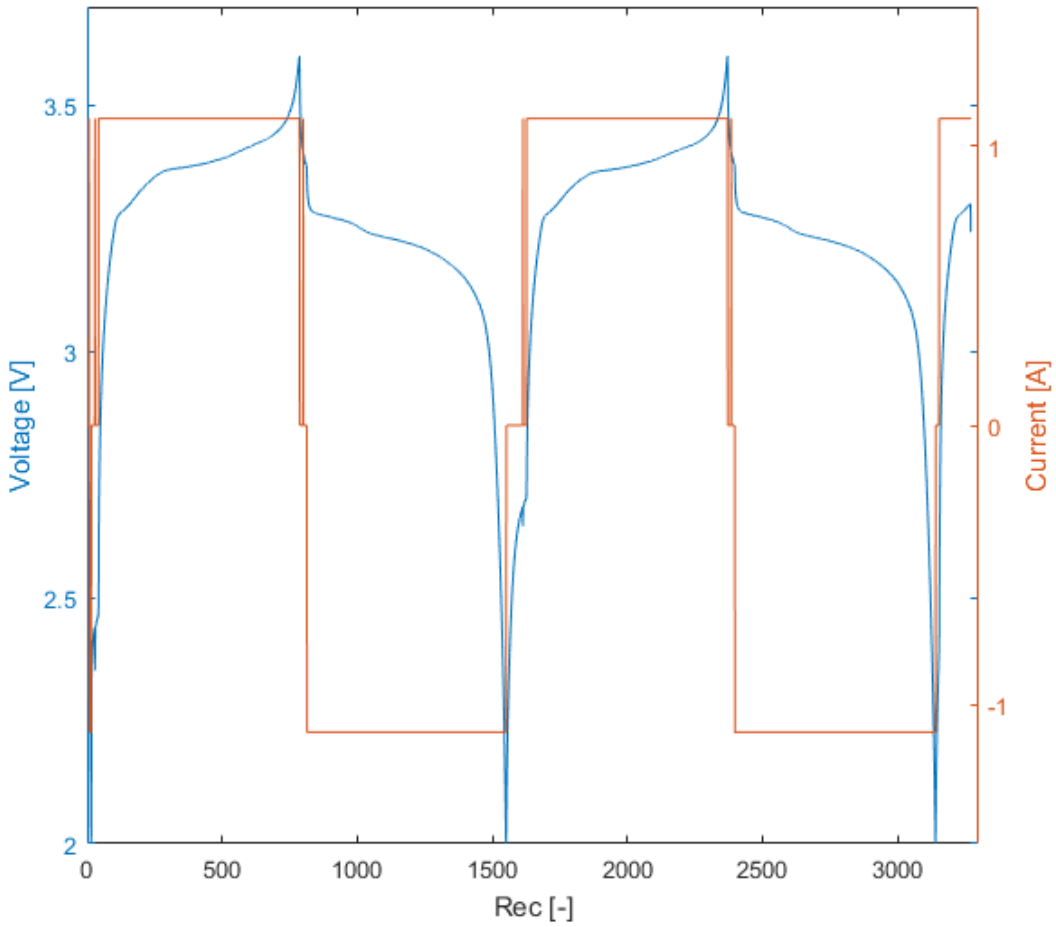


Figure 4.7. Break-in of Cell 001

the cell.

As explained in Section 4.1.1 the capacity of previous tested battery cells decreases after increasing slightly at the first cycles. Figure 4.8 shows the averaged charge capacities of the cells during the first cycles at break-in and rate variation test of the lithium iron phosphate battery cell. The trend of an increase of the capacity during the first cycles is not determined. The capacity stays at 1.1Ah with minimal deviations as listed in Table A.3 in Appendix A.3.

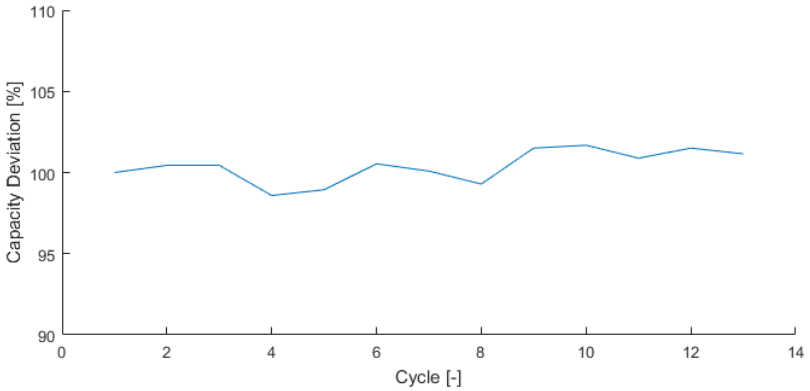

Figure 4.8. Averaged capacities for the first cycles

### 4.3.4 AC Impedance

The lithium iron phosphate battery cell has an averaged internal resistance of 20.9m Ω for values between 18.16mΩ and 33.5mΩ like shown in Table A.4 in Appendix E. This is a low internal resistance compared to other battery cells (AC Imp of $LiCoO_2$ = 60mΩ [7]). The measured data do not meet exactly the AC Imp in the data sheet (see Table 4.1) because of the additional impedances of the electrical leads in the test setup. The low AC Imp of the lithium iron phosphate battery cell results in a particularly stable charge and discharge curve and enables safe cell performances at high charge and discharge rates.
Cell 017 was detected as a bad cell during the test because its AC Imp was higher than average with a value of 50.40mΩ. This cell was excluded from further experimental tests.

### 4.3.5 Discharge Capacity and Watt Hour Efficiency

Figure 4.9 shows the discharge curve of the cells at three different temperatures (30°C, 10°C and 5°C). As mentioned, the cells are discharged primarily with a constant discharge voltage and at the end of the discharge process the voltage decreases strongly. The plotted data show the dependence of the capacity on the temperature. The lower the temperature the lower the capacity at a given value of discharge voltage. This means that the capacity at the end of the discharge is lower at low temperatures than at higher temperatures. Additionally, this results in a faster discharge and faster charge of the cells as shown in Figure 4.10. In this figure the capacity is plotted over

Table 4.2. Watt hour efficiency

| Temperature [°C] | Watt hour efficiency [-] | Rel. watt hour efficiency [%] |
|---|---|---|
| 30 | 0.936815 | 93.6815 |
| 10 | 0.964089 | 96.408 |
| 5 | 0.921754 | 92.1754 |

the recorded data. The capacity loss from 30°C to 5°C is 13.24% for the discharge process and 18.14% for the charge process. These capacity losses are low in comparison with other lithium ion battery cells [17]. Figure 4.11 shows the voltage during the discharge and the charge of the cell at different temperatures. This diagram shows the recovery of the cell during the discharge and charge processes. The lower the temperature the better the recovery of the cell and the higher the starting voltage of the following charge process.

The averaged relative watt hour efficiencies at three different temperatures are listed in Table 4.2. A dependence on the temperature is not identifiably. However the relative efficiency is lower than 100% because of losses in charge caused by secondary reactions in the cell like electrolysis of water or other redox reactions of the active material [17].

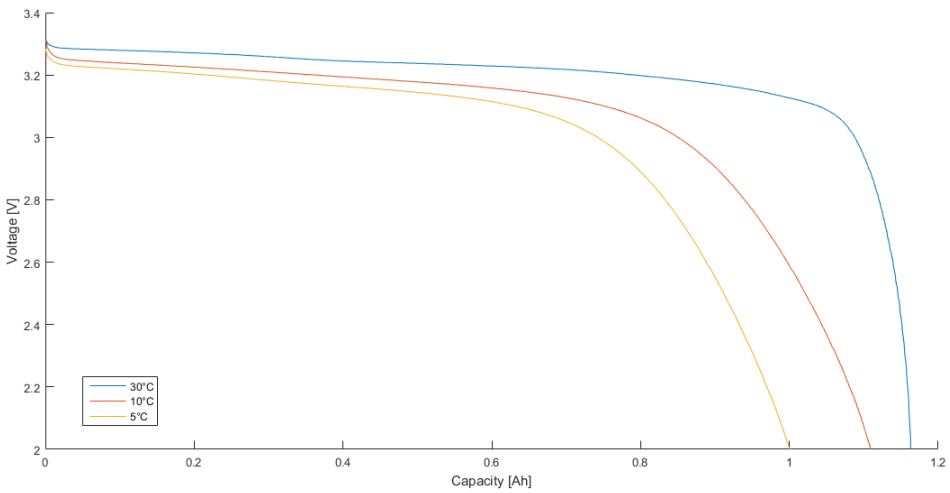


Figure 4.9. Discharge capacity at different temperatures, Part 1

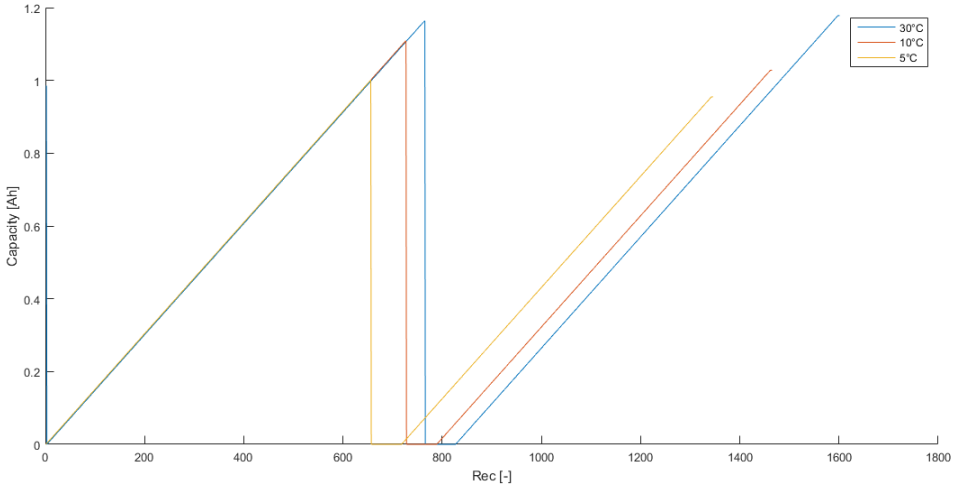


Figure 4.10. Discharge capacity at different temperatures, Part 2

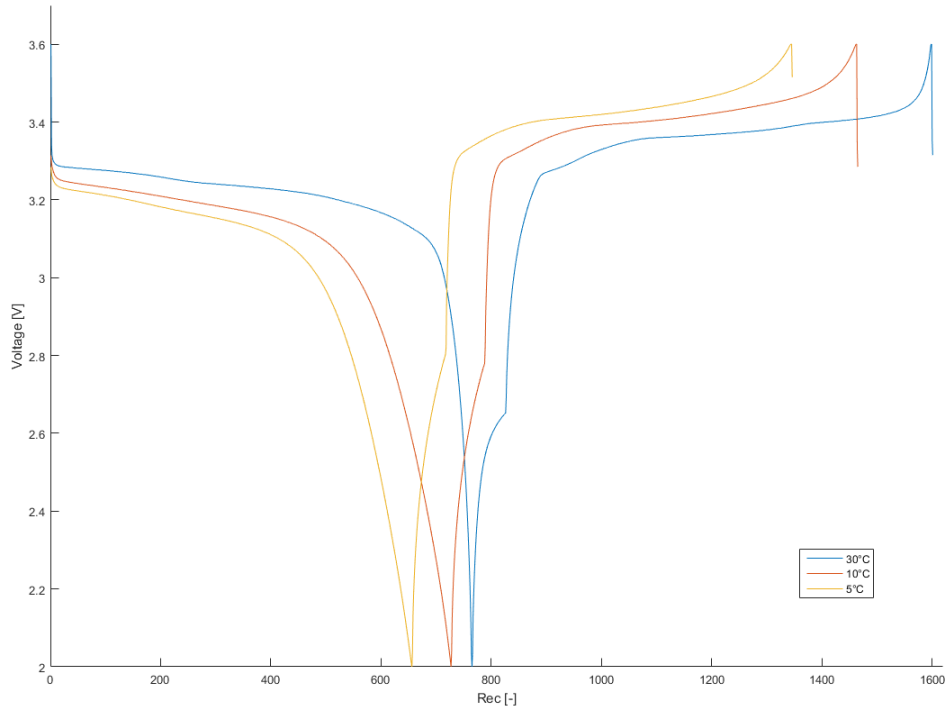


Figure 4.11. Discharge and charge voltage at different temperatures

### 4.3.6 Rate Variation

As mentioned in Chapter 2, the capacity of a cell decreases with increasing discharge current. Figure 4.12 shows the decreasing tendency of the capacity of the cells at higher discharge rates. Figure 4.13 shows the recovery of the voltage of the cells during the rest step of five minutes after the discharge at different discharge rates. The higher the discharge rate, the faster the cell is recovered. This results in a higher start voltage of the next cycle. Additionally these collected data are used to evaluate the Matlab Simulink Model presented in Chapter 5.

### 4.3.7 Temperature Variation

Figure 4.14 shows the dependence of the capacity of the cells on the temperature via discharge curves. The lower the temperature, the lower the capacity of the cell

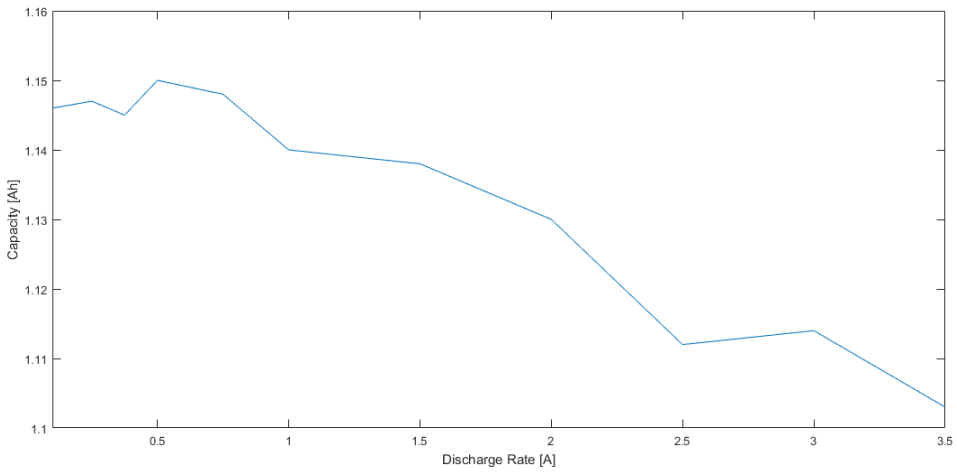


Figure 4.12. Discharge capacity at different discharge rates

and consequentially, the lower the temperature the less time is needed to charge and discharge the cell. Additionally, the resulting lower capacity at lower temperature is displayed in Figure 4.10. The collected data of this test are used to evaluate the Matlab Simulink model presented in Chapter 5.

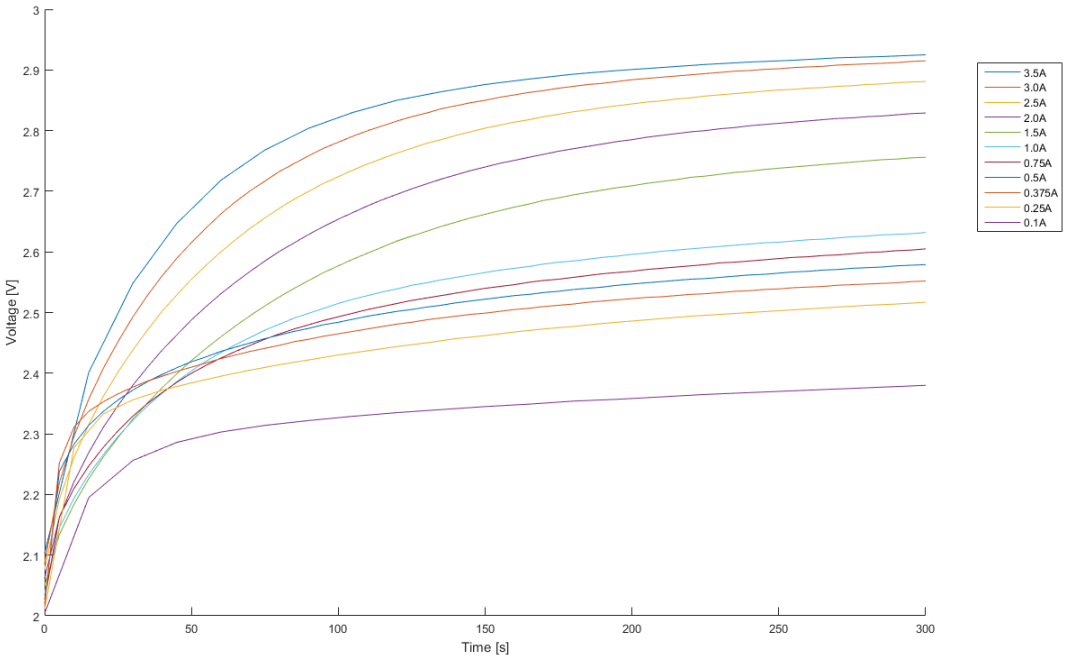


Figure 4.13. Voltage drift during the rest step after discharge at different discharge rates

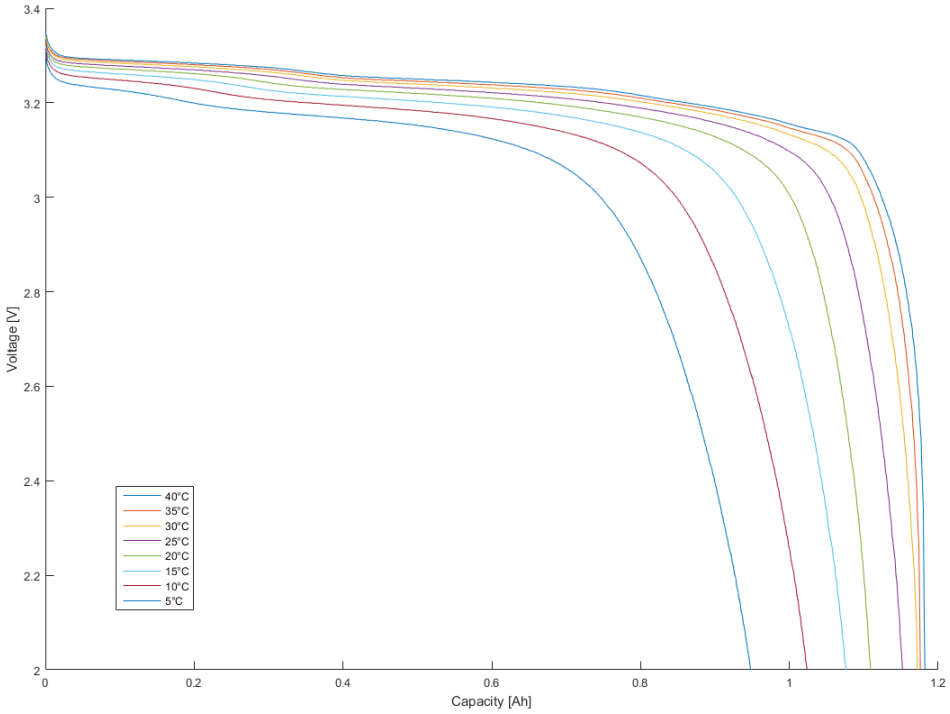


Figure 4.14. Discharge capacity at different temperatures

THIS PAGE INTENTIONALLY LEFT BLANK

# CHAPTER 5:
# Simulink Model

This chapter deals with the function of the model designed to simulate the operation of the power system of NPSAT1. The model is implemented in Matlab Simulink and reflects the real-life behaviour of the satellite's power system.
A model is a very important part of technology development. Simulated tests with a model may simplify the component selection and reduce the amount of physical testing. Therefore, these model-based tests increase the efficiency and effectiveness of the development process and help to reduce development costs.
In this work, a new battery technology for the NPSAT1 is tested to determine if it is more effective than the currently used one. To identify if the battery cell works acceptably in the respective application under certain conditions, it is necessary to perform tests with a model. The model considered is a Matlab Simulink model of the satellite power system including the solar panels, the power-supplied subsystems and the battery.

## 5.1 Model Implementation

Figure 5.1 shows the Simulink model of the power supply system of NPSAT1. In general, it is divided into three main parts: the solar panel input (red box), the duty cycle of the spacecraft (yellow box) and the battery calculation portion (blue box). The following sections focus on these parts and the function and operation of each section is explained.

### 5.1.1 Solar Panel Input

The solar panel input (red box) located at the top left in Figure 5.1 is shown in detail in Figure 5.2. The electrical power provided by the solar panels is used to power experiments which are carried out onboard during the operation and to charge the battery. During operation, the satellite orbits around the earth and the angle the sun strikes the solar panels is changing constantly. Due to this change, the effective

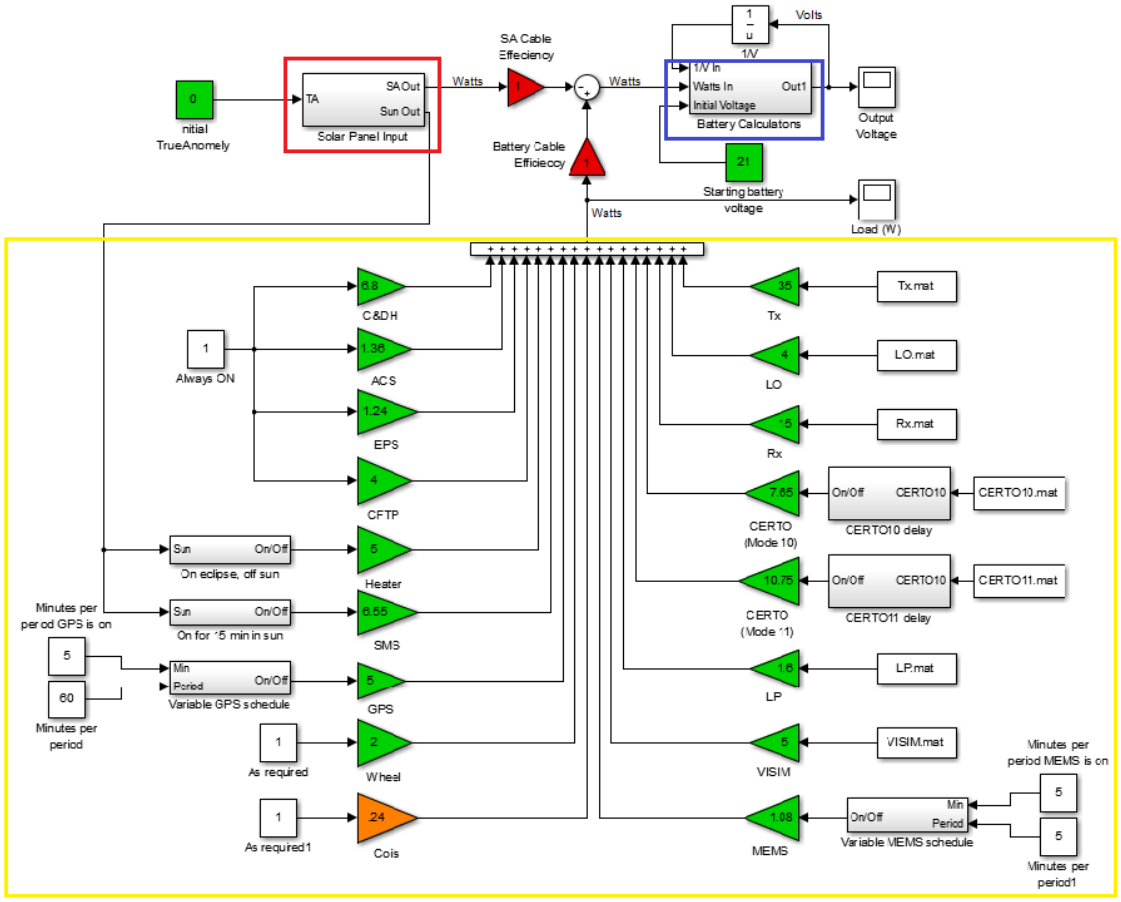


Figure 5.1. NPSAT1 power supply system model

surface of the panel and consequently the produced power, varies.

The main source of data for the solar panel in the model is a Matlab file called "solar_power_per angle.m." This file determines that the described model is referring to a spacecraft-centered coordinate system for all calculations. The fact that the position of the satellite is always constant in this coordinate system and the sun, therefore, orbits around the spacecraft, facilitates the varying power calculations. Furthermore, the file contains model constants of the solar panel to calculate the total generated power; this calculation occurs every 0.5 degree the sun orbits around the satellite. The orbit altitude output of the m-file is the input for the model part to calculate the orbital period. Additionally, the user has to define the spacecraft's true anomaly to determine where the sun starts in its orbit around the spacecraft. The third input is the simulation time. These three inputs are used to determine the

current orbit angle between 0 and 360 degrees.

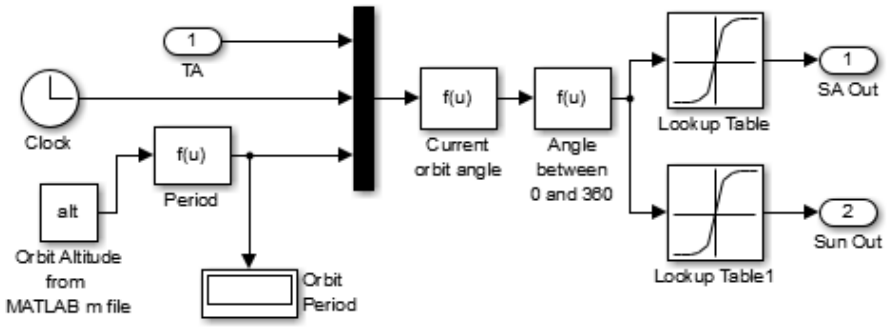


Figure 5.2. Solar panel model

The determined orbit angle is the input for two lookup tables which are populated by executing the m-file. One of the tables outputs the total power generated by the solar panels and the other outputs a 1 or a 0 depending if the solar panel is in sunlight or in eclipse respectively.

To determine the effective surface area of the solar panel at a given angle, Formula 5.1 is used. It is a transformation which allows calculation of the $\beta$ angle for each face of the spacecraft for a given $\Delta A_Z$. For better comprehension, the relations of the angles are shown in Figure 5.3. To simplify the schematic, the NPSAT1 is reduced to eight sites.

$$cos(\beta) = cos(\gamma)cos(\beta'_S) + sin(\gamma)sin(\beta'_S)cos(\Delta A_Z) \tag{5.1}$$

| | | |
|---|---|---|
| $\beta$ | = | Angle between the normal vector n of the solar panel surface and the sun [°] |
| $\gamma$ | = | Angle between the normal vector n of the solar panel surface and the orbit pole [°] |
| $\beta'_S$ | = | Complement of the angle between the sun and the orbit plane of the NPSAT1 [°] |
| $\Delta A_Z$ | = | Angle as the sun orbits around the spacecraft [°] |

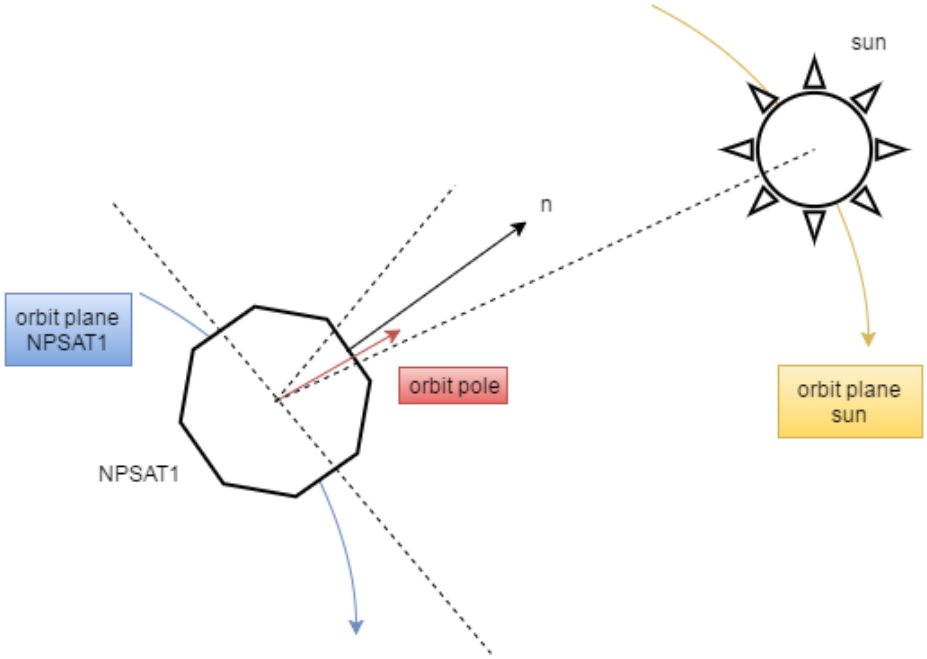


Figure 5.3. Simplified schematic of the sun orbiting the NPSAT1

The NPSAT1 is a twelve sided spacecraft. There are twelve $\gamma$ angles with 30 degree increments. Due to the fact that the leading portion of the spacecraft is an edge, the resulting eleven $\gamma$ angles are 15°, 45°, 75°, 105°, 135°, 165°, 195°, 225°, 285°, 315°and 345°. The results of the calculation are stored in a matrix.

The two times the sun is not striking the surface of the solar panels occur when the spacecraft is in eclipse and when the sun is shining on the back of the solar panel. The former is determined by the Inequality 5.2 whose result is stored in the variable "SUN". If the result of Inequality 5.2 is true, the spacecraft is in eclipse and the value 0 is stored for the $\Delta A_Z$ angle calculation. Likewise if it is false the spacecraft is in sunlight and the value 1 is stored.

$$sin(\Delta A_Z) > sin(A_Z - cos^{-1}(\frac{cos(\beta)}{sin(\beta'_S)})) \tag{5.2}$$

The effective surface area of the solar panel defines the amount of power produced by the panel. The following criteria are used to calculate the cosine of $\beta$ for every side of the spacecraft. Previous experiments resulted in a proportional decrease of the effective surface area due to the reduction of $\beta$ from 70° to 0°. Angles from 70°

to 80° sustain an additional degradation of produced power, which increases linearly for every degree. Angles from 80° to 90° show a zero power output. At angles greater than 90°, which occur when the sun is not shining on the panel, the power output is zero as well. If a $\beta$ angle greater than 80° occurs, the cosine value is set to 0. If a $\beta$ angle greater than 70° occurs, the cosine value is degraded by the degradation factor. Otherwise, if the angle is between 0° and 70°, the calculated cosine of the $\beta$ angle is left as the cosine value.
When the sun is shining at the back of the spacecraft, the $\beta$ angle is greater than 80° so that the power output is zero due to the fact that the cosine value is set to 0. There is no additional determination for this occurrence because it is already considered.
In the next step, the sum of the described cosine values is multiplied by the surface area of the panels and the effective surface area of the solar panels is produced. To determine the actual power produced by this area the value has to be multiplied by the solar constant and the solar panel efficiency. Additionally, it is multiplied by the "SUN" variable and the result of zero power output occurs if the spacecraft is in eclipse. Otherwise the result is the total power produced by the solar panels for a given $\Delta A_Z$ angle. The total power, $\Delta A_Z$ angle and the "SUN" variable are stored in a matrix to provide access to the previously mentioned lookup tables for further considerations.

### 5.1.2 Duty Cycle of the Spacecraft

The power requirements of the spacecraft depend on the selection and the amount of the components needed to be powered on. Therefore, each component has its own individual input as shown in Figure 5.1 marked by the yellow box. The inputs are implemented as gain blocks as shown in Figure 5.4, for example. The value of the gain block, located in the middle of the triangle, defines the component's corresponding power requirement in watts. The input of the gain block depends on the scheduling category, so that components which are always on receive the constant value input of 1 as shown in Figure 5.1 for the Attitude Control System ACS gain block, for example. The product of this value and the component wattage is the output of the considered component. Components like the wheels, as shown in Figure 5.1 at the lower left, which are scheduled manually are controlled by the Satellite Tool Kit STK. The output of the STK is converted to a Matlab file which inputs a 0 or a

1 respectively to the gain block depending on whether the component is off or on at a given time. Likewise the output of the gain block is the required power of the component in watts for a given time. Components powered for a certain time period are controlled by a function block as shown in Figure 5.1 for the GPS gain block. The input to the gain block is provided by the simulation of 0 or 1 through a function block which operates by a given time interval.

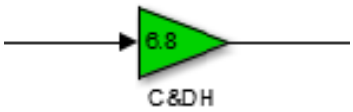


Figure 5.4. Gain block of the command and data handler

All outputs of the power-required components are joined together in an addition block. This block sums the total power requirement for the spacecraft and outputs the wattage at a certain moment in time which is the input for the addition block with the solar panel input.

### 5.1.3 Battery Calculations

The power for the components of the spacecraft are provided first by the solar panel and when needed, by the battery. The excess of power produced by the solar panel is used to charge the battery. Therefore, at times when the solar panel is not able to provide the required power, the battery is also used to power the components.
The output from the solar panel power and the component power requirement are combined by an addition block displayed at the center on top of Figure 5.1. The output of this block provides the information if the battery is currently charging or discharging by being a negative or positive value respectively. Charging of the battery implies that the solar panels produce more energy than needed by the components whereby discharging implies that the battery has to contribute to supplying power.
The positive or negative power output of the addition block is sent to a multiplying block as shown in Figure 5.5. This block multiplies the power in watts and the reciprocal of the battery voltage in volts and outputs the current in amps. This

output is processed by the equation shown in Formula 5.3. The derived values of $\alpha$ and $\beta$ are stored in lookup tables.

$$SOD[i(t), T(t), t] = \frac{1}{Q} \cdot \int_0^t (\alpha[i(t)] \cdot \beta[T(t)] \cdot i(t))dt \tag{5.3}$$

| | | |
|---|---|---|
| $\alpha$ | = | Rate factor [-] |
| $\beta$ | = | Temperature factor [-] |
| i | = | Current [Amps] |
| t | = | Time [s] |
| T | = | Temperature [°C] |
| Q | = | Charge quantity [As] |

In the next step, the current, the $\alpha$ and the $\beta$ values presented in detail in Section 5.1.4, are multiplied to yield an instantaneous current for a given moment in time. After integration, which outputs the capacity in ampere-seconds, a divide by the charge quantity follows. The output is the SOD of the battery. By definition, an SOD of zero signifies a completely discharged battery and an SOD of one signifies a fully charged battery.
Furthermore, the SOD of the battery is part of a sum which compensates the equilibrium potential variation $\nu$ caused by temperature changes. The considered equation is represented in Formula 5.4.

$$\nu[i(t), T(t), t] = \sum\nolimits_{k=0}^{n} c_k \cdot SOD^k[i(t), T(t), t] + \Delta E(T) \tag{5.4}$$

| | | |
|---|---|---|
| $\nu$ | = | Equilibrium potential variation [V] |
| c | = | Number of cells [-] |
| $\Delta E(T)$ | = | Temperature correction term [-] |

In this model the summation is considered in an additional lookup table. The addition of the $\Delta E(T)$ stored in the $\Delta E(T)$ lookup table occurs in the addition block at the right of Figure 5.5. The determination of $\Delta E(T)$ is explained in detail in Section 5.1.5. The output of the described block is multiplied by the number of cells in series used in the battery and the output occurs as the battery voltage as a slope throughout the duration of the simulation. The ambient temperature is set by entering the value

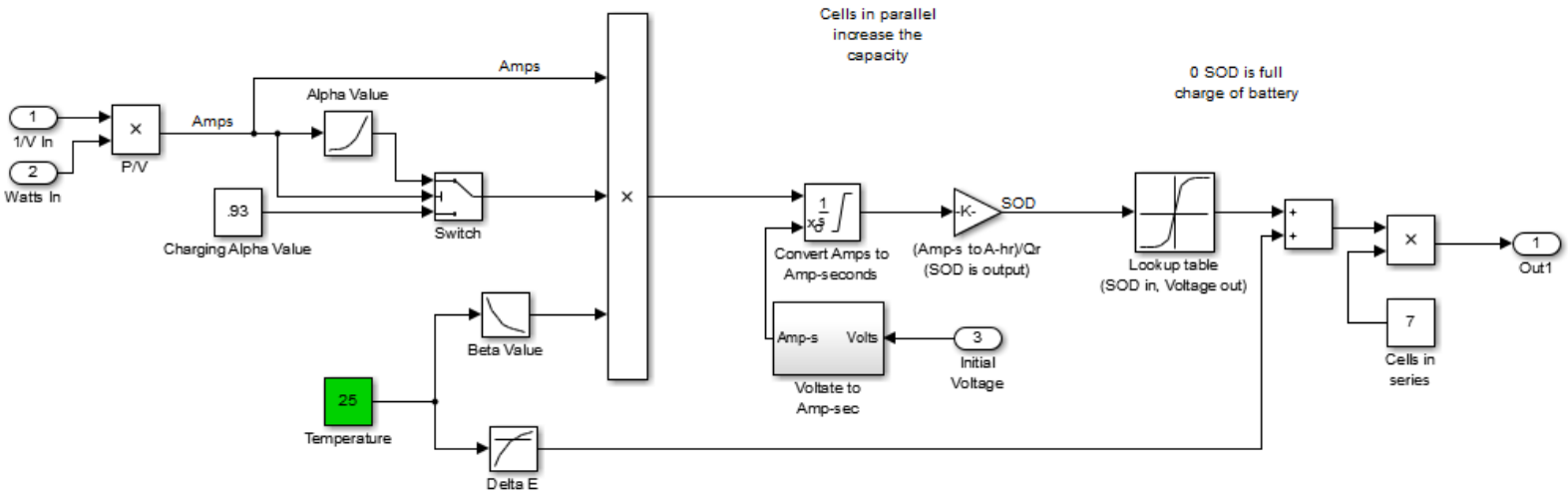


Figure 5.5. Battery calculations

in °C in the green block labeled "Temperature" at the lower left of Figure 5.5.
In case the battery is not fully charged at the beginning of the simulation, there are certain provisions for a starting voltage input for the model as shown in Figure 5.6, a detailed display of the voltage to amps transformation block in Figure 5.5. The first step is to divide the starting voltage by the number of cells in series because the data in the lookup tables are referring to one individual cell. The output of the division is the voltage adjusted to one cell and the input for a lookup table. The output of this lookup table is the current SOD based on the cell voltage which is multiplied by the battery capacity $Q_r$ to convert the value of the SOD to the current ampere-hour of the battery. In order to complete this block, the value is converted to amps and finally becomes the input value for the integral at the center of Figure 5.5. The main cause of the transformation block shown in Figure 5.6 is to ensure that all calculations during the simulation begin with the present SOD of the battery.

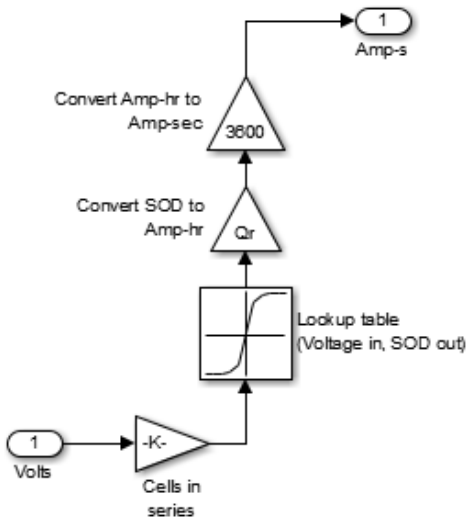


Figure 5.6. Block to transform voltage to ampere-seconds

### 5.1.4 Determination of $\alpha$ and $\beta$ Values

The first step of the calculation of $\alpha$ and $\beta$ values is to define a reference rate and reference temperature close to the expected median operating current or tempera-

ture respectively. In this model the reference rate is 0.375Amps and the reference temperature is 25°C.

### $\alpha$ Value

$\alpha$ is the rate factor needed to compensate for the differences in discharge curves. $\alpha$ is determined by recording discharge curves of one cell for different discharge rates and one charge rate implemented in the rate variation test presented in Section 4.1.3. At the specific time intervals of 5s and 10s for higher or 15s for lower discharge rates data is collected and stored in an excel spreadsheet. Additionally, a polynomial for each rate is defined which fits the generated discharge curve and a lookup table with data points is generated. To determine the $\alpha$ value Formula 5.5 is used.

$$\alpha(i) = \frac{a}{b} \tag{5.5}$$

The a and b values in Table 5.1 are determined by normalizing the SOD for all rates to the SOD of the reference rate. This is implemented by dividing the current ampere-hour value of a given rate by the maximum ampere-hour value of the reference curve. Additionally, the reference curve has to be shifted so that the starting voltage of the curve is equal to the desired starting voltage of the $\alpha$ value. This is implemented by adding the initial voltage difference between the given rate and the reference rate to all values on the given rates. Finally the alpha values are represented in Figure 5.7 as a function of the rate.

Table 5.1. $\alpha$ value determination

| Rate [amps] | a | b | $\alpha$ |
|---|---|---|---|
| 0.100 | 0.99825 | 1.03870 | 0.96106 |
| 0.250 | 0.99825 | 1.00208 | 0.99618 |
| 0.375 | 1.00000 | 1.00000 | 1.00000 |
| 0.500 | 0.99825 | 1.00437 | 0.99391 |
| 0.750 | 0.99825 | 1.00262 | 0.99564 |
| 1.000 | 0.99825 | 0.99563 | 1.00263 |
| 1.500 | 0.99825 | 0.99389 | 1.00439 |
| 2.000 | 0.99825 | 0.98690 | 1.01150 |
| 2.500 | 0.99825 | 0.97991 | 1.01872 |
| 3.000 | 0.99825 | 0.97293 | 1.02603 |
| 3.500 | 0.99825 | 0.96332 | 1.03626 |

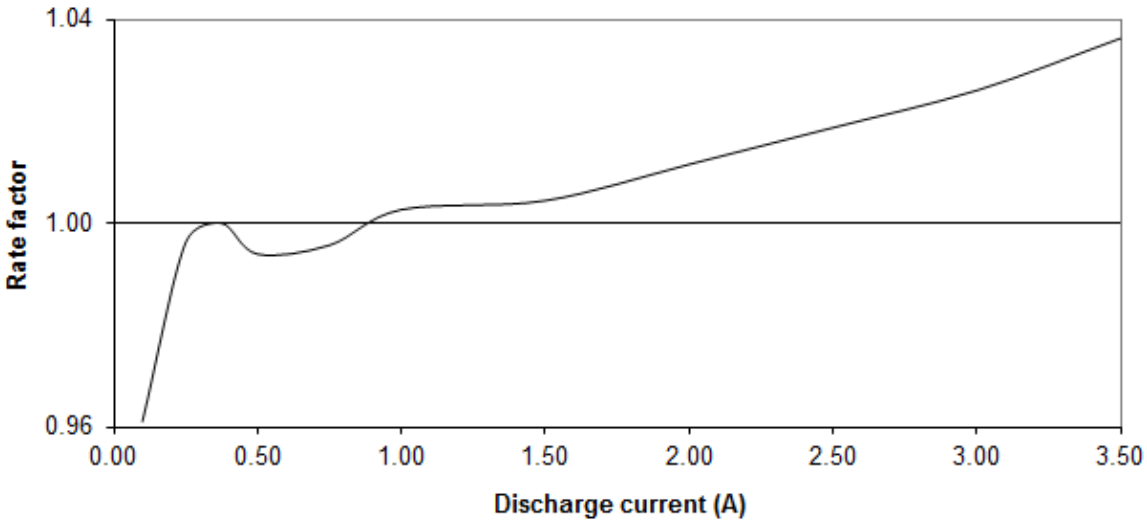


Figure 5.7. Rate factor values

**$\beta$ Value**

$\beta$ is the temperature factor needed to compensate for the differences in discharge curves at different temperatures. It is determined by recording discharge curves of one cell for different temperatures along with the reference rate implemented in the temperature variation test presented in Section 4.1.4. The data from the curves are

Table 5.2. $\beta$ value determination

| Temperature [°C] | c | d | $\beta$ |
|---|---|---|---|
| 5 | 0.97654 | 0.74633 | 1.30845 |
| 10 | 0.98534 | 0.84311 | 1.16870 |
| 15 | 0.99267 | 0.91202 | 1.08842 |
| 20 | 0.99560 | 0.96628 | 1.03035 |
| 25 | 1.00000 | 1.00000 | 1.00000 |
| 30 | 1.00293 | 1.02639 | 0.97714 |
| 35 | 1.00585 | 1.04399 | 0.96347 |
| 40 | 1.00585 | 1.05572 | 0.95277 |

graphed and listed in a lookup table. To determine the $\beta$ value for a given rate, Formula 5.6 is used.

$$\beta(T) = \frac{c}{d} \tag{5.6}$$

The c and d values shown in Table 5.2 are determined by normalizing the SOD for all temperatures to the SOD of the reference temperature and adding the initial voltage difference between the given temperature and the reference temperature to all values at the given temperature. Due to this procedure the reference curve is shifted and the starting voltage is equal to the desired starting voltage of the $\beta$ value. The result is shown in Figure 5.8.

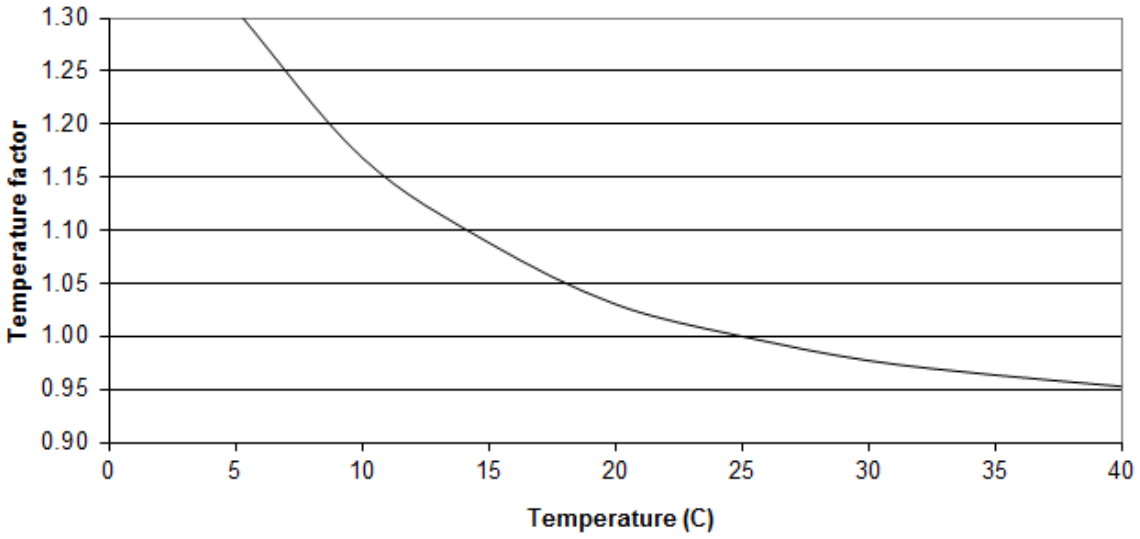


Figure 5.8. Temperature factor values

### 5.1.5 Determination of $\Delta E(T)$ Values

$\Delta E(T)$ is the temperature correction term used to compensate the differences between initial voltages at different temperatures. The $\Delta E(T)$ values for a given rate are determined by using the same discharge curves as used for the beta value determination. The calculation is implemented by an excel spreadsheet subtracting the initial voltage for each temperature from the initial voltage of the reference temperature. Additionally, the data shown in Table 5.3 are used to produce the graph in Figure 5.9 which shows a trend line for the calculated data.

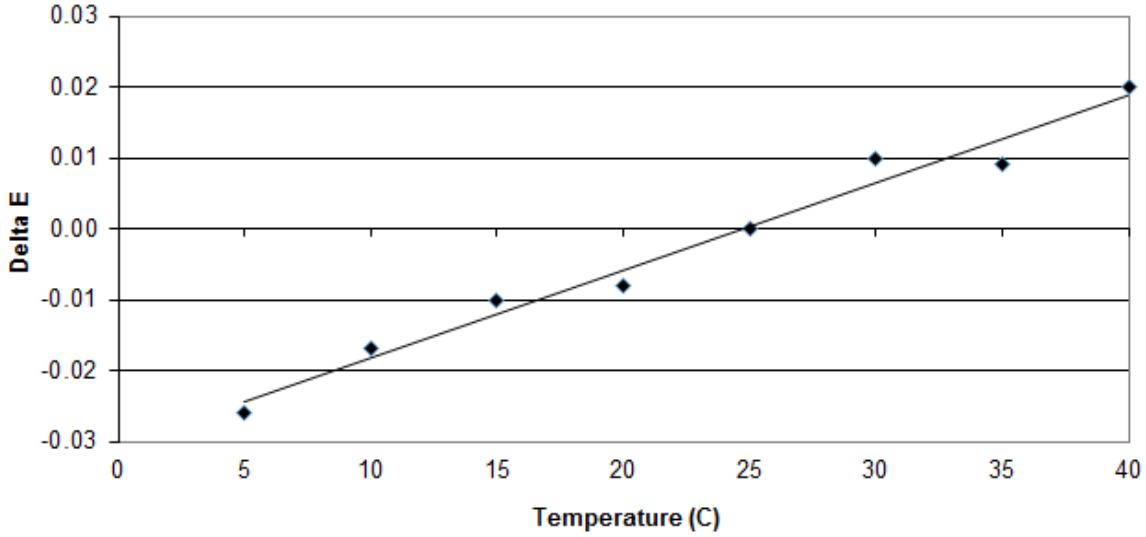


Figure 5.9. Temperature correction term values

Table 5.3. $\Delta E(T)$ value determination

| Temperature [°C] | Start Voltage [V] | $\Delta E$ |
|---|---|---|
| 5 | 3.30600 | -0.02600 |
| 10 | 3.31500 | -0.01700 |
| 15 | 3.32200 | -0.01000 |
| 20 | 3.32400 | -0.00800 |
| 25 | 3.33200 | 0.00000 |
| 30 | 3.34200 | 0.01000 |
| 35 | 3.34100 | 0.00900 |
| 40 | 3.35200 | 0.02000 |

## 5.2 Simulation Result

This section deals with the result of the NPSAT1 power supply model by using the previously collected data as parameters. First the parameter configuration in the simulation model is explained to enable to run the simulation. Additionally, the result of the simulation is presented and its significance is analyzed.

### 5.2.1 Parameter Configuration

To run the simulation the Matlab file "solar_panel_per_angle.m" has to be opened. In addition to the solar panel characteristics the battery parameters are programmed in this file. For the simulation of the battery containing lithium iron phosphate battery cells, the cell capacity is defined as 1.1Ah and the number of cells in series in a string is defined as 7. Additionally, the number of cells in parallel is set to 7. After running the file, the Matlab workspace is filled with variables for the simulation model. The simulation model "NPSAT1_model" is opened in Matlab Simulink and the "Starting battery voltage" has to be changed to 23.1V for the lithium iron phosphate battery cell simulation. This value is the result of the summation of seven voltages of 3.3V in series. The $\alpha$, $\beta$ and $\Delta$E(T) values are input in the battery calculations by opening each block and filling the table data with the calculated data. Additionally, the battery temperature can be varied by setting the temperature input. A timeframe of 604800s (seven days) for the simulation is defined.

### 5.2.2 Simulation Data Analysis

After setting the required model parameters, the simulation is started. The output of the simulation is the battery voltage as it cycles through the entire simulation timeframe at a temperature of 25°C. The data are stored in a matrix and plotted as shown in Figure 5.10. The plot starts at a battery voltage of 23.1V as defined in the simulation model. While running through three cycles the voltage slightly increases with the lowest battery voltage of 23.925V at the first discharge. Afterwards, the battery mainly cycles between a voltage of 3.758V and 3.184V. During three time periods the battery voltage decreases to 23.170 during discharge.

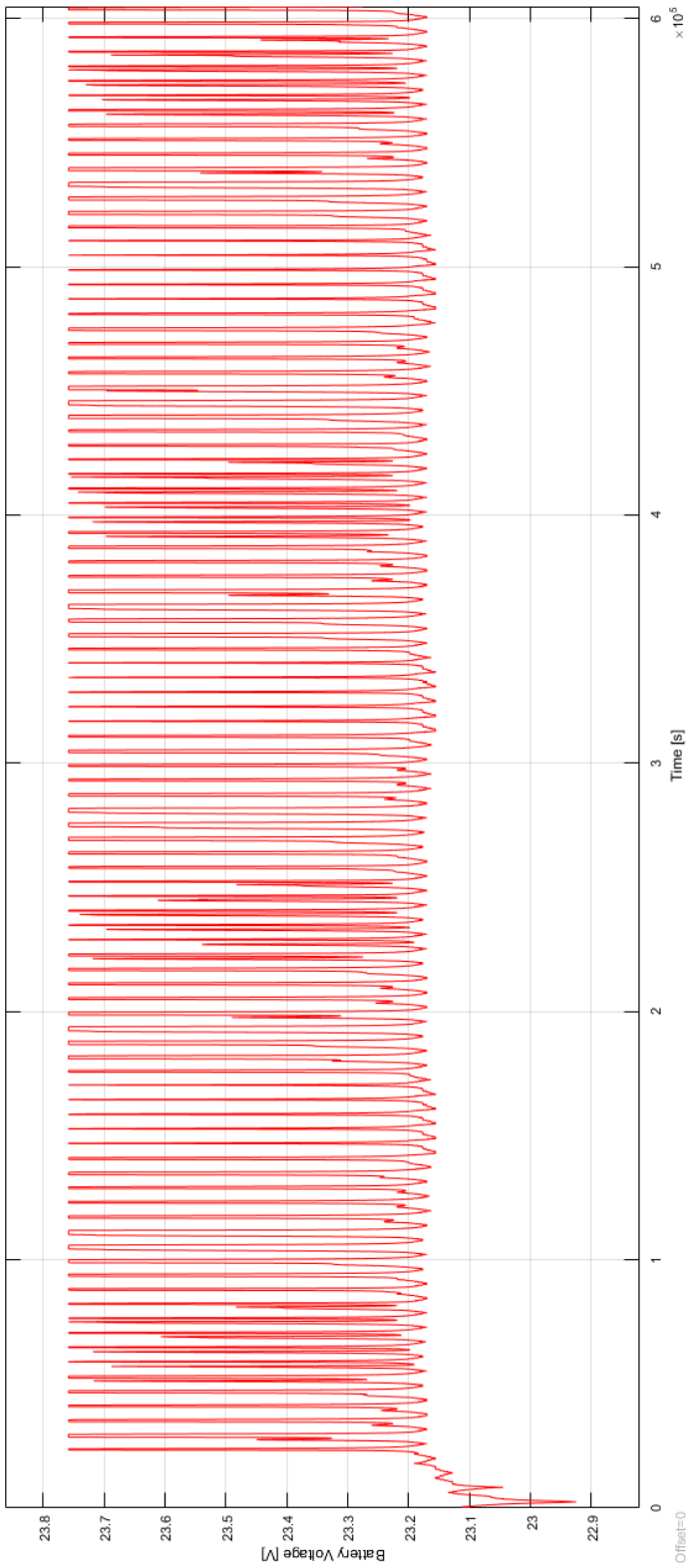


Figure 5.10. Simulation result

THIS PAGE INTENTIONALLY LEFT BLANK

# CHAPTER 6:
# Conclusion

This thesis deals with an investigation if the lithium iron phosphate battery cell APR18650M1 of A123 Systems is suitable for satellite systems of the Space Systems Academic Group of NPS. The lithium iron phosphate battery cell tested in this research is a lithium ion battery cell with ordinary characteristics and performances. In comparison with other lithium ion battery cells the nominal voltage and the nominal capacity of the tested cell is not high. Additionally, the energy density of the lithium iron phosphate battery cell is at the lower range of comparable lithium iron battery cells.

However, lithium iron phosphate battery cells have a large number of advantages. The cathode material, which contributes greatly to the improvement of battery cells, is environmental friendly and has an orthorhombic crystal structure. This structure offers great safety by means of high robustness and good thermal stability. Synthesized materials which are inexpensive and easily available are used to obtain lithium iron phosphate so that the overall cost of lithium iron phosphate battery cells are low in comparison with other lithium ion battery cells.

The tests indicate that the battery cell shows good performance by offering a constant voltage during the discharge process. Furthermore, a good recovery of the cell voltage during rest phases is identified. The capacity loss of the cell depends on the operation temperature and is low in comparison with other lithium ion battery cells. The AC impedance measured is outstandingly low for a battery cell. This enables to charge and discharge the cell with high rates without an increase in temperature. Due to this fact, the lithium iron phosphate battery cells have an innovative potential with regard to safety.

The Matlab Simulink model tested with the collected data results in a good battery performance without limitations for the power supply system of the satellite. Due to this fact and the cell characteristics, the lithium iron phosphate battery cell can be suggested for use in further space systems provided that additional tests show equal results.

THIS PAGE INTENTIONALLY LEFT BLANK

# CHAPTER 7:
# Outlook

This thesis helps to demonstrate if lithium iron phosphate battery cells are useful for power supply systems of space satellite systems. Additional tests explained in Appendix A should be performed to determine more specific cell characteristics. Furthermore, a lifetime test of the cells to evaluate the cycle life would contribute to decide if the cell is useful for space satellite systems.
Because of the low capacity and low nominal voltage in comparison with other lithium ion battery cells the Matlab Simulink model can be used to simulate a battery consisting of more than 49 cells. Although, the available space for the battery and the safety of the battery has to be considered in this case.

THIS PAGE INTENTIONALLY LEFT BLANK

# APPENDIX: Appendix

THIS PAGE INTENTIONALLY LEFT BLANK

# APPENDIX A:
# Additional tests

This chapter provides additional test procedures to determine the performance of the A123 Systems' lithium iron phosphate battery cell.

## A.1 Open Circuit Voltage Decay

The open circuit voltage decay (OCVD) test is done while the cells are charging or discharging at specific charge intervals. These intervals are based on the SOC so that at a SOC of 25%, 50% and 75% the rate of decay is observed for 20 seconds while the cell is disconnected from the external power supply. Figure A.1 (a) [11] shows a quantitative illustration of the open circuit voltage decays of four different cell types. Five seconds after starting the measurement the open circuit is achieved and the voltage decreases. The slope of the decay depends on the characteristic of the examined cell. Cell D in Figure A.1 (a) shows a higher gradient than, for example, cell A so that cell D has a higher open circuit voltage decay. In general the decay rates are flat. If they are steep, those cells should be eliminated from consideration.

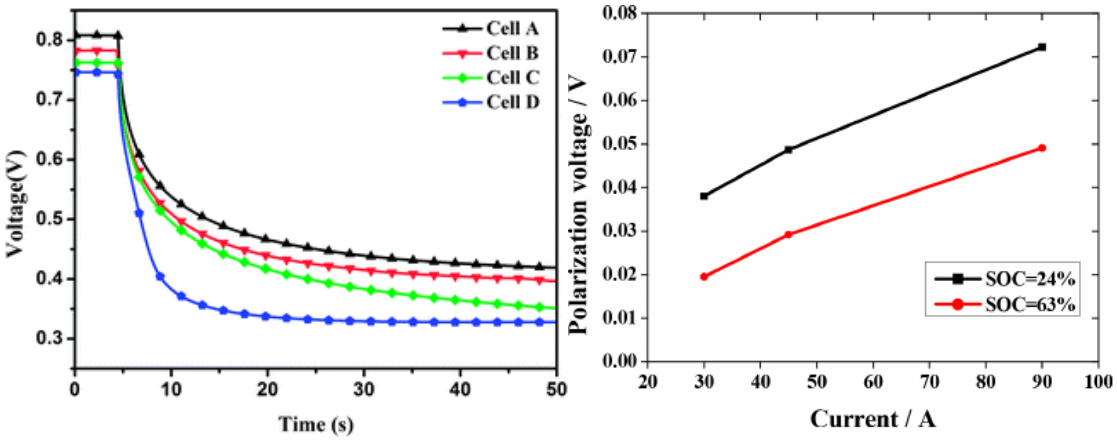


((a)) Open circuit voltage decay [11] ((b)) Polarization [12]

Figure A.1. OCVD and polarization test [11], [12]

## A.2 Polarization

By measuring the voltage-current relationship, the electrochemical activity of a cell is determined periodically. The polarization test includes applying a required current in charge mode and discharge mode for 20s at a time. The SOC remains the same at the end of the test as it was at the beginning of the test. The chosen SOC levels are 25%, 50% and 75%. The voltage data are plotted as a function of current as shown in Figure A.1 (b) [12] for the SOC of 24% and 63%. The more linear the curves, the better the result. If the curves are not linear, the mass transport is poor. Additionally it is possible to determine the internal resistance of the cells by the slope of the curves at each SOC.

## A.3 Hysteresis

The hysteresis effect of a cell is the difference between the 50% SOC and the 50% DOD capacities. It is determined by stopping the discharge process at 50% SOC and 50% DOD and measuring open circuit voltage VOC after allowing a ceratin rest period for the cell. The difference between the measured voltages is called hysteresis. Hysteresis occurs because the chemical reaction during charging lags behind the application of the charging voltage and when the cell is discharging, there is a delay before the full current can be delivered through the load [13]. The Figure A.2 [13] shows the

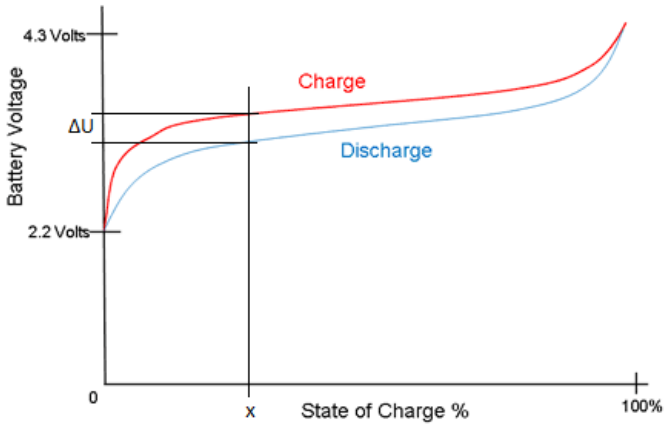


Figure A.2. Hysteresis effect [13]

hysteresis effect of a lithium battery by indicating the difference ΔU between the voltage of the charging process compared to the voltage of the discharging process

for a specific SOC of x%. Rest periods during the charging or discharging process can help to reduce the difference due to hysteresis by accommodating the chemical reaction times.

THIS PAGE INTENTIONALLY LEFT BLANK

# APPENDIX B: Guidance for Lithium Ion Battery Cell Testing with MACCOR

The following sections deal with guidelines for lithium ion battery cell testings with MACCOR. Special attention is given to the prevention of potential danger during testings and the safe handling with lithium cells. These guidelines are extracted from official testing and safety instructions [27], [28].

## A.1 Naval Postgraduate School, SSAG Lithium Ion Battery Handling Guidance and Emergency Procedures

### A.1.1 Lithium Ion Battery Handling Procedures for Guarded Operations

The following procedures are based on personal experience but also include input from ?Guidelines on Lithium-ion Battery Use in Space Applications (NASA/TM-2009-215751). Before performing any tests, it is necessary to refer to the section describing the handling and emergency procedures for li-ion batteries and cells. The following is a list of actions to take when handling li-ion cells.

- In general, lithium battery operations require an attendant. Operations of Lithium-ion cells requires the handler to continuously monitor the work area for potential shorting hazards. Lithium ion cells have the capacity discharge at up to 10 times their rated capacity. $LiFePO_4$ (lithium iron phosphate) cells have an even higher short circuit currents. For special situations that require unattended operations, an SOP must be established.
- All personnel in the operations space must be made aware of the lithium battery operations.
- All personnel in the operations space must be made aware of what to do in case of an ignition-like event.

  - Space evacuation
  - Fume avoidance and clearance
  - Location of fire-fighting equipment
  - Management of remains
- Don?t allow cells to rest on metal fixtures without some restraint that prohibits shorting of the cells such as non-conductive adhesive tape covering the electrodes.
- When storing cells that allow cell electrodes to contact each other such as in anti-static bags, cover at least one electrode with tape.
- During assembly protect batteries from shorting by using original packaging or something specifically designed to be similar.
- When attaching solder tabs to cells use the parallel gap resistance welder to weld solder tabs to cells. Do not solder directly to the cell electrodes.
- Return Lithium cells and batteries to a controlled storage area in original containers, or something specifically designed to be similar when test, assembly or fabrication process is interrupted or completed.
- Store Lithium ion cells in NPS approved storage lockers. $LiFePO_4$ batteries must be stored in metal cabinets or $LiFePO_4$ bags with ceramic tiles in accordance with the NPS $LiFePO_4$ SOP. Keep storage away from flammable or hazardous materials. Storage must be labelled ?"Lithium Battery Storage only"?.
- Never short-circuit a li-ion cell or discharge above the manufacturer?s suggested maximum discharge rate ? usually 2C for lithium ion cells or 10C for $LiFePO_4$ cells.
- Never overheat or subject lithium-ion cells to temperatures higher than manufacturer?s suggested maximum temperature
- Never discharge lithium ion cells to an end-of-discharge voltage (EODV) lower than manufacturer?s suggested minimum voltage ? usually 2.5V for hard carbon, 3.0 for Graphite and 2.0V for $LiFePO_4$ Other chemistries may differ.
- Dispose of properly using NPS requirements for lithium ion cells. If possible, discharge battery before turning in. If a discharge is not possible, cover the terminals with non-conductive adhesive tape and label the battery as ?charged?. Batteries (and remains after they have set and cooled without incident for 24

hours) can be placed in any of the NPS battery buckets placed about campus. Do not mutilate cells.

### A.1.2 Lithium Ion Battery Emergency Procedures

**Exposure to Electrolyte**

- Eyes
  - If eyes become contaminated with electrolyte flush them thoroughly for 15 minutes minimum. While flushing eyes roll them and lift eyelids.
  - Do not put neutralizing solution in eyes.
  - Call 911. Get medical attention immediately
- Skin exposure
  - If electrolyte gets on the skin or clothing flush the area with water. If any indication of irritation, burning, or reactions persists, call 911. Get medical attention immediately.

**Cell Leaking, Venting or Increased Temperature**

- If cells are leaking, venting or increasing in temperature
  - Do not inhale fumes. They are toxic. If fumes cannot be avoided, evacuate the space and others in the vicinity of fumes. Call 911 and request support for a lithium battery fire.
  - Properly equipped personnel may remove the batteries to a safe area. A shovel or protective gloves are required to handle a leaking, venting, or hot battery. Do not risk inhaling fumes to move a battery. If there is danger of inhaling fumes, then evacuate, call 911 and request support for a lithium battery fire.
  - If leaking or venting is minor and stabilized and the opportunity allows, disconnect the battery/cells from other equipment. If the cells are showing any indication of thermally running away, such as increasing venting, increasing leaking, or building smoke, then do not attempt to disconnect equipment until the cells have stabilized. Turn off the equipment at its source if the opportunity allows.
- If cell ruptures,
  - Do not inhale fumes. They are toxic. If fumes cannot be avoided, evacuate the space and others in the vicinity of fumes. Call 911 and request support for a lithium battery fire.

  - Monitor the battery for at least 45 minutes.
  - After 45 minutes, look for the opportunity to disconnect the charger.
  - After 45 minutes, with protective gloves or a shovel, move the battery to a safe location.
- In the event that an unrelated fire breaks out in the area where batteries are stored and if there is time, safely remove any lithium batteries from that area.

## A.2 SSAG MACCOR Lithium Battery Tester, Attended and Unattended Operations SOP

The Space Systems Academic Group has a battery test lab (Bullard Hall Rm 112) that is used to characterize batteries under various charge/discharge regimens and at controlled temperatures. This document describes the operating procedures when testing lithium ion cells using the MACCOR battery test system located in this test lab. This is not a step-by-step procedure but rather a list of practices that must be followed to insure a safe work area and to reduce risk of accident.

The battery test lab includes a MACCOR battery test unit with 16 channels that provide programmable charge and discharge currents at programmable voltages. In addition, the tester has 16 auxiliary channels for temperature monitoring of the cells. A Polyscience recirculator is connected to two cold plates that have attached pods where each pod is capable of holding one 18650 sized lithium ion cell. Electrical leads from the MACCOR are attached to the pods where they then allow electrical contact to the cell electrodes.

The MACCOR tester is designed for stand-alone operation if the configuration and programming practices below are followed. Controlling the charge and discharge regimens is accomplished with MACCOR proprietary software that relies on parameters input by the user. An application note on how to program the MACCOR system safety features is available from Ron Phelps.

Surrounding the two cold plates are polycarbonate enclosures with 6.35mm thick walls.

- Clear away all flammable or hazardous materials
- Review applicable best practices of NPS $LiFePO_4$ SOP (current is version 1.4b JAN 2016).

- Review the SSAG Lithium Ion Battery Handling Guidance and Emergency Procedures (current is 06Jun2016)
- When programming the MACCOR global safety settings for the first time, refer to the Global_safety_settings_MACCOR.pdf application note.
- Never program a charge/discharge current or voltage within a MACCOR procedure that exceeds the manufacturer?s suggested operating specifications of the cell being tested.
- Use program features to restrict the maximum currents and voltages a test cell can sustain to safe limits such that if these limits are exceed the MACCOR tester will halt the test and the cell will not be damaged. A description
- Always turn on the smaller of the two wall fans in the battery test lab to prevent the MACCOR system from overheating. During work hours you may keep the door open when battery testing is in progress.
- Place NPS provided ceramic tiles beneath the polycarbonate enclosures

**For unattended operations**

- The MACCOR Battery Management System must be used.
- Ensure the enclosure is labeled as FAR 25.853 Aircraft Grade polycarbonate.
- Ensure ceramic tiles are in place beneath the test enclosure.
- Use all safety features of the MACCOR battery management system. When programming the MACCOR system, either
  - Have another knowledgeable person review the MACCOR program parameters to verify the program will not exceed the cell ratings for voltage or current ? or ?
  - Run the program fully attended to completion to verify proper operation.

THIS PAGE INTENTIONALLY LEFT BLANK

# APPENDIX C:
# Test Procedures

This chapter contains the test procedures of the $\alpha$ and $\beta$ value and the discharge capacity determination. The test procedures implemented by the BuildTest software of MACCOR are presented in figures and key steps are explained in detail.

## A.1 Alpha Value Determination Test Sequence

Figures A.1, A.2, A.3 and A.4 show the test procedure of the $\alpha$ value determination. Step 1 includes the safety sequence as explained in Section 4.2.2 for the break in test. It follows an AC Imp test and a rest sequence. Afterwards the cells traverse eleven cycles with decreasing discharge rates as presented in 5.1.4. Step 58 includes a charging sequence to a safe storage voltage of 3.3V.

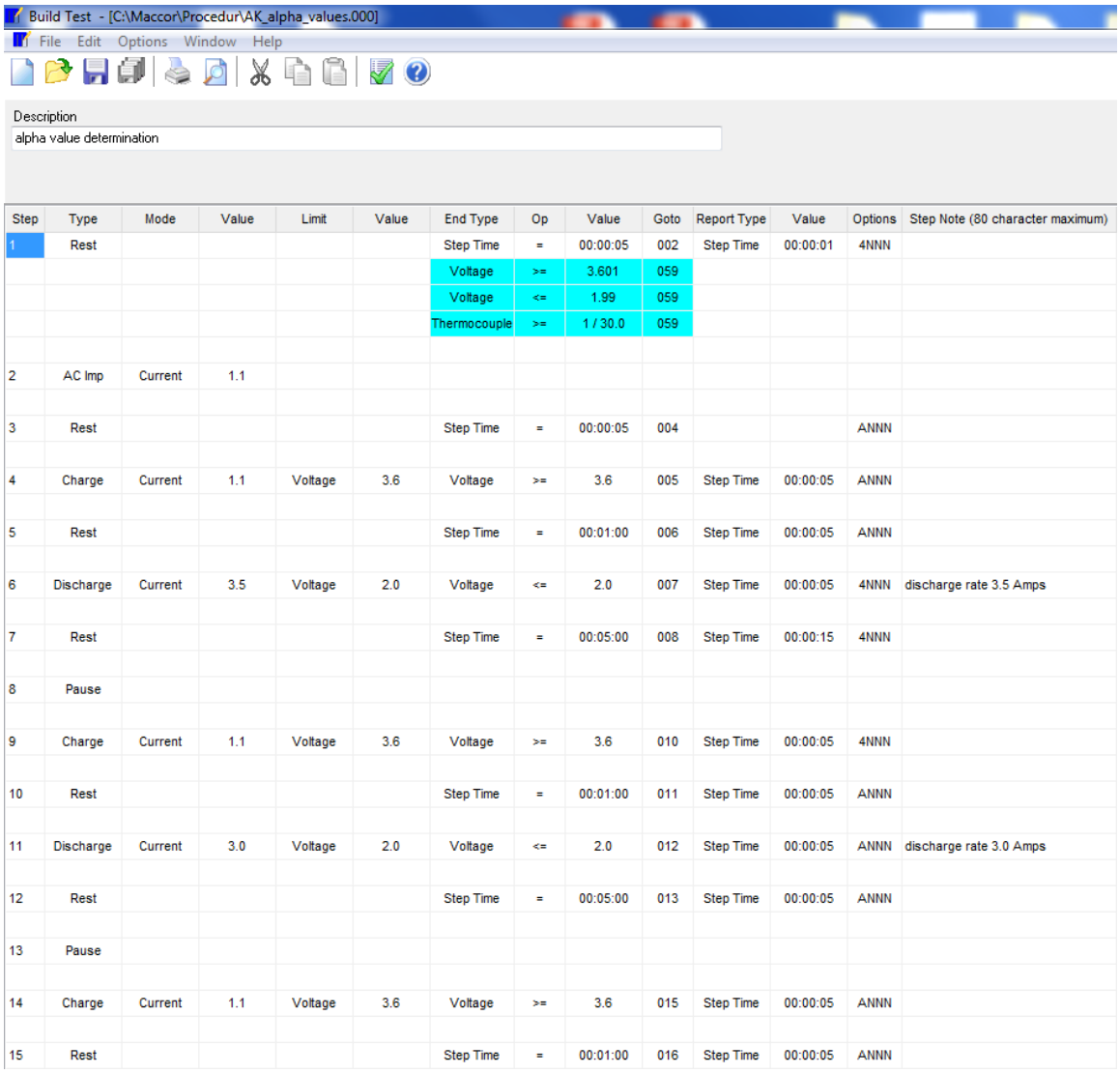


| Step | Type | Mode | Value | Limit | Value | End Type | Op | Value | Goto | Report Type | Value | Options | Step Note (80 character maximum) |
|---|---|---|---|---|---|---|---|---|---|---|---|---|---|
| 1 | Rest | | | | | Step Time | = | 00:00:05 | 002 | Step Time | 00:00:01 | 4NNN | |
| | | | | | | Voltage | >= | 3.601 | 059 | | | | |
| | | | | | | Voltage | <= | 1.99 | 059 | | | | |
| | | | | | | Thermocouple | >= | 1 / 30.0 | 059 | | | | |
| 2 | AC Imp | Current | 1.1 | | | | | | | | | | |
| 3 | Rest | | | | | Step Time | = | 00:00:05 | 004 | | | ANNN | |
| 4 | Charge | Current | 1.1 | Voltage | 3.6 | Voltage | >= | 3.6 | 005 | Step Time | 00:00:05 | ANNN | |
| 5 | Rest | | | | | Step Time | = | 00:01:00 | 006 | Step Time | 00:00:05 | ANNN | |
| 6 | Discharge | Current | 3.5 | Voltage | 2.0 | Voltage | <= | 2.0 | 007 | Step Time | 00:00:05 | 4NNN | discharge rate 3.5 Amps |
| 7 | Rest | | | | | Step Time | = | 00:05:00 | 008 | Step Time | 00:00:15 | 4NNN | |
| 8 | Pause | | | | | | | | | | | | |
| 9 | Charge | Current | 1.1 | Voltage | 3.6 | Voltage | >= | 3.6 | 010 | Step Time | 00:00:05 | 4NNN | |
| 10 | Rest | | | | | Step Time | = | 00:01:00 | 011 | Step Time | 00:00:05 | ANNN | |
| 11 | Discharge | Current | 3.0 | Voltage | 2.0 | Voltage | <= | 2.0 | 012 | Step Time | 00:00:05 | ANNN | discharge rate 3.0 Amps |
| 12 | Rest | | | | | Step Time | = | 00:05:00 | 013 | Step Time | 00:00:05 | ANNN | |
| 13 | Pause | | | | | | | | | | | | |
| 14 | Charge | Current | 1.1 | Voltage | 3.6 | Voltage | >= | 3.6 | 015 | Step Time | 00:00:05 | ANNN | |
| 15 | Rest | | | | | Step Time | = | 00:01:00 | 016 | Step Time | 00:00:05 | ANNN | |

Figure A.1. Alpha value determination test sequence, Part 1

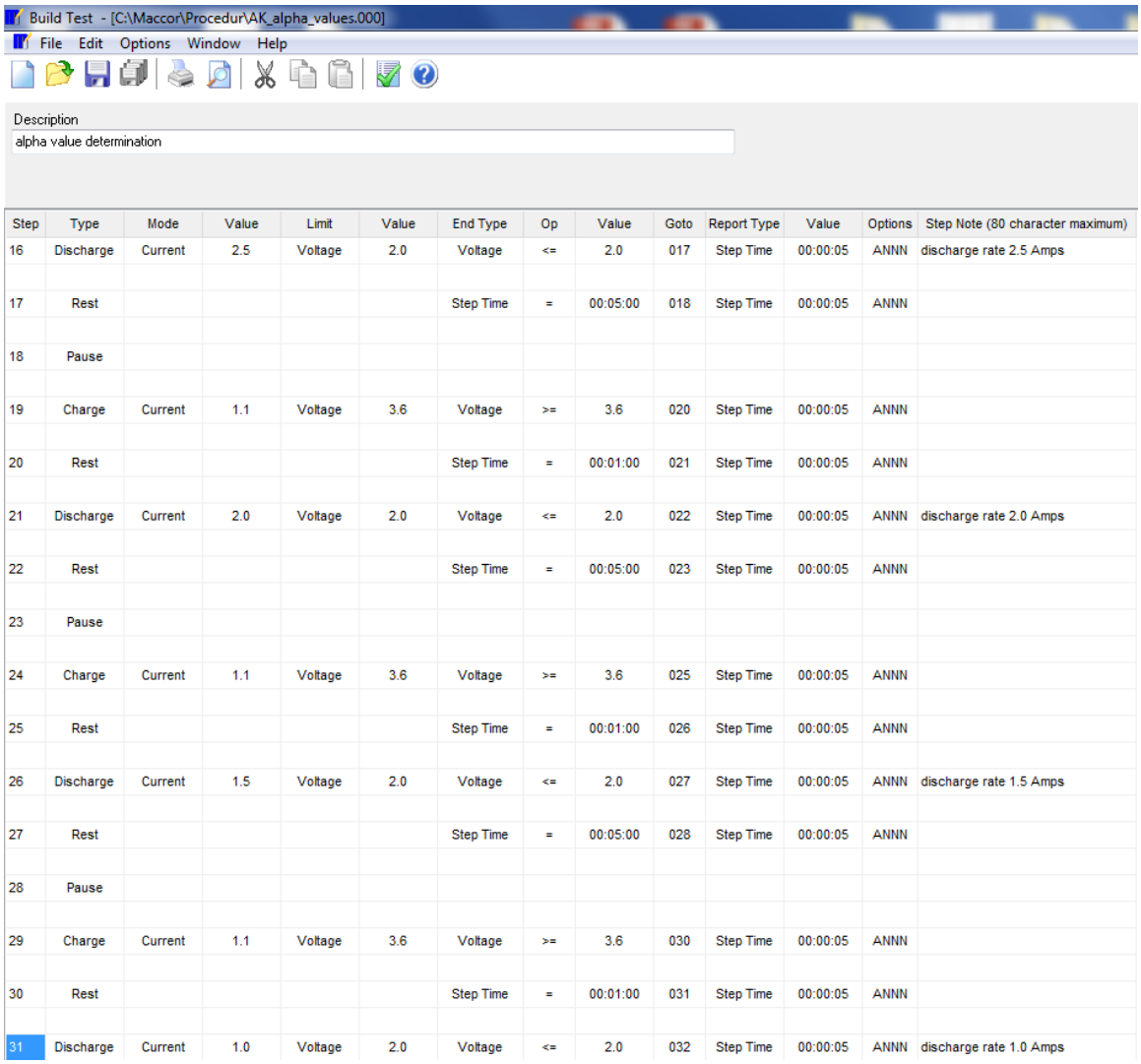


| Step | Type | Mode | Value | Limit | Value | End Type | Op | Value | Goto | Report Type | Value | Options | Step Note (80 character maximum) |
|---|---|---|---|---|---|---|---|---|---|---|---|---|---|
| 16 | Discharge | Current | 2.5 | Voltage | 2.0 | Voltage | <= | 2.0 | 017 | Step Time | 00:00:05 | ANNN | discharge rate 2.5 Amps |
| 17 | Rest | | | | | Step Time | = | 00:05:00 | 018 | Step Time | 00:00:05 | ANNN | |
| 18 | Pause | | | | | | | | | | | | |
| 19 | Charge | Current | 1.1 | Voltage | 3.6 | Voltage | >= | 3.6 | 020 | Step Time | 00:00:05 | ANNN | |
| 20 | Rest | | | | | Step Time | = | 00:01:00 | 021 | Step Time | 00:00:05 | ANNN | |
| 21 | Discharge | Current | 2.0 | Voltage | 2.0 | Voltage | <= | 2.0 | 022 | Step Time | 00:00:05 | ANNN | discharge rate 2.0 Amps |
| 22 | Rest | | | | | Step Time | = | 00:05:00 | 023 | Step Time | 00:00:05 | ANNN | |
| 23 | Pause | | | | | | | | | | | | |
| 24 | Charge | Current | 1.1 | Voltage | 3.6 | Voltage | >= | 3.6 | 025 | Step Time | 00:00:05 | ANNN | |
| 25 | Rest | | | | | Step Time | = | 00:01:00 | 026 | Step Time | 00:00:05 | ANNN | |
| 26 | Discharge | Current | 1.5 | Voltage | 2.0 | Voltage | <= | 2.0 | 027 | Step Time | 00:00:05 | ANNN | discharge rate 1.5 Amps |
| 27 | Rest | | | | | Step Time | = | 00:05:00 | 028 | Step Time | 00:00:05 | ANNN | |
| 28 | Pause | | | | | | | | | | | | |
| 29 | Charge | Current | 1.1 | Voltage | 3.6 | Voltage | >= | 3.6 | 030 | Step Time | 00:00:05 | ANNN | |
| 30 | Rest | | | | | Step Time | = | 00:01:00 | 031 | Step Time | 00:00:05 | ANNN | |
| 31 | Discharge | Current | 1.0 | Voltage | 2.0 | Voltage | <= | 2.0 | 032 | Step Time | 00:00:05 | ANNN | discharge rate 1.0 Amps |

Figure A.2. Alpha value determination test sequence, Part 2

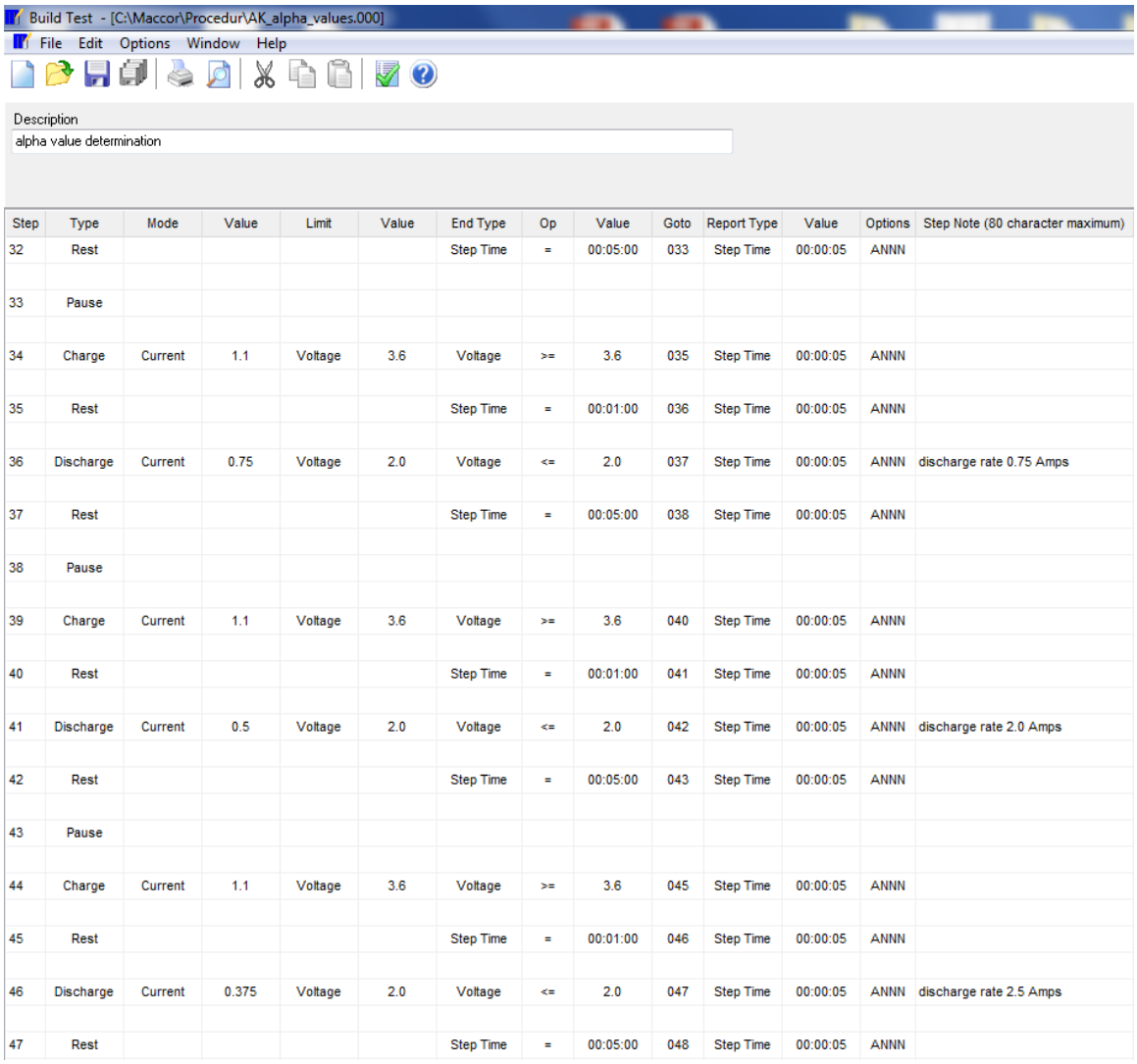


| Step | Type | Mode | Value | Limit | Value | End Type | Op | Value | Goto | Report Type | Value | Options | Step Note (80 character maximum) |
|---|---|---|---|---|---|---|---|---|---|---|---|---|---|
| 32 | Rest | | | | | Step Time | = | 00:05:00 | 033 | Step Time | 00:00:05 | ANNN | |
| 33 | Pause | | | | | | | | | | | | |
| 34 | Charge | Current | 1.1 | Voltage | 3.6 | Voltage | >= | 3.6 | 035 | Step Time | 00:00:05 | ANNN | |
| 35 | Rest | | | | | Step Time | = | 00:01:00 | 036 | Step Time | 00:00:05 | ANNN | |
| 36 | Discharge | Current | 0.75 | Voltage | 2.0 | Voltage | <= | 2.0 | 037 | Step Time | 00:00:05 | ANNN | discharge rate 0.75 Amps |
| 37 | Rest | | | | | Step Time | = | 00:05:00 | 038 | Step Time | 00:00:05 | ANNN | |
| 38 | Pause | | | | | | | | | | | | |
| 39 | Charge | Current | 1.1 | Voltage | 3.6 | Voltage | >= | 3.6 | 040 | Step Time | 00:00:05 | ANNN | |
| 40 | Rest | | | | | Step Time | = | 00:01:00 | 041 | Step Time | 00:00:05 | ANNN | |
| 41 | Discharge | Current | 0.5 | Voltage | 2.0 | Voltage | <= | 2.0 | 042 | Step Time | 00:00:05 | ANNN | discharge rate 2.0 Amps |
| 42 | Rest | | | | | Step Time | = | 00:05:00 | 043 | Step Time | 00:00:05 | ANNN | |
| 43 | Pause | | | | | | | | | | | | |
| 44 | Charge | Current | 1.1 | Voltage | 3.6 | Voltage | >= | 3.6 | 045 | Step Time | 00:00:05 | ANNN | |
| 45 | Rest | | | | | Step Time | = | 00:01:00 | 046 | Step Time | 00:00:05 | ANNN | |
| 46 | Discharge | Current | 0.375 | Voltage | 2.0 | Voltage | <= | 2.0 | 047 | Step Time | 00:00:05 | ANNN | discharge rate 2.5 Amps |
| 47 | Rest | | | | | Step Time | = | 00:05:00 | 048 | Step Time | 00:00:05 | ANNN | |

Figure A.3. Alpha value determination test sequence, Part 3

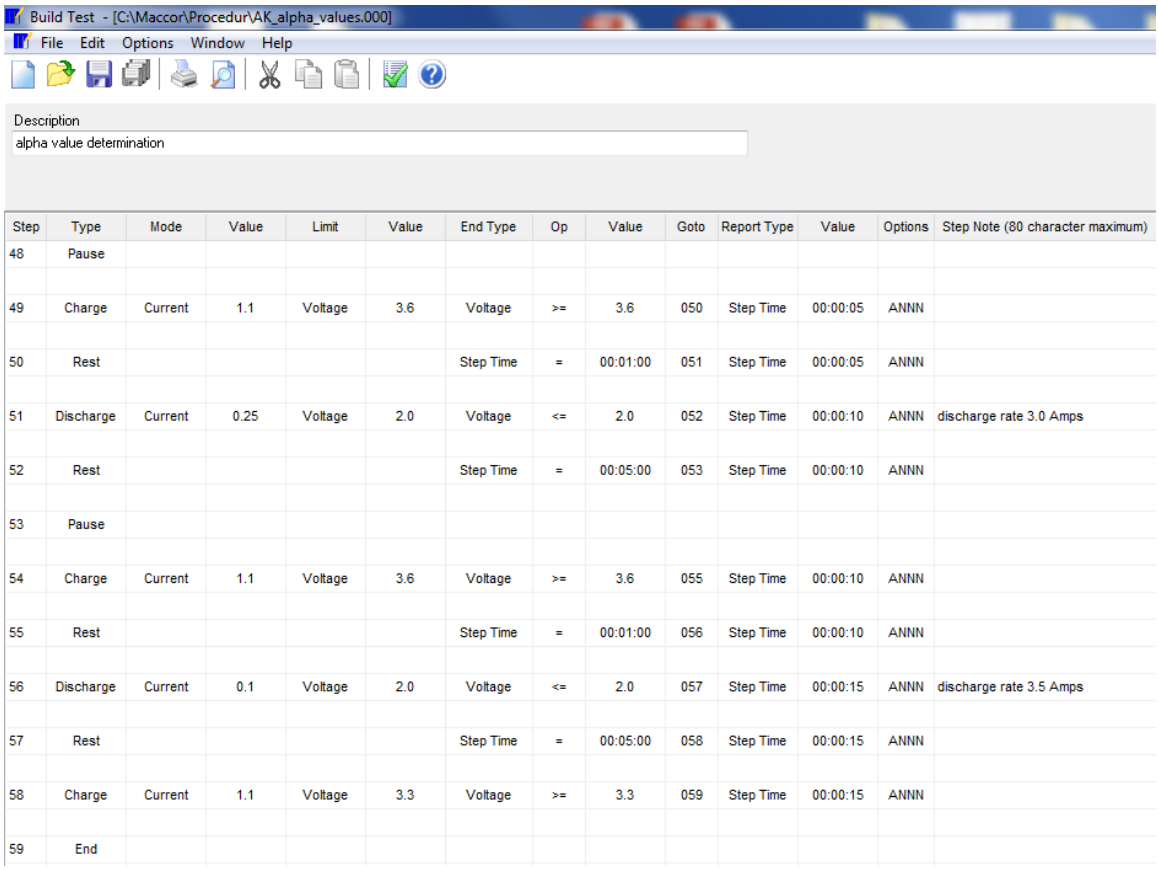


| Step | Type | Mode | Value | Limit | Value | End Type | Op | Value | Goto | Report Type | Value | Options | Step Note (80 character maximum) |
|---|---|---|---|---|---|---|---|---|---|---|---|---|---|
| 48 | Pause | | | | | | | | | | | | |
| 49 | Charge | Current | 1.1 | Voltage | 3.6 | Voltage | >= | 3.6 | 050 | Step Time | 00:00:05 | ANNN | |
| 50 | Rest | | | | | Step Time | = | 00:01:00 | 051 | Step Time | 00:00:05 | ANNN | |
| 51 | Discharge | Current | 0.25 | Voltage | 2.0 | Voltage | <= | 2.0 | 052 | Step Time | 00:00:10 | ANNN | discharge rate 3.0 Amps |
| 52 | Rest | | | | | Step Time | = | 00:05:00 | 053 | Step Time | 00:00:10 | ANNN | |
| 53 | Pause | | | | | | | | | | | | |
| 54 | Charge | Current | 1.1 | Voltage | 3.6 | Voltage | >= | 3.6 | 055 | Step Time | 00:00:10 | ANNN | |
| 55 | Rest | | | | | Step Time | = | 00:01:00 | 056 | Step Time | 00:00:10 | ANNN | |
| 56 | Discharge | Current | 0.1 | Voltage | 2.0 | Voltage | <= | 2.0 | 057 | Step Time | 00:00:15 | ANNN | discharge rate 3.5 Amps |
| 57 | Rest | | | | | Step Time | = | 00:05:00 | 058 | Step Time | 00:00:15 | ANNN | |
| 58 | Charge | Current | 1.1 | Voltage | 3.3 | Voltage | >= | 3.3 | 059 | Step Time | 00:00:15 | ANNN | |
| 59 | End | | | | | | | | | | | | |

Figure A.4. Alpha value determination test sequence, Part 4

## A.2 Beta Value Determination Test Sequence

Figures A.5, A.6 and A.7 show the test procedure of the $\beta$ value determination. Step 1 includes the safety sequence as explained in Section 4.2.2 for the break in test. The thermocouple is changed to 45°C because the determination of the beta values occurs with a temperature increase to 40°C. The battery cells are charged and discharged with a charge and discharge rate of 1.1Amps eight times with eight different ambient temperatures (40°C, 35°C, 30°C, 25°C, 20°C, 15°C, 10°C, 5°C). An AC Imp test follows before every cycle to determine a dependence of the internal resistance of the battery cell on temperature. The pause steps between the cycles are implemented to adjust the required temperature. When the specific temperature is achieved, a

manual restart is necessary to proceed the test. At the end of the test procedure the cells are charged to a safe storage voltage of 3.3V and a capacity of 0.55Ah.

Build Test - [C:\Maccor\Procedur\AK_beta_values.000]

File Edit Options Window Help

Description

beta value determination

| Step | Type | Mode | Value | Limit | Value | End Type | Op | Value | Goto | Report Type | Value | Options | Step Note (80 character maximum) |
|---|---|---|---|---|---|---|---|---|---|---|---|---|---|
| 1 | Rest | | | | | Step Time | = | 00:00:05 | 002 | Step Time | 00:00:01 | 4NNN | |
| | | | | | | Voltage | >= | 3.601 | 043 | | | | |
| | | | | | | Voltage | <= | 1.99 | 043 | | | | |
| | | | | | | Thermocouple | >= | 1 / 45.0 | 043 | | | | |
| 2 | AC Imp | Current | 1.1 | | | | | | | | | | Verify good conductivity, set cell temp to 40°C |
| 3 | Charge | Current | 1.1 | Voltage | 3.6 | Voltage | >= | 3.6 | 004 | Step Time | 00:00:05 | 4NNN | top off cell |
| 4 | Rest | | | | | Step Time | = | 00:05:00 | 005 | Step Time | 00:00:05 | 4NNN | |
| 5 | Discharge | Current | 1.1 | Voltage | 2.0 | Voltage | <= | 2.0 | 006 | Step Time | 00:00:05 | 4NNN | |
| 6 | Pause | | | | | | | | | | | | Pause to change temperature to 35°C |
| 7 | AC Imp | Current | 1.1 | | | | | | | | | | |
| 8 | Charge | Current | 1.1 | Voltage | 3.6 | Voltage | >= | 3.6 | 009 | Step Time | 00:00:05 | 4NNN | |
| 9 | Rest | | | | | Step Time | = | 00:05:00 | 010 | Step Time | 00:00:05 | 4NNN | |
| 10 | Discharge | Current | 1.1 | Voltage | 2.0 | Voltage | <= | 2.0 | 011 | Step Time | 00:00:05 | 4NNN | |
| 11 | Pause | | | | | | | | | | | | Pause to change temperature to 30°C |
| 12 | AC Imp | Current | 1.1 | | | | | | | | | | |
| 13 | Charge | Current | 1.1 | Voltage | 3.6 | Voltage | >= | 3.6 | 014 | Step Time | 00:00:05 | 4NNN | |
| 14 | Rest | | | | | Step Time | = | 00:05:00 | 015 | Step Time | 00:00:05 | 4NNN | |
| 15 | Discharge | Current | 1.1 | Voltage | 2.0 | Voltage | <= | 2.0 | 016 | Step Time | 00:00:05 | 4NNN | |

Figure A.5. Beta value determination test sequence, Part 1

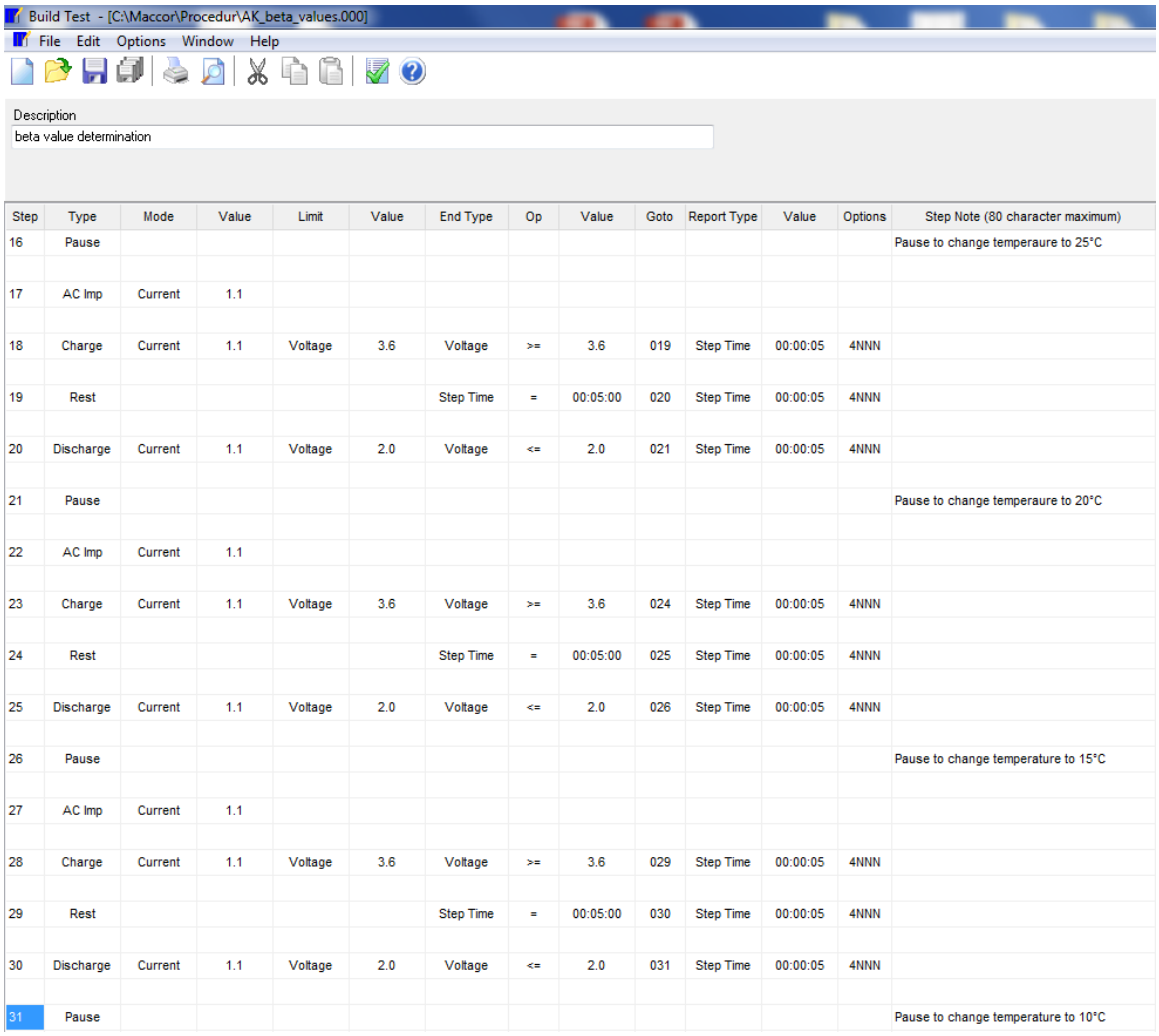


| Step | Type | Mode | Value | Limit | Value | End Type | Op | Value | Goto | Report Type | Value | Options | Step Note (80 character maximum) |
|---|---|---|---|---|---|---|---|---|---|---|---|---|---|
| 16 | Pause | | | | | | | | | | | | Pause to change temperaure to 25°C |
| 17 | AC Imp | Current | 1.1 | | | | | | | | | | |
| 18 | Charge | Current | 1.1 | Voltage | 3.6 | Voltage | >= | 3.6 | 019 | Step Time | 00:00:05 | 4NNN | |
| 19 | Rest | | | | | Step Time | = | 00:05:00 | 020 | Step Time | 00:00:05 | 4NNN | |
| 20 | Discharge | Current | 1.1 | Voltage | 2.0 | Voltage | <= | 2.0 | 021 | Step Time | 00:00:05 | 4NNN | |
| 21 | Pause | | | | | | | | | | | | Pause to change temperaure to 20°C |
| 22 | AC Imp | Current | 1.1 | | | | | | | | | | |
| 23 | Charge | Current | 1.1 | Voltage | 3.6 | Voltage | >= | 3.6 | 024 | Step Time | 00:00:05 | 4NNN | |
| 24 | Rest | | | | | Step Time | = | 00:05:00 | 025 | Step Time | 00:00:05 | 4NNN | |
| 25 | Discharge | Current | 1.1 | Voltage | 2.0 | Voltage | <= | 2.0 | 026 | Step Time | 00:00:05 | 4NNN | |
| 26 | Pause | | | | | | | | | | | | Pause to change temperature to 15°C |
| 27 | AC Imp | Current | 1.1 | | | | | | | | | | |
| 28 | Charge | Current | 1.1 | Voltage | 3.6 | Voltage | >= | 3.6 | 029 | Step Time | 00:00:05 | 4NNN | |
| 29 | Rest | | | | | Step Time | = | 00:05:00 | 030 | Step Time | 00:00:05 | 4NNN | |
| 30 | Discharge | Current | 1.1 | Voltage | 2.0 | Voltage | <= | 2.0 | 031 | Step Time | 00:00:05 | 4NNN | |
| 31 | Pause | | | | | | | | | | | | Pause to change temperature to 10°C |

Figure A.6. Beta value determination test sequence, Part 2

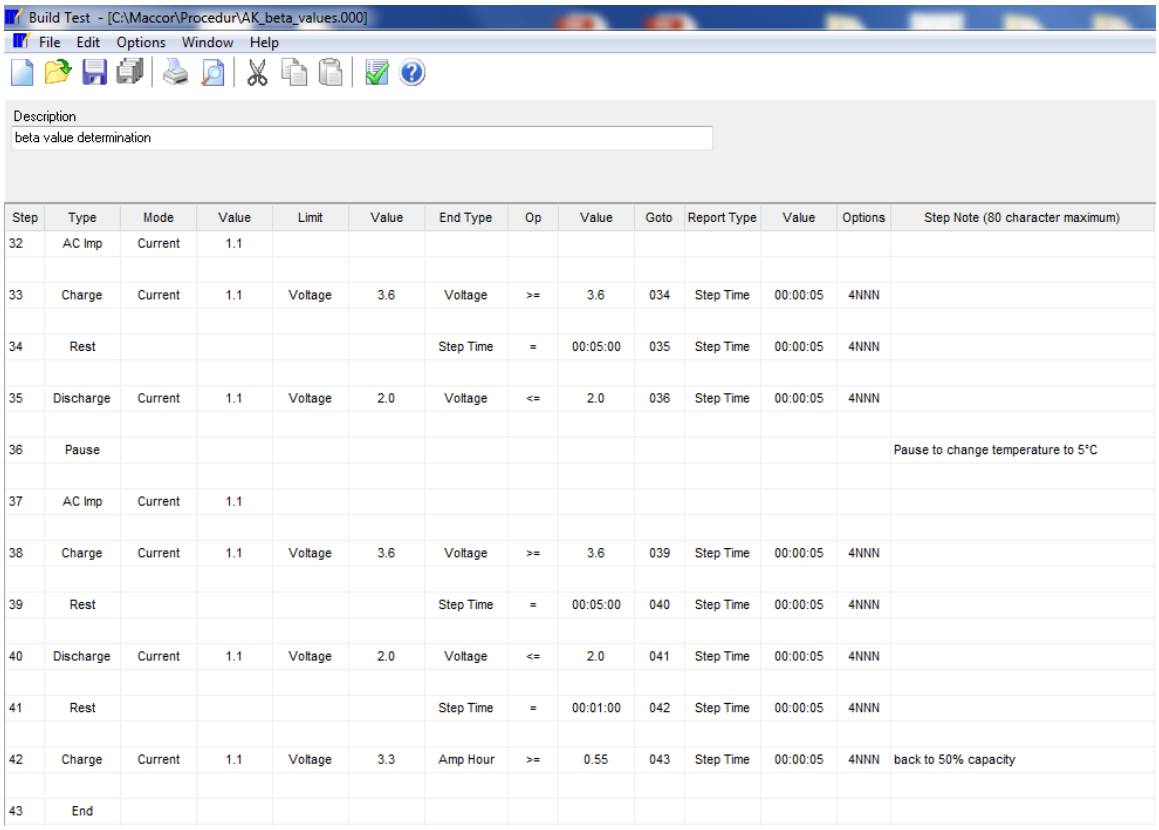


| Step | Type | Mode | Value | Limit | Value | End Type | Op | Value | Goto | Report Type | Value | Options | Step Note (80 character maximum) |
|---|---|---|---|---|---|---|---|---|---|---|---|---|---|
| 32 | AC Imp | Current | 1.1 | | | | | | | | | | |
| 33 | Charge | Current | 1.1 | Voltage | 3.6 | Voltage | >= | 3.6 | 034 | Step Time | 00:00:05 | 4NNN | |
| 34 | Rest | | | | | Step Time | = | 00:05:00 | 035 | Step Time | 00:00:05 | 4NNN | |
| 35 | Discharge | Current | 1.1 | Voltage | 2.0 | Voltage | <= | 2.0 | 036 | Step Time | 00:00:05 | 4NNN | |
| 36 | Pause | | | | | | | | | | | | Pause to change temperature to 5°C |
| 37 | AC Imp | Current | 1.1 | | | | | | | | | | |
| 38 | Charge | Current | 1.1 | Voltage | 3.6 | Voltage | >= | 3.6 | 039 | Step Time | 00:00:05 | 4NNN | |
| 39 | Rest | | | | | Step Time | = | 00:05:00 | 040 | Step Time | 00:00:05 | 4NNN | |
| 40 | Discharge | Current | 1.1 | Voltage | 2.0 | Voltage | <= | 2.0 | 041 | Step Time | 00:00:05 | 4NNN | |
| 41 | Rest | | | | | Step Time | = | 00:01:00 | 042 | Step Time | 00:00:05 | 4NNN | |
| 42 | Charge | Current | 1.1 | Voltage | 3.3 | Amp Hour | >= | 0.55 | 043 | Step Time | 00:00:05 | 4NNN | back to 50% capacity |
| 43 | End | | | | | | | | | | | | |

Figure A.7. Beta value determination test sequence, Part 3

## A.3 Discharge Capacity

The test procedure of the discharge capacity test is shown in Figures A.8 and A.9. Step 1 includes the safety sequence as explained in Section 4.2.2 for the break-in test. The thermocouple is changed to 35°C because the highest ambient temperature is adjusted to 30°C in this test. After an AC Imp test the cells are charged from the safe storage voltage to 3.6V. Step 4 is a pause to adjust the temperature to 30°C. Afterwards, the test starts with the first cycle. Two additional cycles follow at temperatures of 10°C and 5°C. At the end of the procedure the temperature is adjusted to 25°C and the cells are charged to a safe storage voltage of 3.3V.

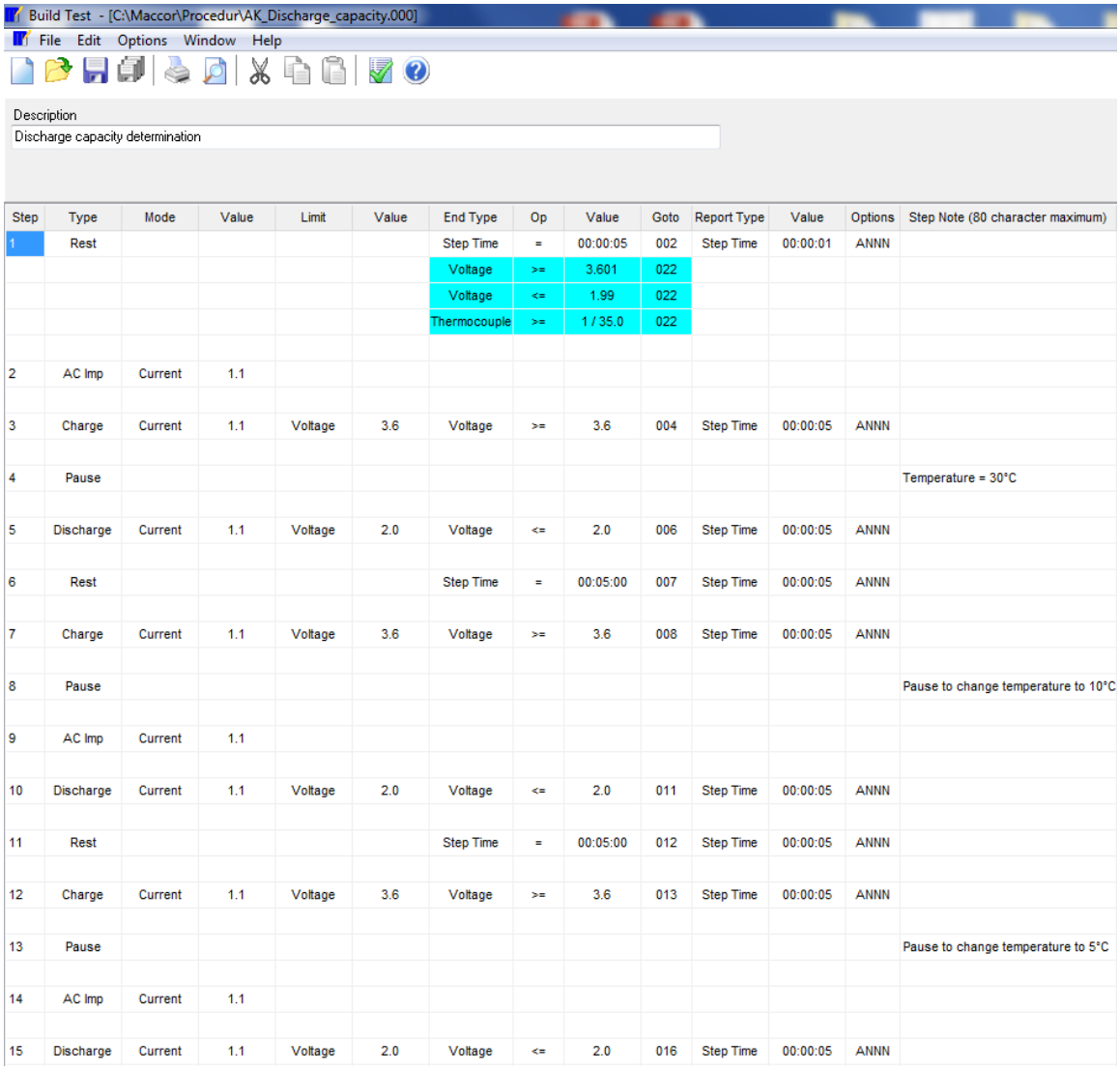


| Step | Type | Mode | Value | Limit | Value | End Type | Op | Value | Goto | Report Type | Value | Options | Step Note (80 character maximum) |
|---|---|---|---|---|---|---|---|---|---|---|---|---|---|
| 1 | Rest | | | | | Step Time | = | 00:00:05 | 002 | Step Time | 00:00:01 | ANNN | |
| | | | | | | Voltage | >= | 3.601 | 022 | | | | |
| | | | | | | Voltage | <= | 1.99 | 022 | | | | |
| | | | | | | Thermocouple | >= | 1 / 35.0 | 022 | | | | |
| 2 | AC Imp | Current | 1.1 | | | | | | | | | | |
| 3 | Charge | Current | 1.1 | Voltage | 3.6 | Voltage | >= | 3.6 | 004 | Step Time | 00:00:05 | ANNN | |
| 4 | Pause | | | | | | | | | | | | Temperature = 30°C |
| 5 | Discharge | Current | 1.1 | Voltage | 2.0 | Voltage | <= | 2.0 | 006 | Step Time | 00:00:05 | ANNN | |
| 6 | Rest | | | | | Step Time | = | 00:05:00 | 007 | Step Time | 00:00:05 | ANNN | |
| 7 | Charge | Current | 1.1 | Voltage | 3.6 | Voltage | >= | 3.6 | 008 | Step Time | 00:00:05 | ANNN | |
| 8 | Pause | | | | | | | | | | | | Pause to change temperature to 10°C |
| 9 | AC Imp | Current | 1.1 | | | | | | | | | | |
| 10 | Discharge | Current | 1.1 | Voltage | 2.0 | Voltage | <= | 2.0 | 011 | Step Time | 00:00:05 | ANNN | |
| 11 | Rest | | | | | Step Time | = | 00:05:00 | 012 | Step Time | 00:00:05 | ANNN | |
| 12 | Charge | Current | 1.1 | Voltage | 3.6 | Voltage | >= | 3.6 | 013 | Step Time | 00:00:05 | ANNN | |
| 13 | Pause | | | | | | | | | | | | Pause to change temperature to 5°C |
| 14 | AC Imp | Current | 1.1 | | | | | | | | | | |
| 15 | Discharge | Current | 1.1 | Voltage | 2.0 | Voltage | <= | 2.0 | 016 | Step Time | 00:00:05 | ANNN | |

Figure A.8. Discharge capacity test sequence, Part 1

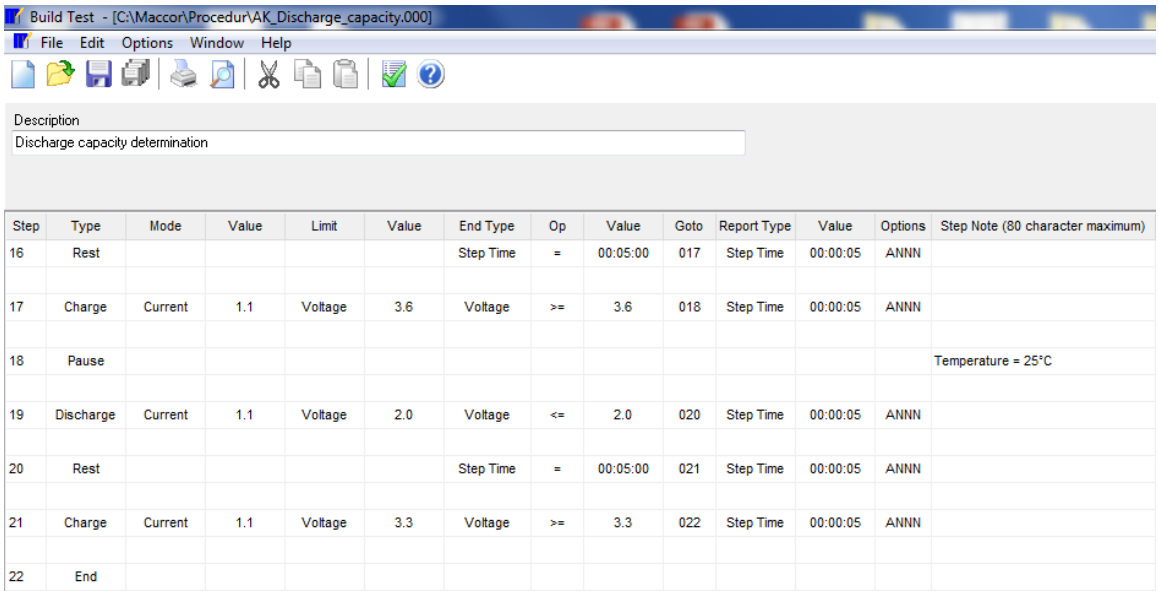


| Step | Type | Mode | Value | Limit | Value | End Type | Op | Value | Goto | Report Type | Value | Options | Step Note (80 character maximum) |
|---|---|---|---|---|---|---|---|---|---|---|---|---|---|
| 16 | Rest | | | | | Step Time | = | 00:05:00 | 017 | Step Time | 00:00:05 | ANNN | |
| 17 | Charge | Current | 1.1 | Voltage | 3.6 | Voltage | >= | 3.6 | 018 | Step Time | 00:00:05 | ANNN | |
| 18 | Pause | | | | | | | | | | | | Temperature = 25°C |
| 19 | Discharge | Current | 1.1 | Voltage | 2.0 | Voltage | <= | 2.0 | 020 | Step Time | 00:00:05 | ANNN | |
| 20 | Rest | | | | | Step Time | = | 00:05:00 | 021 | Step Time | 00:00:05 | ANNN | |
| 21 | Charge | Current | 1.1 | Voltage | 3.3 | Voltage | >= | 3.3 | 022 | Step Time | 00:00:05 | ANNN | |
| 22 | End | | | | | | | | | | | | |

Figure A.9. Discharge capacity test sequence, Part 2

# APPENDIX D:
# MACCOR Software Program

The following Figures in this chapter show screenshots of the interface of the MACCOR software program presented in Section 4.2.3.

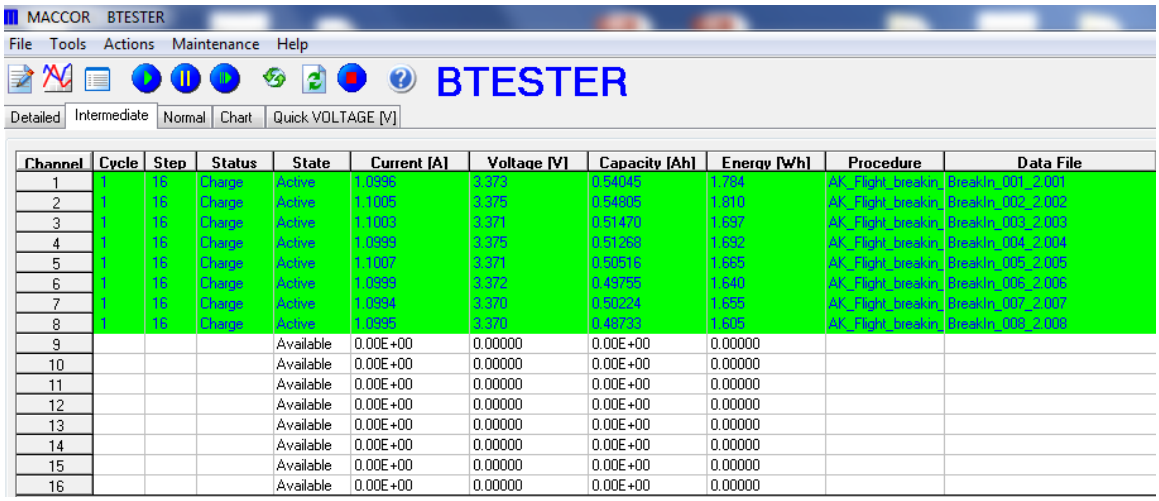


| Channel | Cycle | Step | Status | State | Current [A] | Voltage [V] | Capacity [Ah] | Energy [Wh] | Procedure | Data File |
|---|---|---|---|---|---|---|---|---|---|---|
| 1 | 1 | 16 | Charge | Active | 1.0996 | 3.373 | 0.54045 | 1.784 | AK_Flight_breakin_ | BreakIn_001_2.001 |
| 2 | 1 | 16 | Charge | Active | 1.1005 | 3.375 | 0.54805 | 1.810 | AK_Flight_breakin_ | BreakIn_002_2.002 |
| 3 | 1 | 16 | Charge | Active | 1.1003 | 3.371 | 0.51470 | 1.697 | AK_Flight_breakin_ | BreakIn_003_2.003 |
| 4 | 1 | 16 | Charge | Active | 1.0999 | 3.375 | 0.51268 | 1.692 | AK_Flight_breakin_ | BreakIn_004_2.004 |
| 5 | 1 | 16 | Charge | Active | 1.1007 | 3.371 | 0.50516 | 1.665 | AK_Flight_breakin_ | BreakIn_005_2.005 |
| 6 | 1 | 16 | Charge | Active | 1.0999 | 3.372 | 0.49755 | 1.640 | AK_Flight_breakin_ | BreakIn_006_2.006 |
| 7 | 1 | 16 | Charge | Active | 1.0994 | 3.370 | 0.50224 | 1.655 | AK_Flight_breakin_ | BreakIn_007_2.007 |
| 8 | 1 | 16 | Charge | Active | 1.0995 | 3.370 | 0.48733 | 1.605 | AK_Flight_breakin_ | BreakIn_008_2.008 |
| 9 | | | | Available | 0.00E+00 | 0.00000 | 0.00E+00 | 0.00000 | | |
| 10 | | | | Available | 0.00E+00 | 0.00000 | 0.00E+00 | 0.00000 | | |
| 11 | | | | Available | 0.00E+00 | 0.00000 | 0.00E+00 | 0.00000 | | |
| 12 | | | | Available | 0.00E+00 | 0.00000 | 0.00E+00 | 0.00000 | | |
| 13 | | | | Available | 0.00E+00 | 0.00000 | 0.00E+00 | 0.00000 | | |
| 14 | | | | Available | 0.00E+00 | 0.00000 | 0.00E+00 | 0.00000 | | |
| 15 | | | | Available | 0.00E+00 | 0.00000 | 0.00E+00 | 0.00000 | | |
| 16 | | | | Available | 0.00E+00 | 0.00000 | 0.00E+00 | 0.00000 | | |

Figure A.1. Intermediate screen of MACCOR

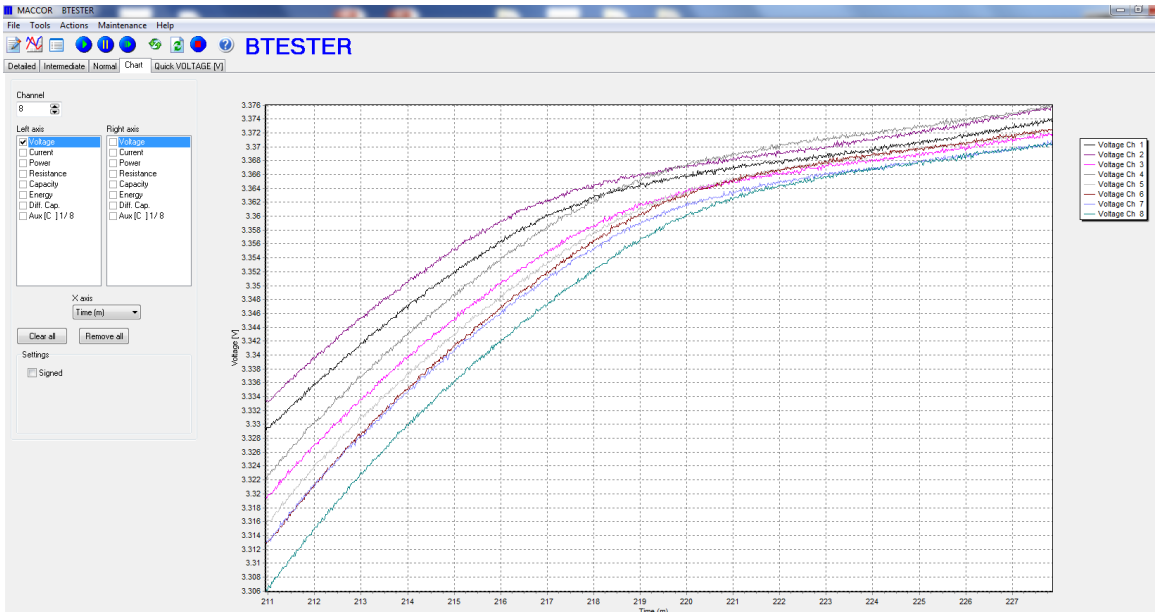


Figure A.2. Chart screen of MACCOR

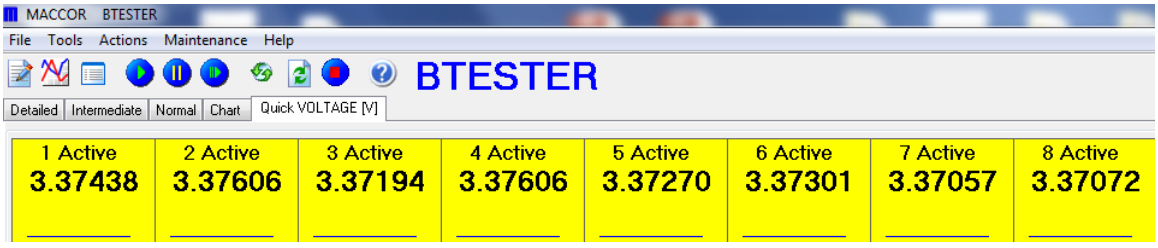


Figure A.3. Quick voltage screen of MACCOR

# APPENDIX E: Spreadsheets

This chapter provides spreadsheets used to record data. Cell 17 is noted as a bad cell, because the AC Imp is 50.4mΩ recorded at the AC Imp test. Cell 50 is damaged by a short circuit caused by a wrong installation in the pod at the break-in test.

## A.1 Open Circuit Voltage

| Cell Number | OCV [V] | Comment |
|---|---|---|
| 1 | 3.2912 | |
| 2 | 3.2891 | |
| 3 | 3.2921 | |
| 4 | 3.2912 | |
| 5 | 3.2911 | |
| 6 | 3.2915 | |
| 7 | 3.2908 | |
| 8 | 3.2909 | |
| 9 | 3.292 | |
| 10 | 3.2917 | |
| 11 | 3.2919 | |
| 12 | 3.2914 | |
| 13 | 3.2917 | |
| 14 | 3.2917 | |
| 15 | 3.2911 | |
| 16 | 3.2917 | |
| 17 | 3.2883 | Bad cell |
| 18 | 3.2889 | |
| 19 | 3.2911 | |
| 20 | 3.2914 | |
| 21 | 3.2915 | |
| 22 | 3.291 | |
| 23 | 3.2924 | |
| 24 | 3.2914 | |
| 25 | 3.2916 | |
| 26 | 3.2909 | |
| 27 | 3.2928 | |
| 28 | 3.2916 | |
| 29 | 3.2913 | |
| 30 | 3.2917 | |
| 31 | 3.2914 | |
| 32 | 3.2916 | |
| 33 | 3.2917 | |
| 34 | 3.2881 | |
| 35 | 3.2912 | |
| 36 | 3.2912 | |
| 37 | 3.2917 | |
| 38 | 3.2918 | |
| 39 | 3.2906 | |
| 40 | 3.2895 | |
| 41 | 3.2885 | |
| 42 | 3.2883 | |
| 43 | 3.2904 | |
| 44 | 3.2913 | |
| 45 | 3.2915 | |
| 46 | 3.2908 | |
| 47 | 3.2896 | |
| 48 | 3.2918 | |
| 49 | 3.2911 | |
| 50 | 3.2912 | Short-Circuit |

Table A.1. Open circuit voltage of the $LiFePO_4$ battery cells

## A.2 Capacity

| Cell Number | Capacity [Ah] | Comment |
|---|---|---|
| 1 | 1.13 | |
| 2 | 1.13 | |
| 3 | 1.14 | |
| 4 | 1.13 | |
| 5 | 1.13 | |
| 6 | 1.13 | |
| 7 | 1.13 | |
| 8 | 1.14 | |
| 9 | 1.13 | |
| 10 | 1.13 | |
| 11 | 1.13 | |
| 12 | 1.13 | |
| 13 | 1.14 | |
| 14 | 1.13 | |
| 15 | 1.13 | |
| 16 | 1.13 | |
| 17 | - | Bad cell |
| 18 | 1.12 | |
| 19 | 1.13 | |
| 20 | 1.13 | |
| 21 | 1.13 | |
| 22 | 1.13 | |
| 23 | 1.13 | |
| 24 | 1.13 | |
| 25 | 1.13 | |

| Cell Number | Capacity [Ah] | Comment |
|---|---|---|
| 26 | 1.13 | |
| 27 | 1.12 | |
| 28 | 1.13 | |
| 29 | 1.12 | |
| 30 | 1.13 | |
| 31 | 1.12 | |
| 32 | 1.13 | |
| 33 | 1.13 | |
| 34 | 1.12 | |
| 35 | 1.12 | |
| 36 | 1.13 | |
| 37 | 1.1 | |
| 38 | 1.13 | |
| 39 | 1.1 | |
| 40 | 1.12 | |
| 41 | 1.12 | |
| 42 | 1.13 | |
| 43 | 1.13 | |
| 44 | 1.13 | |
| 45 | 1.13 | |
| 46 | 1.13 | |
| 47 | 1.12 | |
| 48 | 1.13 | |
| 49 | 1.13 | |
| 50 | - | Short-Circuit |

Table A.2. Capacity of the $LiFePO_4$ battery cells

## A.3 Capacity Deviation

| Cycle | Capacity [Ah] | Rel. Capacity [%] | Rel. Deviation [%] |
|---|---|---|---|
| 1 | 1.13 | 100 | 0 |
| 2 | 1.135 | 100.4424779 | 0.442477876 |
| 3 | 1.135 | 100.4424779 | 0.442477876 |
| 4 | 1.114 | 98.5840708 | 1.415929204 |
| 5 | 1.118 | 98.9380531 | 1.061946903 |
| 6 | 1.124 | 100.5366726 | 0.53667263 |
| 7 | 1.131 | 100.0884956 | 0.088495575 |
| 8 | 1.122 | 99.2920354 | 0.796460177 |
| 9 | 1.147 | 101.5044248 | 1.504424779 |
| 10 | 1.149 | 101.6814159 | 1.681415929 |
| 11 | 1.14 | 100.8849558 | 0.884955752 |
| 12 | 1.147 | 101.5044248 | 1.504424779 |
| 13 | 1.143 | 101.1504425 | 1.150442478 |

Table A.3. Capacity deviation of the first 13 cycles of the $LiFePO_4$ battery cells

## A.4 AC Impedance

| Cell Number | AC Imp [mΩ] | Comment |
|---|---|---|
| 1 | 21.19 | |
| 2 | 20.21 | |
| 3 | 19.71 | |
| 4 | 23.74 | |
| 5 | 20.54 | |
| 6 | 20.79 | |
| 7 | 19.16 | |
| 8 | 19.63 | |
| 9 | 19.78 | |
| 10 | 18.45 | |
| 11 | 18.7 | |
| 12 | 19.84 | |
| 13 | 19.26 | |
| 14 | 20.79 | |
| 15 | 20.65 | |
| 16 | 19.07 | |
| 17 | 50.4 | Bad cell |
| 18 | 21.39 | |
| 19 | 19.59 | |
| 20 | 20.61 | |
| 21 | 19.18 | |
| 22 | 19.53 | |
| 23 | 18.96 | |
| 24 | 18.85 | |
| 25 | 21.05 | |

| Cell Number | AC Imp [mΩ] | Comment |
|---|---|---|
| 26 | 20.67 | |
| 27 | 19.31 | |
| 28 | 23.31 | |
| 29 | 33.5 | |
| 30 | 21.45 | |
| 31 | 22.16 | |
| 32 | 20.26 | |
| 33 | 20.11 | |
| 34 | 20.64 | |
| 35 | 19.24 | |
| 36 | 25.55 | |
| 37 | 32.09 | |
| 38 | 20.19 | |
| 39 | 21.43 | |
| 40 | 19.66 | |
| 41 | 19.98 | |
| 42 | 21.32 | |
| 43 | 18.16 | |
| 44 | 20.15 | |
| 45 | 21.31 | |
| 46 | 22.13 | |
| 47 | 22.16 | |
| 48 | 19.34 | |
| 49 | 18.63 | |
| 50 | - | Short-Circuit |

Table A.4. AC Impedance of the $LiFePO_4$ battery cells

# Bibliography


[1] Unknown, "Materials science battery case study," online: http://depts.washington.edu/matseed/batteries/MSE/index.html 05/06/2016, 2016.

[2] Anonymous, "Open circuit voltage vs. temperature at various states-of-charge (soc) for a wet low maintenance (sb/ca) or standard (sb/sb) battery table," online: http://jgdarden.com/batteryfaq/carfaq4.htmindex 05/11/2016, 2016.

[3] R. Allain, "Could you start your car with d-cell batteries?" online: http://www.wired.com/2012/10/could-you-start-your-car-with-d-cell-batteries/ 05/12/2016, 2012.

[4] I. Misiucenko, G. A. Martsinovskiy, B. C. Constantinovich, R. G. Khorenyan, and S. Nikolay, "Current interrupt device for batteries," online: http://www.google.com/patents/US7763375 05/19/2016, 2006.

[5] A. K. Maini and V. Agrawal, *Satellite Technology : Principles and Applications (2)*. Wiley, 2010.

[6] G. Prater, D. Sakoda, and A. Grant, "Overview of the naval postgraduate school small satellite, npsat1," Tech. Rep., 2004.

[7] G. Cheruvally, *Materials Science Foundations, Volume 38 : Lithium Iron Phosphate: A Promising Cathode-Active Material for Lithium Secondary Batteries*. Trans Tech Publications, 2008.

[8] Anonymous, "Apr18650 lithium ion cylindrical cell," online: http://www.a123systems.com/lifepo4-battery-cell.htm 06/28/2016, 2016.

[9] J. Molenda, A. Kulka, A. Milewska, W. Zajc, and K. Konrad Ywierczek, "Structural, transport and electrochemical properties of lifepo4 substituted in lithium and iron sublattices (al, zr, w, mn, co and ni)," *Department of Hydrogen Energy, Faculty of Energy and Fuels, AGH University of Science and*, 2013.

[10] I. Buchmann, "Bu-701: How to prime batteries," online: http://batteryuniversity.com/learn/article/howtoprimebatteries 05/31/2016, 2011.

[11] W.-Q. Wu, J.-Y. Liao, H.-Y. Chen, X.-Y. Yu, C.-Y. Su, and D.-B. Kuang, *Dye-sensitized solar cells based on a double layered TiO2 photoanode consisting of hierarchical nanowire arrays and nanoparticles with greatly improved photovoltaic performance.* J. Mater. Chem, 2012.

[12] Y. Jiang, C. Zhang, W. Zhang, W. Shi, and Q. Liu, "Modeling charge polarization voltage for large lithium-ion batteries," *Journal of Industrial Engineering and Management*, 2013.

[13] Anonymous, "Battery chargers and charging methods," online: http://www.mpoweruk.com/chargers.htm 05/31/2016, 2005, woodbank Communications.

[14] K. Bazzi, "Nanostrucured lithium iron phosphate as cathode material for lithium ion-batteries," Ph.D. dissertation, Wayne State University, 2014.

[15] Anonymous, "Safety data sheet for high power lithium ion cell, phosphate-based," *A123 Systems Regulation*, 2009.

[16] I. Buchmann, "Bu-802b: What does elevated self-discharge do?" online: http://batteryuniversity.com/learn/article/elevatingselfdischarge 05/11/2016, 2016, cadex Electronics Inc.

[17] T. B. Reddy, *Linden's Handbook of Batteries*. Mc Graw Hill, 2011, vol. Fourth Edition.

[18] R. Hensley, J. Newmann, and M. Rogers, "Battery technology charges ahead," *McKinseyCompany*, 2014.

[19] I. Buchmann, "Bu-806a: How heat and loading affect battery life," online: http://batteryuniversity.com/learn/article/howheatandharshloadingreducesbatterylife 05/12/2016, 2016, cadex Electronics Inc.

[20] Z. Chen, Y. Qin, and K. Amine, *Chemical Overcharge Protection of Lithim-Ion Cells*. Nova Science Publishers, Inc., 2010.

[21] D. Sakoda, J. Horning, and R. Panholzer, *Small Satellites: Past, Present and Future*, H. Helvajian and S. W. Janson, Eds. The Aerospace Press, 2008, chapter 9: The Naval Postgraduate School Small Satellite Program.

[22] B. Greiner, "In-situ-messungen an lithium-ionen-batterien mit dem adiabatischen reaktionskalorimeter," Deutsches Zentrum fr Luft- und Raumfahrt e.V. (DLR), Stuttgart; Institut fr Technische Thermodynamik; Abteilung Elektrochemische Energietechnik, Fachgruppe Batterietechnik, Tech. Rep., 2012.

[23] X.-C. Tang, L.-X. Li, Q.-L. Lai, X.-W. Song, and L.-H. Jiang, "Investigation on diffusion behavior of li+ in lifepo4 by capacity intermittent titration technique (citt)," *Electrochim. Acta*, 2009.

[24] W.-J. Zhang, "Structure and performance of lifepo4 cathode materials: A review, j. power," 2011.

[25] P. Xiao, Z. Q. Deng, A. Manthiram, and G. Henkelmann, "Calculations of oxygen stability in lithium-rich layered cathodes," *The Journal of Physical Chemistry*, 2012.

[26] Anonymous, "Cylindrical battery pack design, validation and assembly guide," *User Documentation*, 2013.

[27] R. L. Phelps, "Naval postgraduate school, ssag lithium ion battery handling guidance and emergency procedures," Naval Postgraduate School, Tech. Rep., 20016.

[28] R. L. Phelps, "Ssag maccor lithium battery tester, attended and unattended operations sop," Naval Postgraduate School, Tech. Rep., 2016.

THIS PAGE INTENTIONALLY LEFT BLANK

# Initial Distribution List

1. Defense Technical Information Center
   Ft. Belvoir, Virginia

2. Dudley Knox Library
   Naval Postgraduate School
   Monterey, California